USAAMRDL-TR-75-31A

INTEGRAL ENGINE INLET PARTICLE SEPARATOR

Volume I – Technology Program

General Electric Company
Aircraft Engine Group
Cincinnati, Ohio 05215

July 1975

Prepared for

EUSTIS DIRECTORATE
U. S. ARMY AIR MOBILITY RESEARCH AND DEVELOPMENT LABORATORY
Fort Eustis, Va. 23604

EUSTIS DIRECTORATE POSITION STATEMENT

The work reported herein represents the first known systematic investigation of the design variables that influence the performance of integral inlet particle separators.

It is expected that the design procedures and performance data described herein will be used in the design of integral inlet particle separators for future Army aircraft gas turbine engines.

Appropriate technical personnel of this Directorate have reviewed this report and concur with the conclusions and recommendations contained herein.

Mr. David B. Cale of the Propulsion Technical Area, Technology Applications Division, served as Project Engineer for this effort.

UNCLASSIFIED

SECURITY CLASSIFICATION OF THIS PAGE (When Data Entered)

REPORT DOCUMENTATION PAGE	READ INSTRUCTIONS BEFORE COMPLETING FORM
1 REPORT NUMBER (19) USAAMRDL-TR-75-31A	2 GOVT ACCESSION NO 3 RECIPIENT'S CATALOG NUMBER
4 TITLE (and Subtitle) (6) INTEGRAL ENGINE INLET PARTICLE SEPARATOR, Volume I, Technology Program,	5 TYPE OF REPORT & PERIOD COVERED (12) Final rept. 6 PERFORMING ORG. REPORT NUMBER
7 AUTHOR(s) (10) Robert J. Duffy Bernard F. Shattuck	8 CONTRACT OR GRANT NUMBER(s) (15) DAAJ02-73-C-0004 new
9 PERFORMING ORGANIZATION NAME AND ADDRESS General Electric Company Aircraft Engine Group Cincinnati, Ohio 45215/Lynn, Mass. 01910	10 PROGRAM ELEMENT, PROJECT, TASK AREA & WORK UNIT NUMBERS 62204A 1G162204AA71 04 001 EK
11 CONTROLLING OFFICE NAME AND ADDRESS Eustis Directorate U.S. Army Air Mobility R&D Laboratory Fort Eustis, Virginia 23604	(11) 12 REPORT DATE July 1975 13 NUMBER OF PAGES 109
14 MONITORING AGENCY NAME & ADDRESS (if different from Controlling Office)	15 SECURITY CLASS (of this report) UNCLASSIFIED 15a DECLASSIFICATION/DOWNGRADING SCHEDULE

(9) Final rept.

16 DISTRIBUTION STATEMENT (of this Report)

Approved for public release; distribution unlimited.

(16) DA-1-G-162204-AA-71

17 DISTRIBUTION STATEMENT (of the abstract entered in Block 20, if different from Report)

(17) 1-G-162204-AA-7104

18 SUPPLEMENTARY NOTES

Volume I of two volumes

19 KEY WORDS (Continue on reverse side if necessary and identify by block number)

Inlet Particle Separator, Design Guide, Integral, Inertial, Axial Scroll, Particle Trajectory, Separation Efficiency, Test Specifications

20 ABSTRACT (Continue on reverse side if necessary and identify by block number)

Volume I of this report describes the results of a 30-month program to design and evaluate integral engine inlet separators in 2, 5, and 15 lb/sec sizes. The separators are designed to remove sand, dust, and single foreign objects from the air entering a turboshaft engine.

(Continued)

to 1473B

DD FORM 1 JAN 73 1473A EDITION OF 1 NOV 65 IS OBSOLETE

UNCLASSIFIED

SECURITY CLASSIFICATION OF THIS PAGE (When Data Entered)

JN

703-168

from 1473A

UNCLASSIFIED

SECURITY CLASSIFICATION OF THIS PAGE(When Data Entered)

Program effort included:

(1) Definition of turboshaft engine environment in terms of amounts and types of ingested materials.

(2) Mechanical and aerodynamic design trade-off studies of integral engine separators followed by full-scale model performance tests of 2 and 15 lb/sec separators.

(3) Detailed design and procurement of 2, 5, and 15 lb/sec separators, and design and procurement of improved components.

(4) Model tests of the separators to obtain detailed aerodynamic and off-design performance data.

(5) Preparation of a separator design guide for integral engine separators in the 2 to 15 lb/sec size range.

The design guide (including environment definition) is presented in Volume II of this report. Volume I documents all other aspects of the program.

1473B

UNCLASSIFIED

SECURITY CLASSIFICATION OF THIS PAGE(When Data Entered)

PREFACE

This final report contains the results of work done to satisfy the requirements of the Integral Engine Inlet Protection Device Technology Program. The program was conducted by General Electric under Contract DAAJ02-73-C-0004 with the Eustis Directorate, U.S. Army Air Mobility Research and Development Laboratory, Fort Eustis, Virginia. It was carried out over a period of 30 months in six phases.

Phase I - Definition of Environment

Phase IIA - Design Trade-Off Definition

Phase IIB - Inlet Scroll Configuration

Phase III - Detailed Separator System Design

Phase IV - Model Hardware and Instrumentation

Phase V - Experimental Evaluation

Phase VI - Preparation of Preliminary Design Guide

Several people who contributed to the program should be recognized. The literature search, which was most of the work of Phase I, was conducted by T.L. De Young. The design and procurement of the models, and the conduct of the test program, were almost entirely done by J.A. Ebacher. Nearly all of the particle trajectory analysis effort was contributed by G.E. Lepine. The aerodynamic data reduction and analysis was done by G.L. Allen. The success of the program was due largely to these contributors.

TABLE OF CONTENTS

LIST OF ILLUSTRATIONS

LIST OF ILLUSTRATIONS - Continued

LIST OF ILLUSTRATIONS - Continued

LIST OF TABLES

INTRODUCTION

The adverse environments in which Army equipment operates impose severe penalties upon gas turbine engine performance, reliability, and life expectancy. Ingested sand, dust, foliage, rain, salt spray, and single foreign objects can cut off or appreciably reduce an unprotected engine's term of service. Numerous studies and development programs have demonstrated that engine inlet protective devices significantly reduce the damaging effects of these various forms of ingested materials. No program, however, has collected the large amount of detailed data relating to the environments encountered by gas turbine engines in the field or under controlled laboratory conditions. Phase I of the Integral Engine Inlet Protection Device Technology Program was designed to accomplish that objective in order to define a representative operating environment in which an inlet protection device is expected to function. The results of Phase I are presented in Volume II.

INDEX TO TECHNICAL DATA

To make this final report as useful as possible, an index to the technical data contained in both volumes of the report is included as Table 1. Table 1 serves a secondary purpose by indicating the parameters which are important to the design of an inlet particle separator.

TABLE 1. INDEX TO TECHNICAL DATA FOR 2-LB/SEC, 5-LB/SEC, AND 15-LB/SEC SEPARATORS
(Volume No. - Page No.)

Parameter	2-Lb/Sec Separators	5-Lb/Sec Separators	15-Lb/Sec Separators
Swirl Vane			
Shape	I-64, II-92, II-97	I-74, II-92, II-97	I-51, I-56, I-57, I-58, I-82, I-84, II-99
Location	II-86	II-86	I-57, I-84, II-86
Solidity	I-64, II-86, II-91, II-92	I-74, II-86, II-91	I-51, I-98, II-86, II-91, II-92
Swirl Vane	I-64, II-19, II-86	I-77, II-19, II-86	I-82, I-87, I-88, I-89, II-19, II-86
Flow Path			
Aerodynamics	I-33, I-63, II-68	I-46, I-73, I-77, II-68	I-56, I-84, II-68
Separator Efficiency	I-64, II-68	I-73, I-74, II-68	I-82, I-83, I-84, I-85, I-92, II-68
Scavenge Flow Ratio	I-66, II-18, II-129, II-132 II-134	I-75, II-18, II-130, II-133, II-134	I-95, I-96, I-98, II-18, II-131, II-133, II-134
Deswirl Vane			
Shape	II-109	II-109	II-109
Location	II-112, II-109	II-112, II-132, II-109	II-112, II-109
Solidity	I-64	II-112	II-112
Scroll Vanes	I-64, II-126	I-76, II-126	II-126

DEFINITION OF ENVIRONMENT

SAND AND DUST

In the helicopter environment at low altitude, especially takeoff and landing over land, sand and dust are always present. They do not generally cause the catastrophic types of failure which often accompany the ingestion of large single objects or masses of foliage, but they continuously erode an engine's mechanical structure and its performance. The MIL-E-5007C specification dust concentration, 1.5 milligrams/ft^3, is less than nearly all sea level and altitude samples which are found in the literature. Most of the recorded concentrations are between 1.5 and 15 mg/ft^3.

However, the size and size distribution of MIL-E-5007C specification dust (C-Spec) are typical of most terrain samples from various locations in the world. As the altitude of the helicopter over the ground increases, the dust tends to become finer but usually not as fine as AC coarse.

FOLIAGE AND RAGS

Foliage or rag ingestion is an important problem since the engine inlet is blocked and the engine must be shut down until the item is removed. However, the item does not usually cause appreciable engine damage. When the ingested foliage or rag is removed, the aircraft becomes operational again. Therefore, there are very few statistics to indicate the magnitude of the foliage ingestion problem, which is probably much larger than available data indicates.

SINGLE FOREIGN OBJECTS

The ingestion of large single objects is the most formidable aircraft environmental problem, since nuts, bolts, safety pins, and other large objects which are left in the aircraft inlet system or dropped on the runway usually cause extensive engine damage. Birds as well as ice which breaks off the fuselage or inlet system, also are important problems.

WEATHER

Weather is important to the aircraft engine's environment primarily because of ice ingested in large chunks which cause serious engine damage. Rain is not as damaging as ice, but it can cause engine mechanical damage and performance loss. Concentration of rain in inlet air at altitude has been recorded at about 8% of the inlet airflow by weight. The engine is required by Specification MIL-E-5007C to operate at concentrations of 5%.

COMBINATIONS OF ELEMENTS

Combinations of various elements of the environment are considered to be relatively unimportant. For instance, an ingested bolt is no more harmful if it is accompained by dust. Wet dust may be less harmful than dry dust, but its importance is removed mainly because wet dust is hard to stir up on the ground. Wet foliage may be more harmful than dry. Tests with wet and damp foliage are therefore recommended.

PRELIMINARY DESIGN

ENGINE AND SEPARATOR SYSTEMS

The T700 integral separator design was selected as the baseline configuration for scaling and designing integral inlet separators in the 2 to 15 lb/sec range because it is an intermediate size, and it represents the latest and most complete integration of accessory, structural and separator requirements. Cross sections and visual descriptions of the T700 separator are shown in Figures 1, 2, and 3.

The T700 was also a convenient choice since the engines used in the 2, 5, and 15 lb/sec designs were selected to be front drive engines with front mounted accessories. The principles of the separator design apply equally well for other engines such as rear drives in this size range. In fact, the designs become simpler when some of the subsystem functions such as power takeoff (PTO) and front drive do not have to be integrated into the design. The engine configurations were based upon engine designs previously studied by General Electric. The 15-lb/sec turboshaft engine is a scaled-up version of the T700 engine, while the 2 and 5 lb/sec engines were based upon a combination of scaling downward plus additional modifications which include: single-stage turbines for both the 2 and 5 lb/sec engine, no axial compressor stages for the 2 lb/sec engine, and two axial stages for the 5 lb/sec engine. Although the separator designs are shown on these engines, they are capable of being used on engines of different makes, sizes, configurations and installations.

Direct scaling of the T700 separator was not possible for the 2 lb/sec engine. Therefore, a T700 type separator design was used as a baseline configuration, but other separator designs were also investigated. The most promising alternate configuration was a scroll separator. This separator, shown in Figure 4, was especially applicable to the 2 lb/sec engine. Some studies of the scroll design in the 5 lb/sec size were started but were dropped when they indicated that the overall volume was larger than it was with the scaled T700 type separator. Alternate design studies were made for both integrated oil tanks and separate oil tanks, for the scroll separator.

Installation requirements are important in prescribing the separator configuration, especially in the 2 lb/sec size. For the scroll separator, the drive shaft is not coaxial with respect to the air inlet as it is in the T700 separator. This results in a different installation setup and separate points of attachment for the inlet. Although the engines on which this separator design was based are principally for aircraft installations with air inlet from the front, they could be used for other applications such as tanks, other ground vehicles, and auxiliary power units. The 2 lb/sec scroll separator is especially versatile and flexible

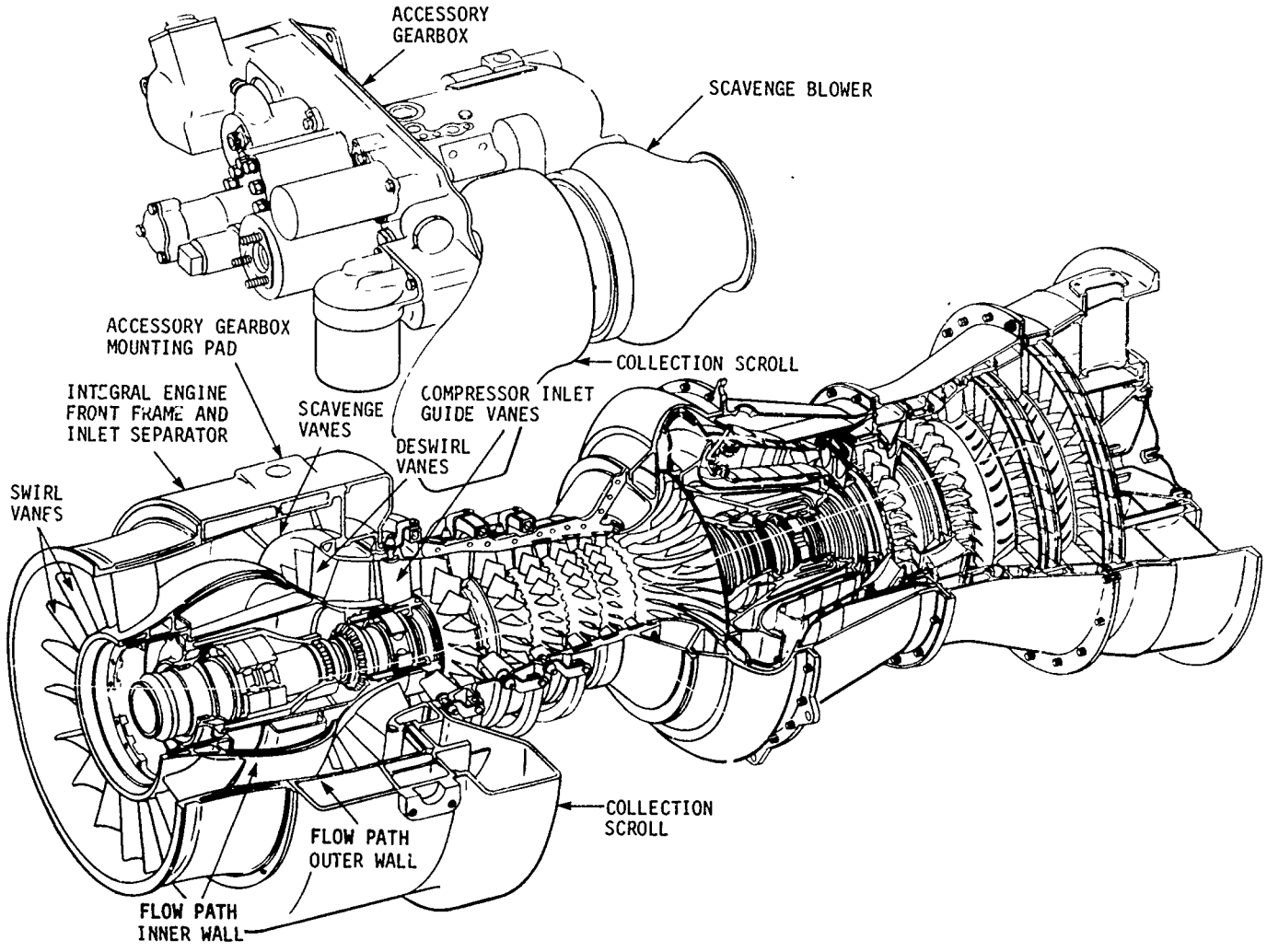

Figure 1. T700 Turboshaft Engine With Inlet Separator.

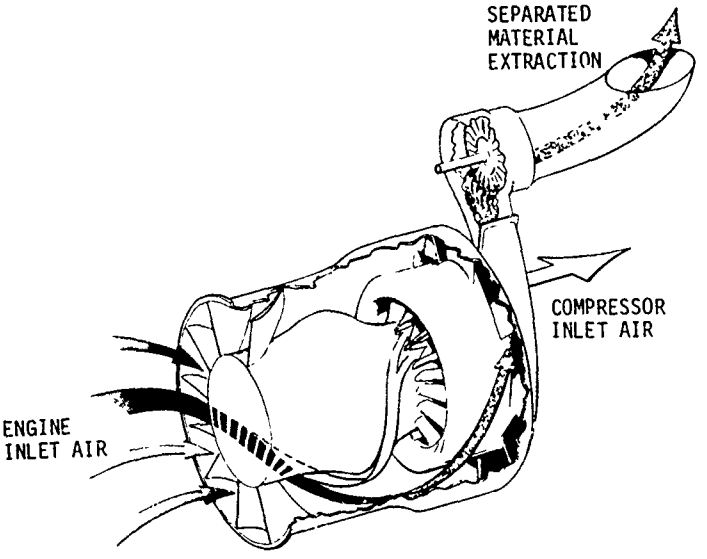

Figure 2. T700 Type Separator Schematic.

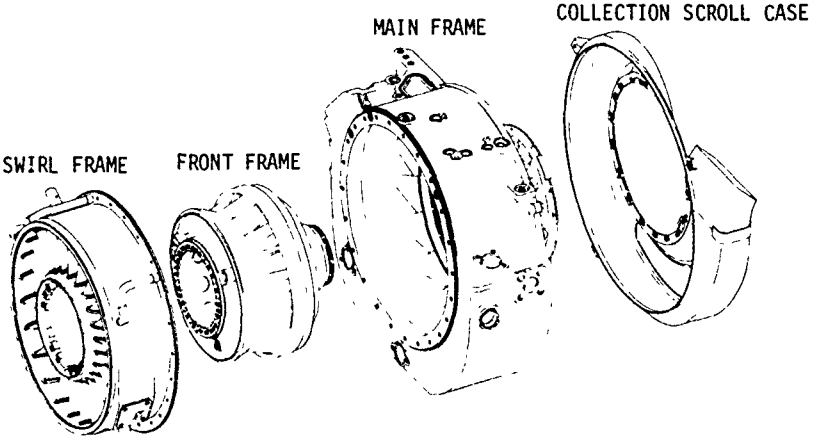

Figure 3. Exploded View of Major Components.

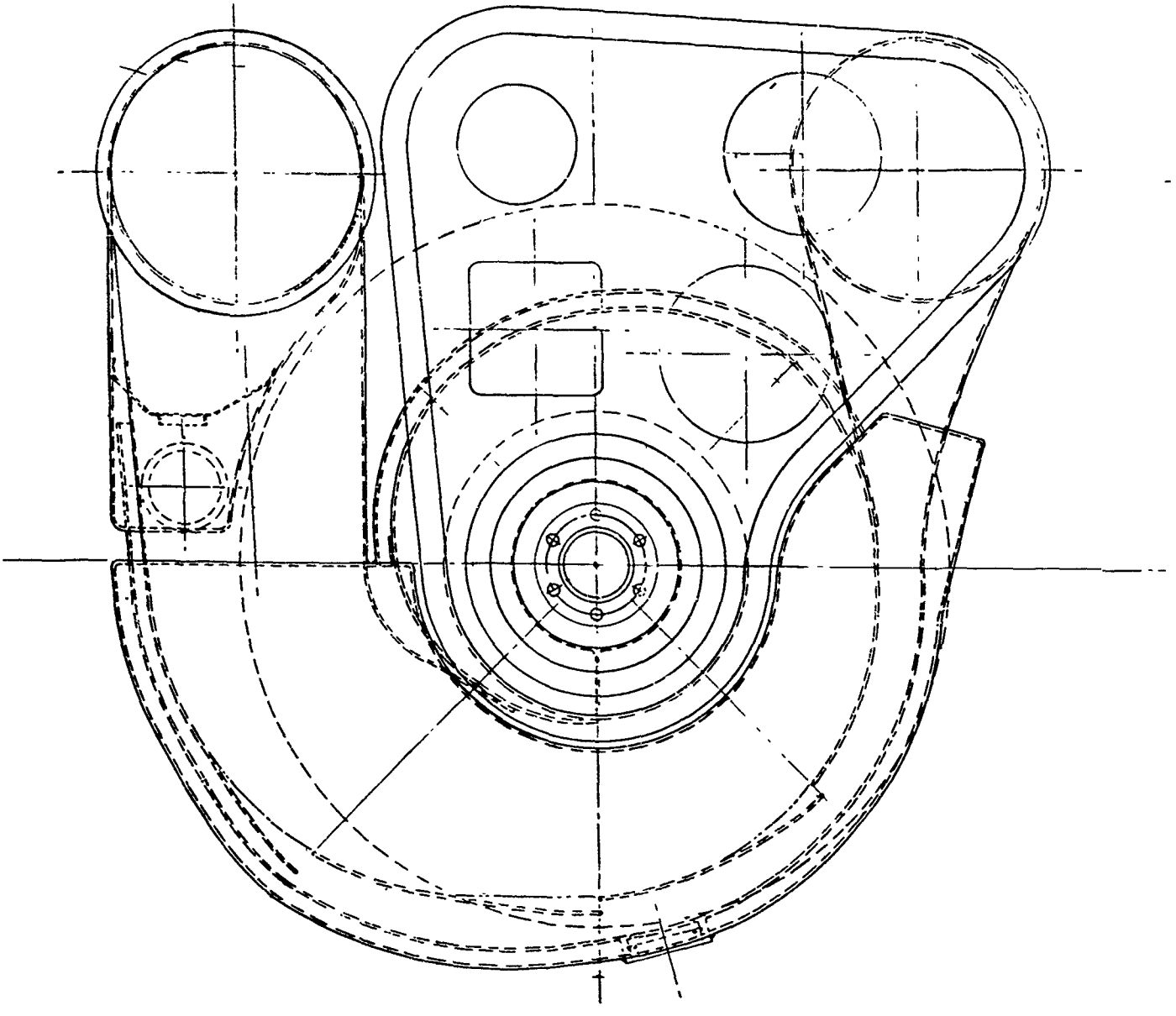

Figure 4. 2 Lb/Sec Turboshaft Engine With Inlet Scroll Separator.

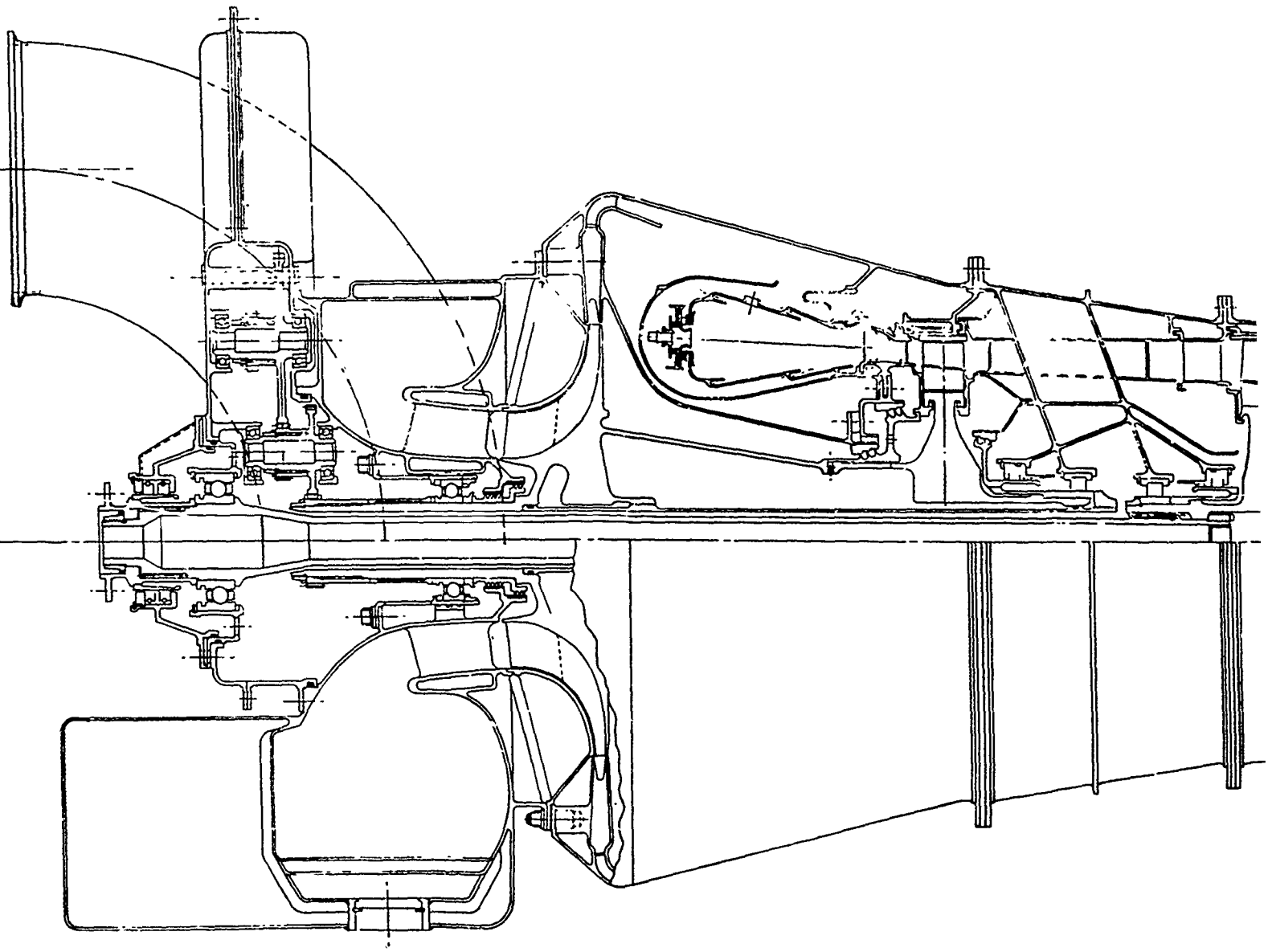

for a variety of different installations, because of the small inlet duct. With a rotatable type elbow inlet, air can be introduced at any angular location over a 360-degree arc.

Another configuration of the scroll separator is illustrated in Figure 5. In this design the inlet air is introduced tangentially into the scroll. The elbow collector has been replaced by a collector located further around the scroll at a location where the scroll turns the incoming air sufficiently to separate out the large foreign objects. Pressure drop in the inlet elbow is thus eliminated, providing an improvement of approximately 5 in. H_2O in pressure drop.

SUBSYSTEMS AND THEIR INTEGRATION

To obtain efficient utilization of space and weight, the separators were designed so that they could be integrated with other engine subsystems. The lube system, accessories and accessory gearbox, power-takeoff (PTO), anti-icing systems, structure of the front frame, aero-thermo systems, and inlet protective devices are engine subsystems that have a direct influence upon each other and upon the engine. Integration considerations were:

1. Accessories and Accessory Power. Accessories, accessory gearboxes (AGB's), and accessory power requirements were considered in the separator studies. Although they are not a part of the basic separator design, the size of the accessory power load and the size and location of the PTO shaft influence separator design. The PTO shafting must be the smallest diameter possible to have minimal effect on separator performance. For improved performance, the 2 lb/sec design was changed to have the PTO shaft go through the swirl vanes rather than through the scavenge air vanes as in the T700 separator. This was accompanied by a reduction in the size of the struts in the compressor inlet and in the scavenge air exhaust.

   In establishing the three different size separators, the PTO shafting, gearing, and splines were sized on the basis of assumed starter loading and then checked against the total assumed accessory power load when running. The accessories for the engines are not directly or equally scalable. Some accessories, such as temperature and pressure sensing accessories, are the same size or nearly the same size regardless of engine rating. Other accessories, such as the blower and lube pump, are more nearly scalable. For the design studies, accessory requirements were scaled or estimated using T700 accessories and ratings as a reference. Table 2 gives some of the requirements.

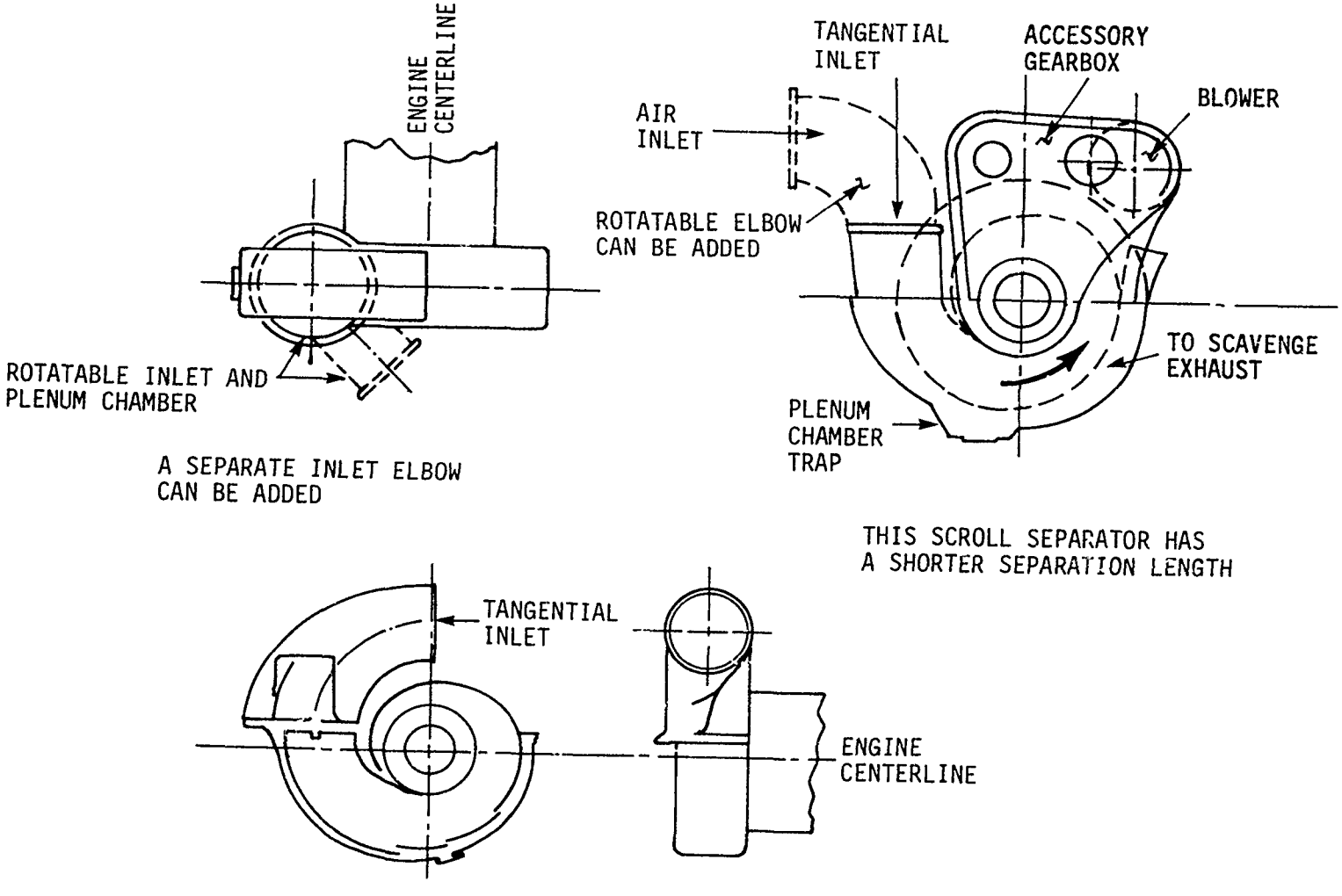

Figure 5. Scroll Separator Tangential Inlet.

TABLE 2. T700 ACCESSORY REQUIREMENTS				
Accessory Requirement	Engine Size (Airflow, lb/sec) 2	5	15	T700
AGB HP	20	40	80	49
Customer HP	8	15	30	15
Starter Torque as % T700	25	55	130	100
Sizes as % T700	60	80	115	100

Accessory requirements for the scroll separator design were somewhat different from those for the T700 type separator. For instance,

a. Both have a completely modular accessory package and gearbox so that the gearbox with accessories can be mounted or removed as a module. For the scroll separator, however, the gearbox is also a support structure for the main power drive shaft, which must be removed before the gearbox can be taken off.
b. The scroll type separator does not provide for a power takeoff shaft (PTO) or bevel gearing. Only spur gearing is used.

2. Oil Tank and Oil Cooling (Oil to Air Heat Exchange). The T700 integral separator incorporates a number of features which were retained for all the scaled T700 type separator designs. These are:
   a. Integral oil tank.
   b. Supplemental oil to air cooling by running oil through the scavenge air vanes.
   c. Thermal compensation of inner and outer separator structural parts by running cooling oil through the scavenge air vanes and around the inner and outer structural parts.
   d. Deaeration of oil by introducing at top and letting it flow over the inner wall of the oil tank.

   Oil flows and oil tank capacities estimated are listed in Table 3.

TABLE 3. OIL SYSTEM REQUIREMENTS AND VOLUMES

Item	Engine Size (Airflow, lb/sec) 2	5	15	T700
Oil Tank Volume (gal, oil only)	1.2	1.5	2.1	1.7
Usable Oil (gal)	.3	.4	.6	.5
Oil Flow (gal/min)	2.5	3.3	4.5	4.0
Dwell Time (sec)	20	20	20	20
Expansion Air Space (% vol)	--	--	--	10-25

For the scroll separator design, supplemental cooling of oil with air is possible by one or more of the following:

a. Integral oil tank.
b. Running oil lines around the outside wall of the scroll - especially at the inlet.
c. Passing oil through structural vanes in front of the compressor.
d. Separate oil-to-air heat exchanger.

For the scroll separator, both integral and separate oil tanks were considered, and there was an air/oil deaerator inside the oil tank to assure good deaeration of the oil.

3. Anti-Icing. Anti-icing of swirl vanes and leading edge of splitter nose was incorporated into the scaled separator designs as it is for the T700 separator.

Anti-icing of the scroll separator for 2 lb/sec size is less of a problem. It can be accomplished by hot oil in tubing, surrounding scroll with oil, and/or oil through structural vanes leading to compressor.

4. Structural Requirements. The structural requirements for the front of the engine are similar in nature and complexity to those for the T700 engine. The T700 type separator provides a satisfactory structure without adversely affecting engine

performance. For the 2 lb/sec size, the vanes must be made longer and larger to carry the structural loads as well as to provide necessary internal flow areas for ducting oil. For the scroll separator in the 2 lb/sec size, the only structural vanes are those at the compressor inlet.

AERODYNAMIC LOSSES

The reference that has been used for all of the axial separator losses is the T700 design. In the initial designs for all core airflows, two principal scaling rules were followed:

1. All dimensions were scaled so that T700 Mach numbers were maintained.

2. T70C turning in vane cascades was retained.

The above rules could be followed for the 5 and 15 lb/sec designs by scaling the T700 design, but the 2 lb/sec design was defined along the inside diameter by the bearing and gearing requirements of the engine, which prevented a direct scale of the T700 separator.

Since turning and passage characteristics of the T700 have been retained, the initial T700 separator cascade and turning loss of 5.6 in. H_2O was used for all the T700 type separators. The friction losses were taken also from T700 test results. The initial T700 separator friction loss of 3.5 in. H_2O was corrected for changes in the ratio of scrubbed area to flow area and for Reynolds number.

PARTICLE SEPARATION

A major objective of any separator study is the determination of particle separation efficiency. The level of efficiency in the preliminary design stages of a program, prior to availability of experimental data, can be obtained by tracing various particles through a specific flow field. This particle tracing or particle trajectory analysis is based upon the classical equations of motion of a particle modified by aerodynamic drag. The equations of motion are:

$$V_r = dr/dt \tag{1}$$

$$V_\theta = r\,(d\theta/dt) \tag{2}$$

$$V_Z = dz/dt \tag{3}$$

$$(dV_r/dt) = (v^2_{\theta/r}) + C(U_r - V_r) \tag{4}$$

$$dV_\theta/dt = C(U_\theta - V_\theta) - (V_r V_\theta)/r \quad (5)$$

$$dV_z/dt = C(U_2 - V_2) \quad (6)$$

where

r, θ, Z are particle radial, circumferential, and axial position components;

U_r, U_θ, U_Z are fluid radial, circumferential, and axial velocity components;

V_r, V_θ, Vz are particle radial, circumferential, and axial velocity components; and

t is Time.

This analysis provides a general overview of the separation problem. Particle Trajectory Analysis is discussed more fully in Volume II, Appendix B. Figure 6 shows the variation of the particle g-force (V_θ^2/r) with average radius. Once the separation force is determined by comparing the particle trajectory to the flow paths, relative performance can be defined. This type of comparison was made in the trade-off study phase of the program.

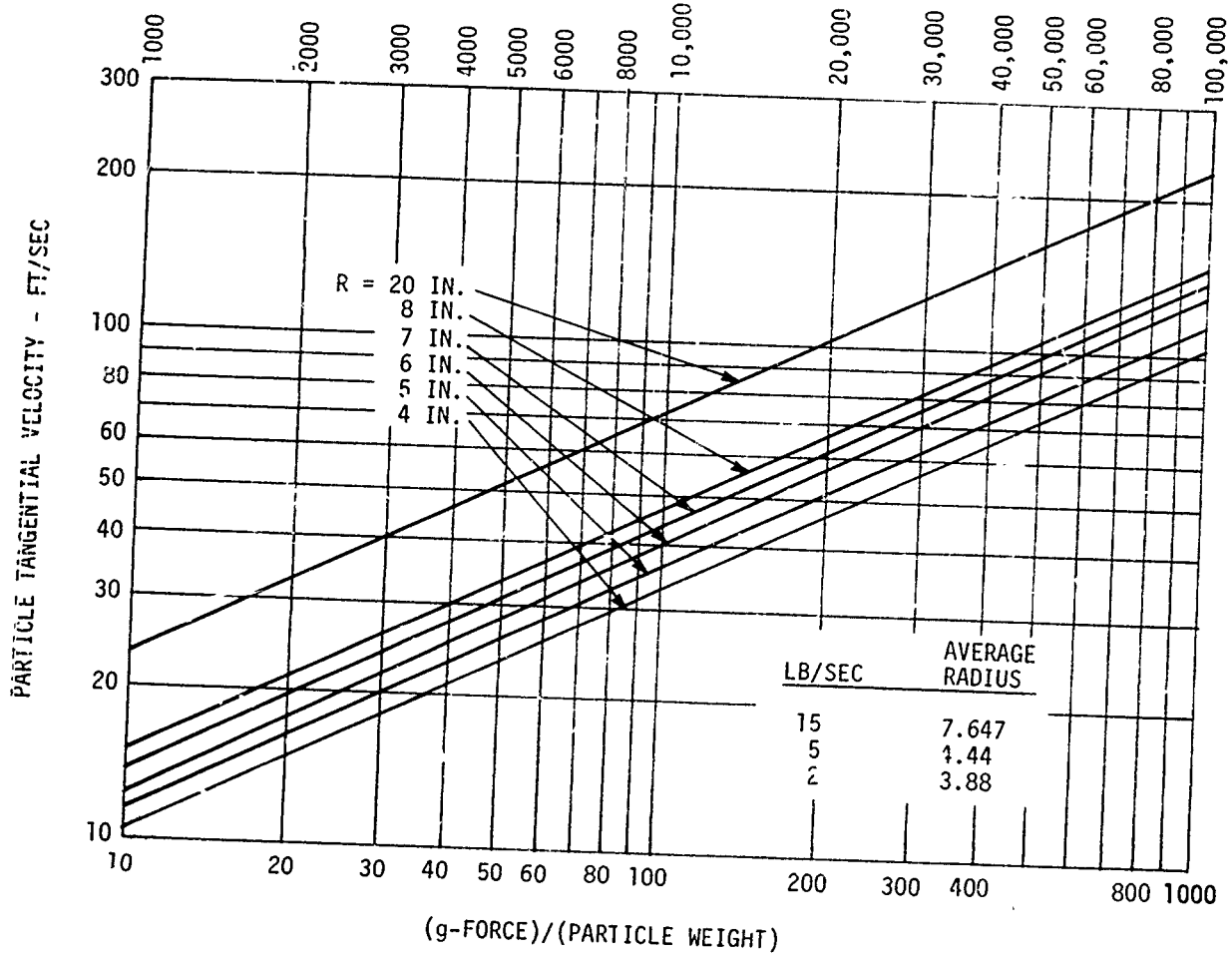

Figure 6. g Forces on a Particle.

MODEL DESIGNS

2 LB/SEC AXIAL SEPARATOR DESIGN

During Phase II of the program, a T700 type separator was designed for the 2 lb/sec turboshaft engine shown in Figure 7. Direct scaling of the T700 separator does not satisfy the mechanical requirements for the 2 lb/sec engine because the inside dimensions of the separator become too small to contain the front bearings and sump. Also, the vanes are not structurally strong enough to carry the engine loads, and they are not large enough internally for functional uses such as porting engine oil or housing a PTO shaft or accessory lines. The T700 type separator can be used in the 2 lb/sec engine if it is made larger in diameter and longer than a direct scale with airflow would dictate. The integral separator design shown incorporates these changes. It has longer and larger swirl, deswirl, and scavenge vanes to carry structural loads and to have enough internal port area for ducting anti-icing air through the swirl vane and oil through the scavenge vanes. A comparison of a scaled T700 separator flow path and the 2 lb/sec model flow path is shown in Figure 8. The figure demonstrates the large divergence of the design from the direct scaled T700 separator.

In the 2 lb/sec design shown in Figure 7, the PTO shaft goes through the swirl vanes instead of the scavenge vanes in order to reduce its adverse effect upon engine performance. The PTO shaft and splines were kept as small as possible to keep vane size to a minimum. Alternate studies were carried out on separator configurations with the PTO shaft located between the swirl and scavenge vanes, and with it passing through the swirl and deswirl vanes. These configurations are shown in Figures 9, 10, and 11.

Preliminary studies on oil flow, oil tank volume, and oil cooling were also carried out for the 2 lb/sec separator and compared to the T700 requirements. The studies showed that approximately 2.5 gal/min of lube oil must be supplied to the bearing sumps and gearbox of the 2 lb/sec engine. This is appreciably higher oil flow than indicated by direct scaling. This also had a direct effect on the size of the oil tank since the T700 oil dwell time requirement of 20 seconds was used. In addition, the increased oil flow requires proportionately more supplemental cooling from the air due to the higher ratio of oil flow to fuel flow.

Because they become relatively more important in the 2 lb/sec engine, special attention was paid to the accessories and accessory gearbox. A 60% scale of T70C accessories was selected for the 2 lb/sec engine. However, actual sizes were not considered critical during the initial part of the program since the AGB is mounted externally to the separator.

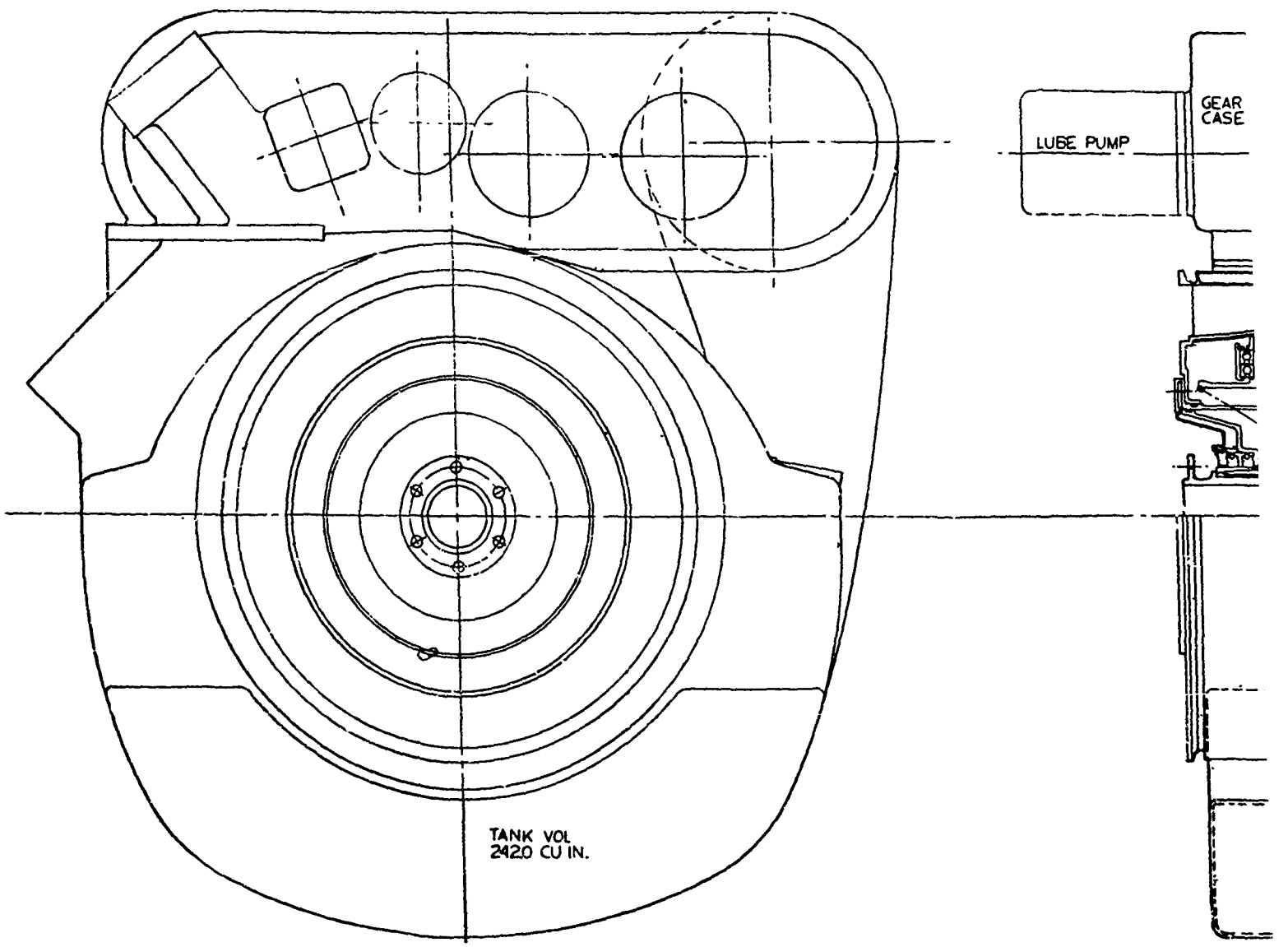

Figure 7. 2 Lb/Sec Engine With Separator.

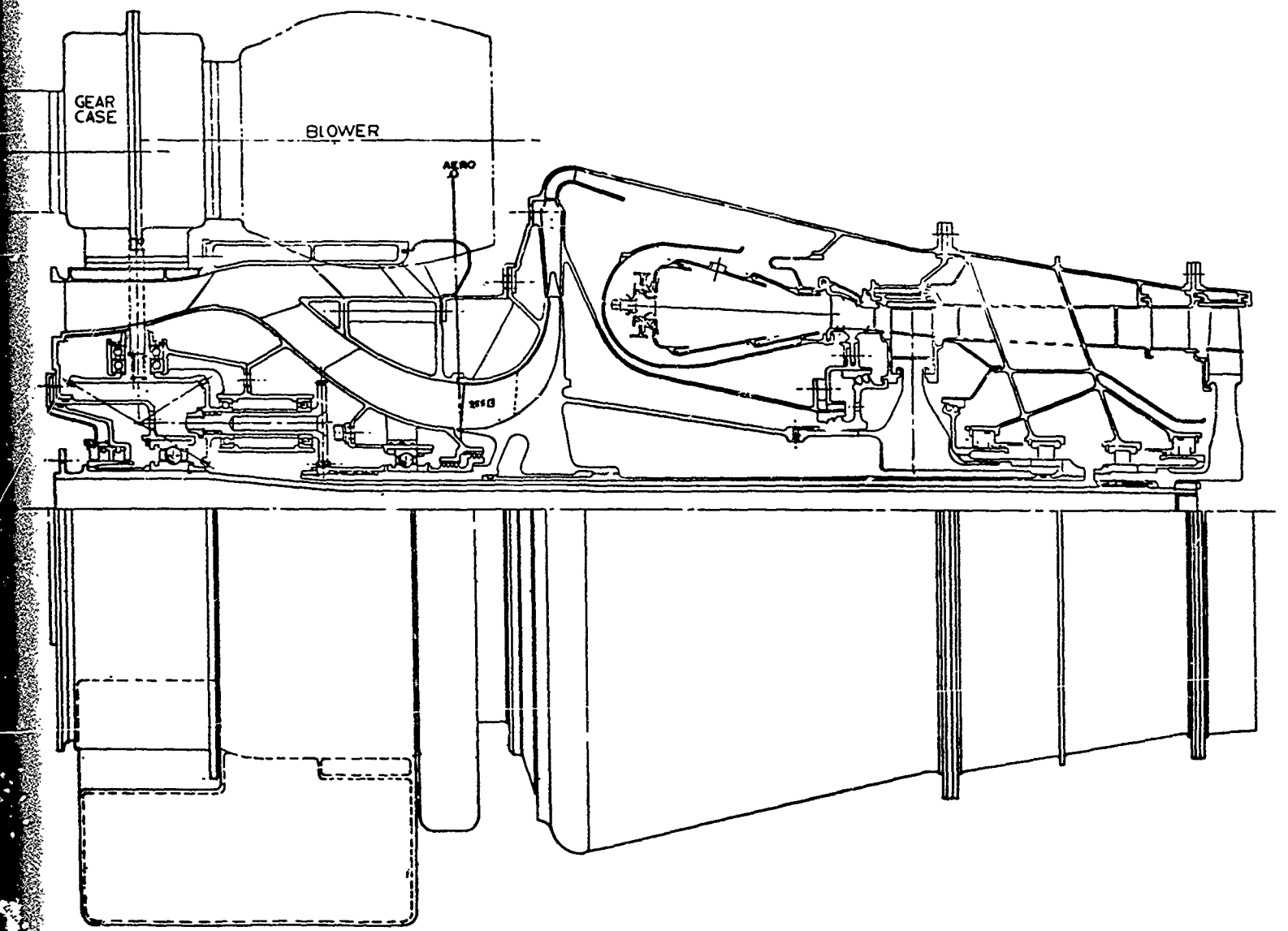
GEAR CASE
BLOWER
AERO

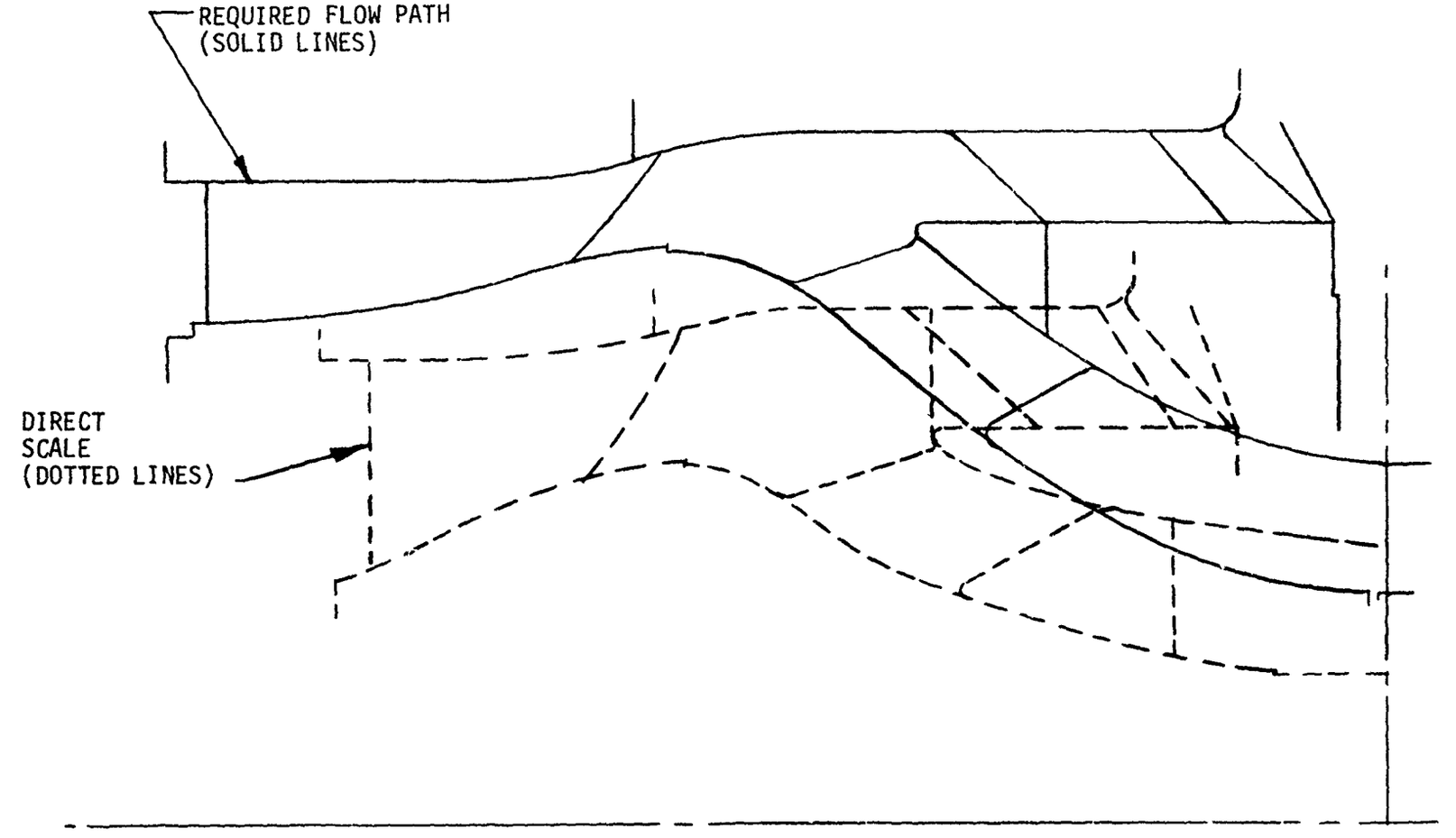

Figure 8. T700 Type Separator Flow Path for 2 Lb/Sec Engine.

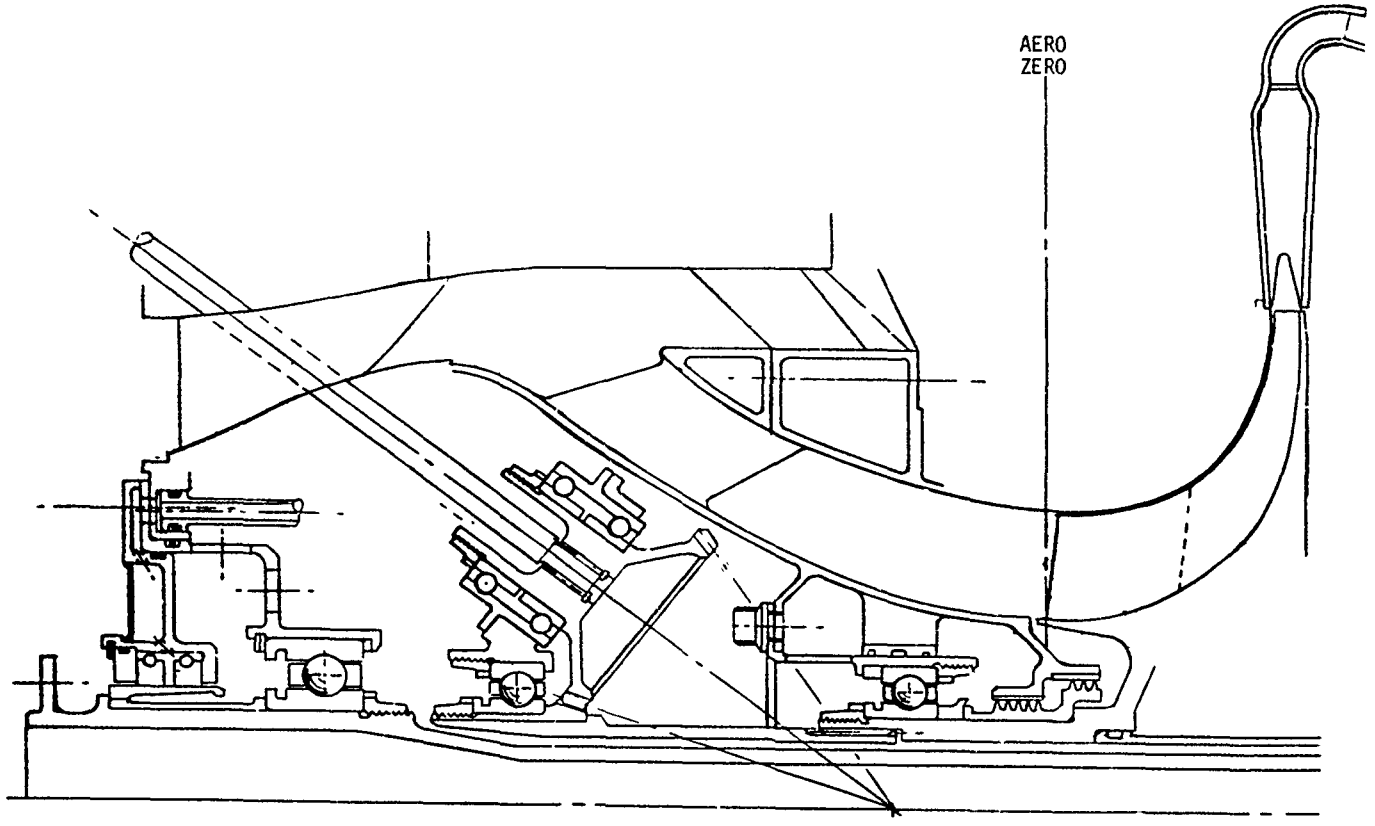

Figure 9. 2 Lb/Sec T700 Type Separator With PTO Shaft Canted Forward.

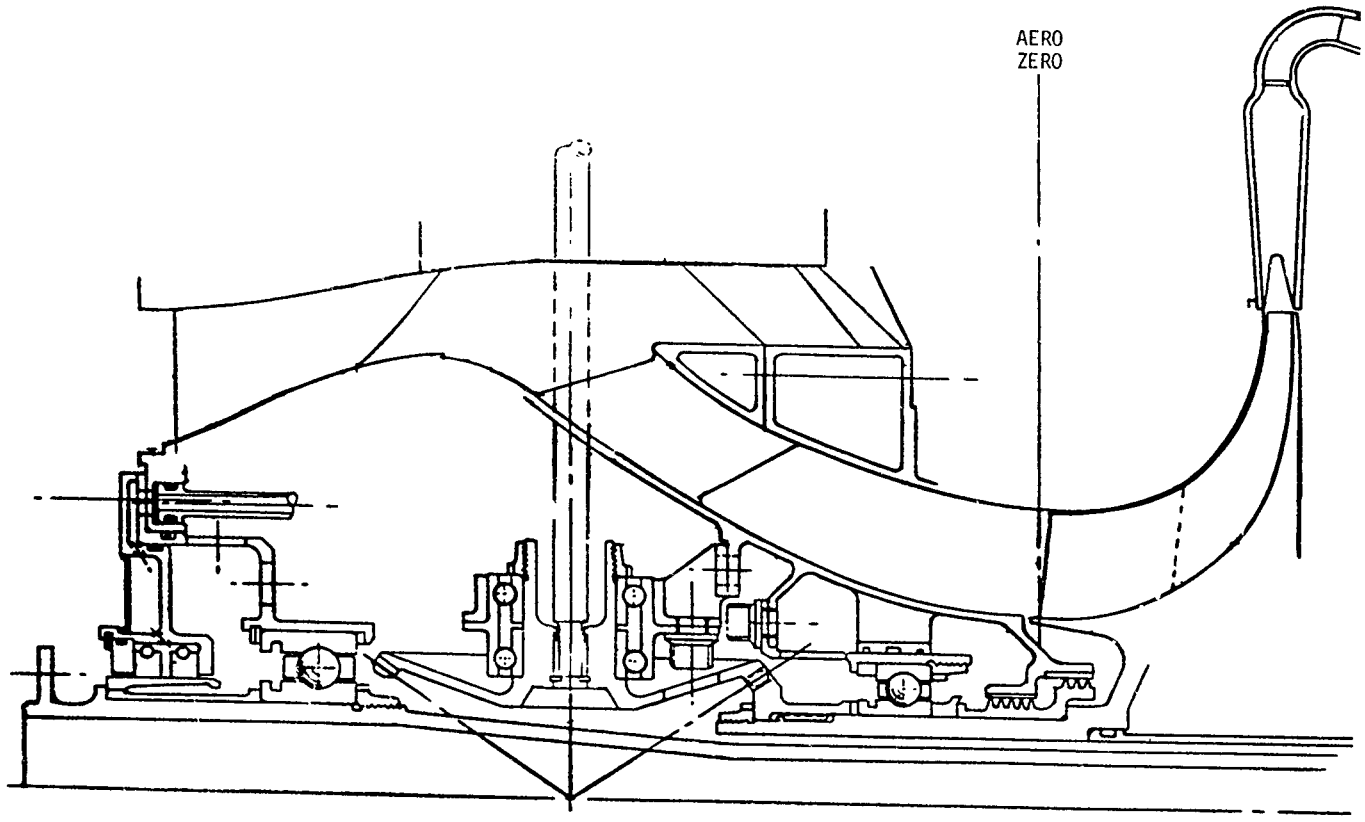

Figure 10. 2 Lb/Sec T70C Type Separator With PTO Shaft Between Swirl Vanes and Scavenge Air Vanes.

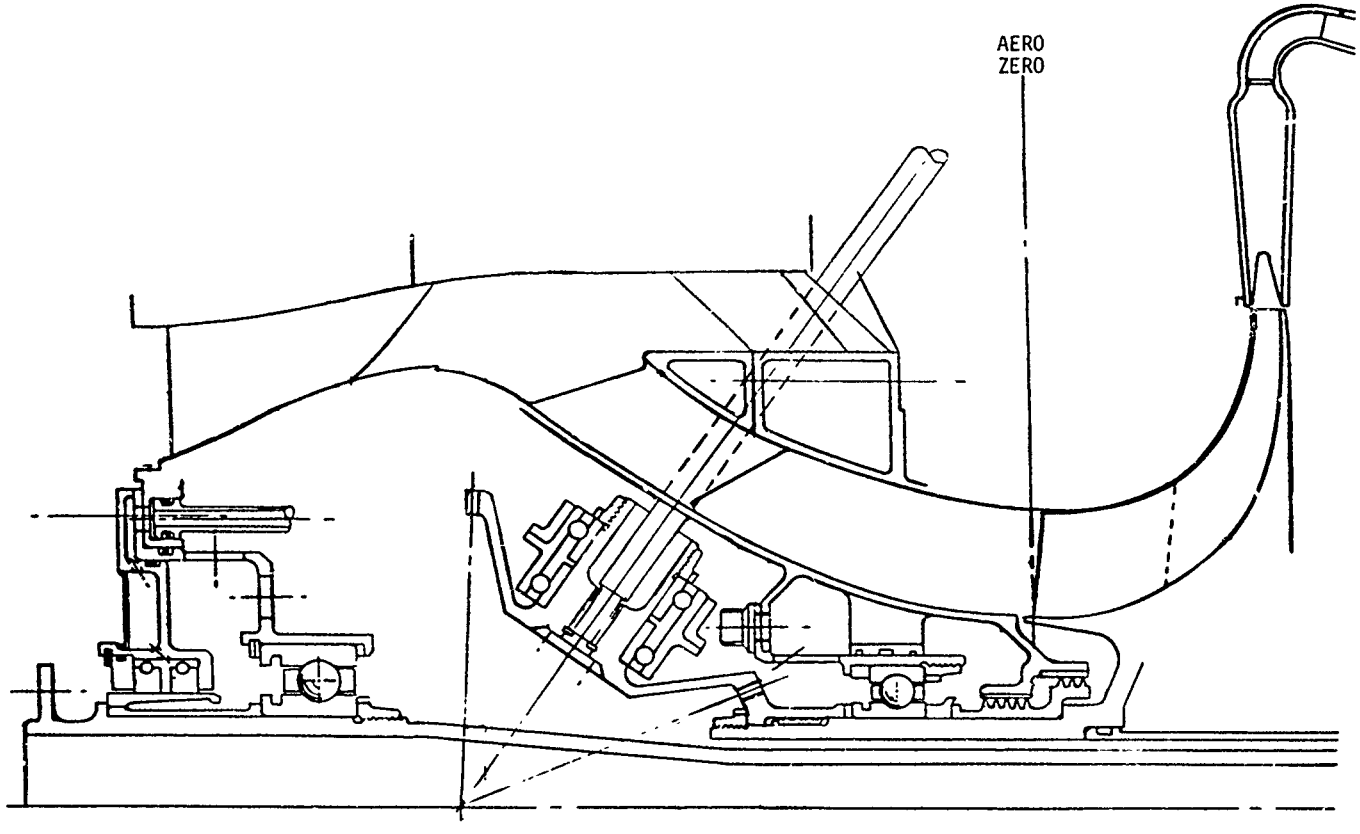

Figure 11. 2 Lb/Sec T700 Type Separator With PTO Shaft Canted Aft.

Aerodynamic Design of 2 lb/sec Axial Separator

Mechanical constraints on the 2 lb/sec separator made scaling of inside diameter and length impossible. T700 Mach numbers and cascade turning were retained, and turning losses were assessed at 5.6 in. H_2O. The impact of size on scrubbing losses was significant since the channel aspect ratio changed substantially as the inner channel wall was forced outward. The average value of the surface area to cross-sectioned area ratio increased by 39% for the 2 lb/sec design. Also, the friction coefficient increased by 15% due to Reynolds number changes. Friction loss therefore was about 154% of the T700 level which was 5.4 in. H_2O. Summation of turning and friction losses gave an estimate of 11.0 in. H_2O for the pressure loss of the 2 lb/sec axial separator. The total pressure loss breakdown can be found in Table 4. In the Phase V tests, a loss of 11.1 in. H_2O was achieved.

TABLE 4. TOTAL PRESSURE LOSS BREAKDOWN - T700 TYPE SEPARATOR

Loss Mechanism	Total Pressure Loss - In. H_2O			
	T700 (1972)	2 lb/sec	5 lb/sec	15 lb/sec
Centerbody Friction	1.3	2.0	1.4	1.2
Splitter Friction	1.0	1.5	1.1	0.9
Swirl Vane Friction	0.4	0.6	0.4	0.4
Deswirl Vane Friction	0.8	1.3	0.8	0.8
Cascade and Turning	5.6	5.6	5.6	5.6
	9.1	11.0	9.3	8.9

2 Lb/Sec Model Features (Figure 12)

The model was made up of four modules. One module is the bellmouth and bullet nose, which are separable and are constructed primarily of fiberglass. The swirl vane cascade and its flow path make up a second discrete unit, which is all aluminum. The vanes are mounted in a manner that allows relatively simple modification of swirl angle within the range of $\pm 10°$. The deswirl vanes are mounted in a similar manner to the swirl vanes, allowing the same flexibility for changes. With the inner and outer flow paths, they form another independent unit. The vanes and outer flow path including the splitter nose are aluminum. As with the swirl and deswirl vanes,

the scroll vanes are attached to the adjacent sections of flow path and comprise another independent unit. The scroll is also detachable and is made of fiberglass. The flexibility of the modular design allowed modification to local contours or overall flow area to be made inexpensively and rapidly during the test phases of the program.

2 Lb/Sec Model Redesign

The flow path for the model tested in Phase V of the program is shown in Figure 13. Forward of the rainstep, the flow path is the same as that of the original 2 lb/sec model. Aft of the rainstep, the splitter lip is hidden behind the inner flow path wall. The Phase II swirl vanes were used for Phase V. Design of the core flow path aft of the rainstep was directed toward achieving small diffusion on the hub and in the deswirl cascade. The core side of the splitter lip was made bellmouth-like to prevent entrance losses. This feature was taken from the 5 lb/sec model design, which had the lowest core total pressure loss, 3.7 in. H_2O, of all models tested with swirl and deswirl vanes removed.

Z FROM AESO "0"	SEPAR HUB R_1
.000	1.475
- 50	1.510
- 1.00	1.620
- 1.50	1.825
- 2.00	2.120
- 2.500	2.480
- 3.00	2.890
- 3.50	3.300
- 3.622	—
- 4.00	3.465
- 4.30	3.480
- 4.30	3.530
- 4.50	3.500
- 5.00	3.395
- 5.50	3.235
- 5.74	—
- 6.00	3.090
- 6.50	3.005
- 7.00	2.970
- 7.375	2.970

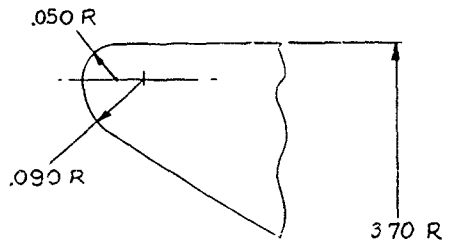

DETAIL "A"
SPLITTER NOSE
10 × SIZE

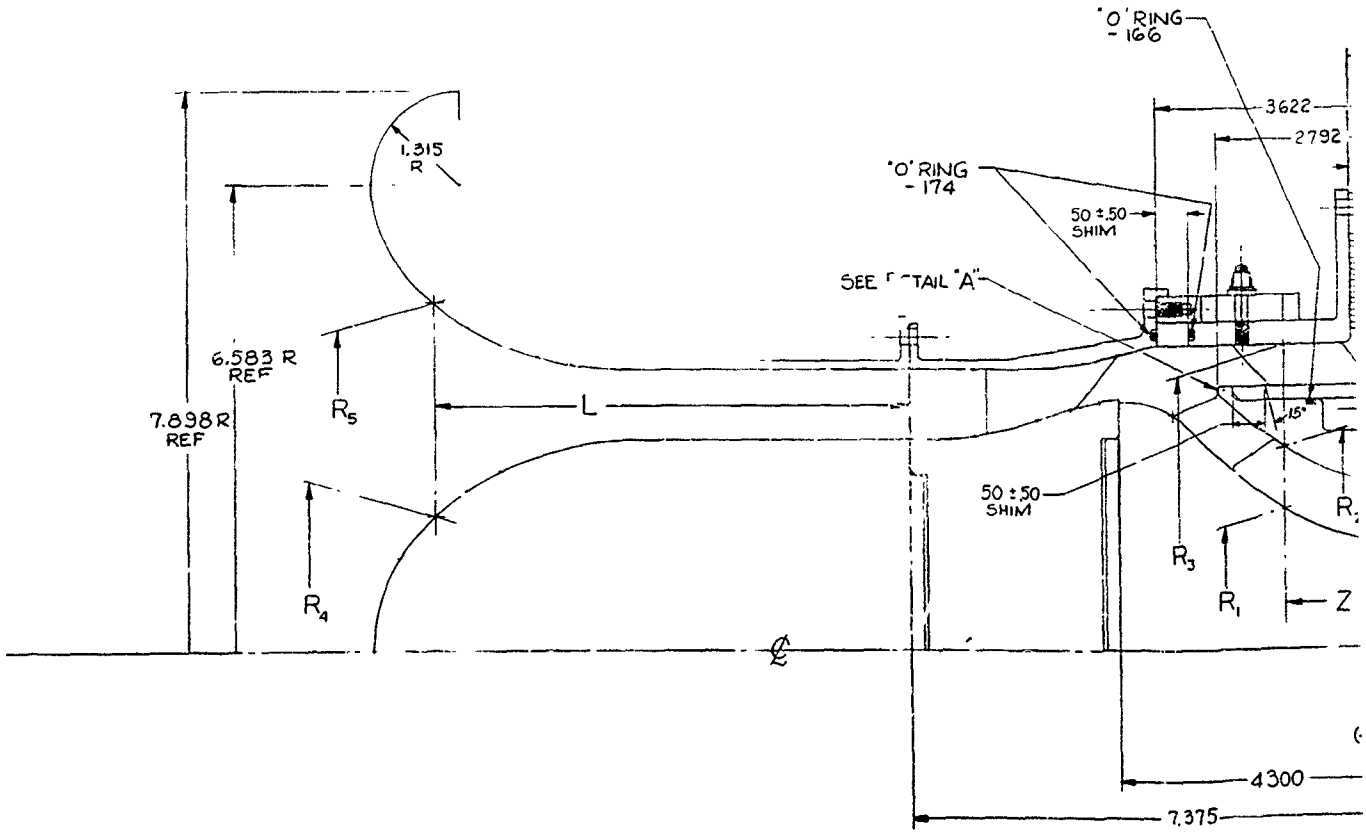

Figure 12. 2 Lb/Sec Inlet Separator Model.

AERO "0"	SEPARATOR FLOWPATH HUB R_1	SPLITTER R_2	OUTER R_3
.000	1.475	2.285	—
.50	1.510	2.335	—
1.00	1.620	2.475	4.285
1.50	1.825	2.695	4.285
2.00	2.120	3.010	4.285
2.500	2.480	3.370	4.285
3.00	2.890	—	4.285
3.50	3.300	—	4.285
3.622	—	—	4.285
4.00	3.465	—	4.225
4.130	3.480	—	4.147
4.330	3.530	—	4.147
4.50	3.500	—	4.095
5.00	3.395	—	4.005
5.50	3.235	—	3.965
5.74	—	—	3.950
6.00	3.090	—	3.950
6.50	3.005	—	3.950
7.00	2.970	—	3.950
7.375	2.970	—	3.950

L FROM SEPARATOR INLET	BULLET NOSE R_4	BELLMOUTH R_5
.00	2.970	3.950
3.95	2.970	3.950
4.50	2.941	3.976
5.00	2.863	4.044
5.50	2.752	4.161
6.00	2.539	4.332
6.50	2.268	4.572
7.00	1.887	4.910
7.50	1.302	5.428
7.90	.000	6.583

COLLECTOR SCROLL ANGULAR LOCATION	B	C
30°	.466	.800
45°	.604	↕
60°	.738	
75°	.880	
90°	1.020	
105°	1.174	↕
120°	1.300	.800
135°	↕	.876
150°		.970
165°		1.060
180°		1.156
195°		1.228
210°		1.314
225°		1.390
240°		1.474
255°		1.556
270°		1.626
285°		1.716
300°		1.790
315°		1.864
330°		1.956
345°	↕	2.032
360°	1.300	2.125

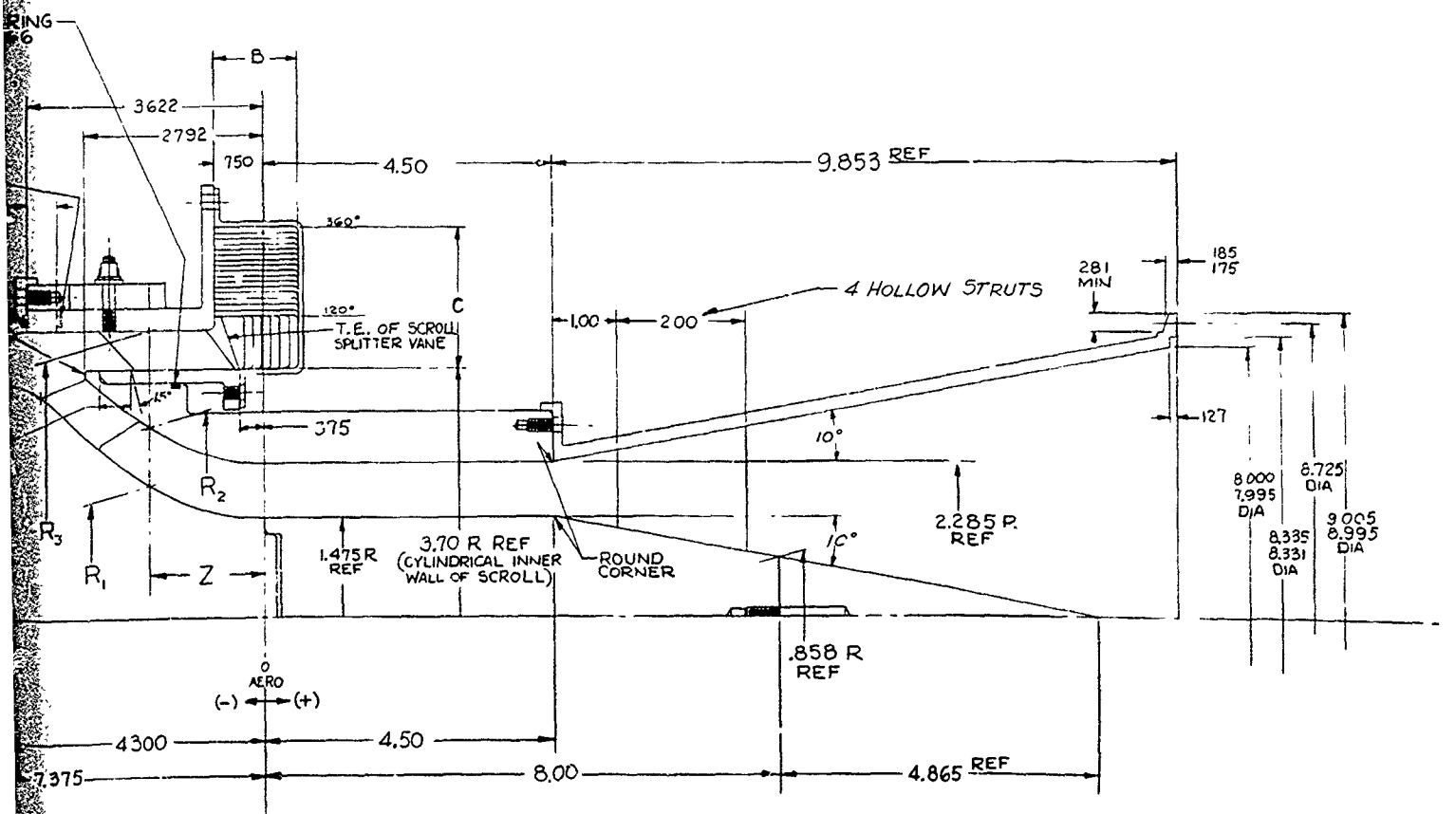

2

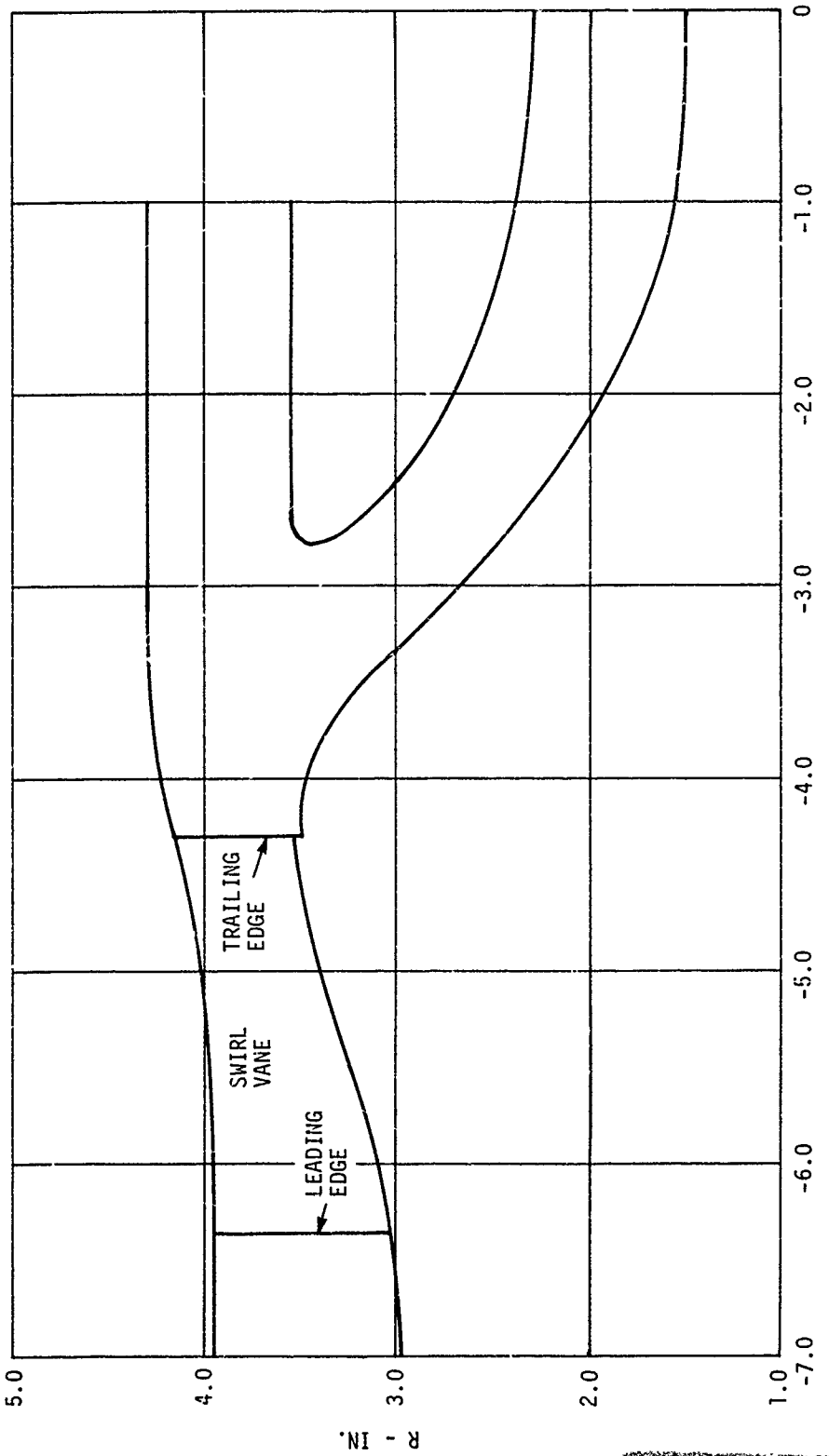

Figure 13. 2 Lb/Sec Model Flow Path With Hidden Splitter Lip.

Figure 14 shows the calculated wall static pressure distribution of the 2 lb/sec model, which is comparable to that of the 5 lb/sec model shown in Figure 15.

Since tests of the 5 lb/sec model indicated that its deswirl vanes performed adequately, the same type of design was used in the 2 lb/sec model.

2 LB/SEC INLET SCROLL SEPARATOR DESIGN

In evaluating separator configurations for the 2 lb/sec turboshaft engine, the small inlet area permitted a number of arrangements that would not be as practical in larger size engines. One result was the inlet scroll separator shown in Figure 4. This separator has approximately the same volume as the T700 type separator for the 2 lb/sec engine but requires an inlet air opening of only 4.36 in. diameter. Although the inlet diameter is small, it is over 50% larger than the diameter of the inlet to the compressor, so the overall pressure drop in the separator is not excessive.

In the scroll design, a plenum chamber is added at the inlet elbow to collect and trap a maximum amount of major-size foreign objects, preventing them from going through the separator and scavenge blower. Scavenge air is taken from this collector and from several locations along the scroll. Scavenge air openings are sized so that only smaller particles like sand can go through the openings. The only exception is the second bleed-off opening, which is at the bottom of the separator. It is large enough to take nuts, bolts, and similar objects if they should get past the collection trap. Cleanout covers to remove trapped objects are located at the inlet elbow (collection trap) and at the second bleed-off opening.

The inlet to a scroll separator is adaptable to a variety of different installations because of the small inlet size. Inlet air can be introduced from any direction by designing the inlet so that it can rotate through 360° or so that it can be removed so that air can be brought in tangentially. An engine design showing tangential introduction of air is shown in Figure 5.

The scroll separator can be used with an integral oil tank, a separate oil tank in the same relative location and space, or a separate oil tank located elsewhere on the engine. Some additional supplemental cooling of the oil and anti-icing of the scroll are obtained from the integral oil tank arrangement. It is necessary, however, to have other means for cooling the oil since there is not enough fuel to do the entire job. Methods investigated include:

1. Wrapping coils of oil around the inlet scroll.

2. Using an oil-to-air heat exchanger.

3. Cooling oil by passing through the scroll struts which are located in front of the compressor.

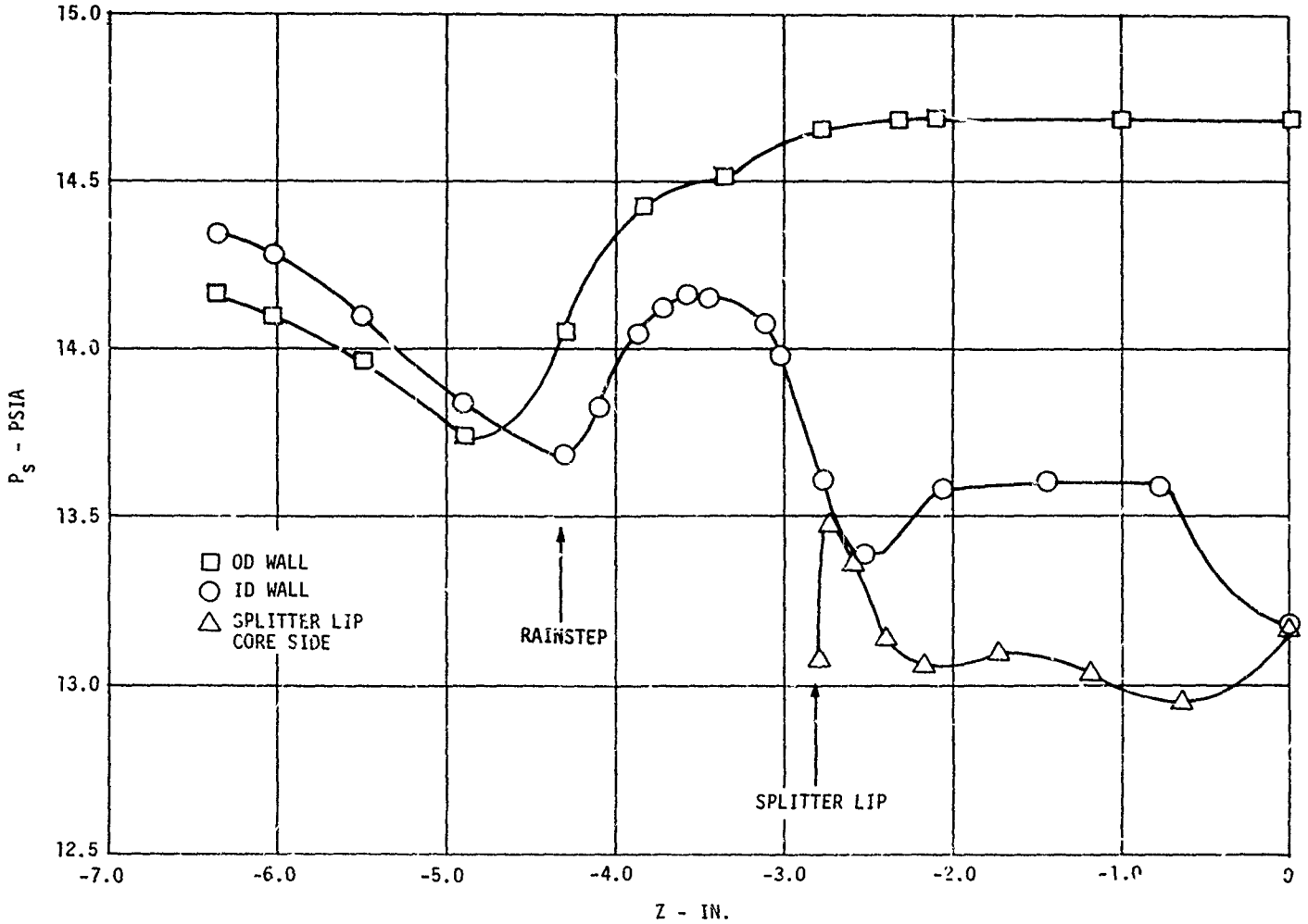

Figure 14. 2 Lb/Sec Model With Hidden Splitter Lip - Predicted Wall Static Pressures.

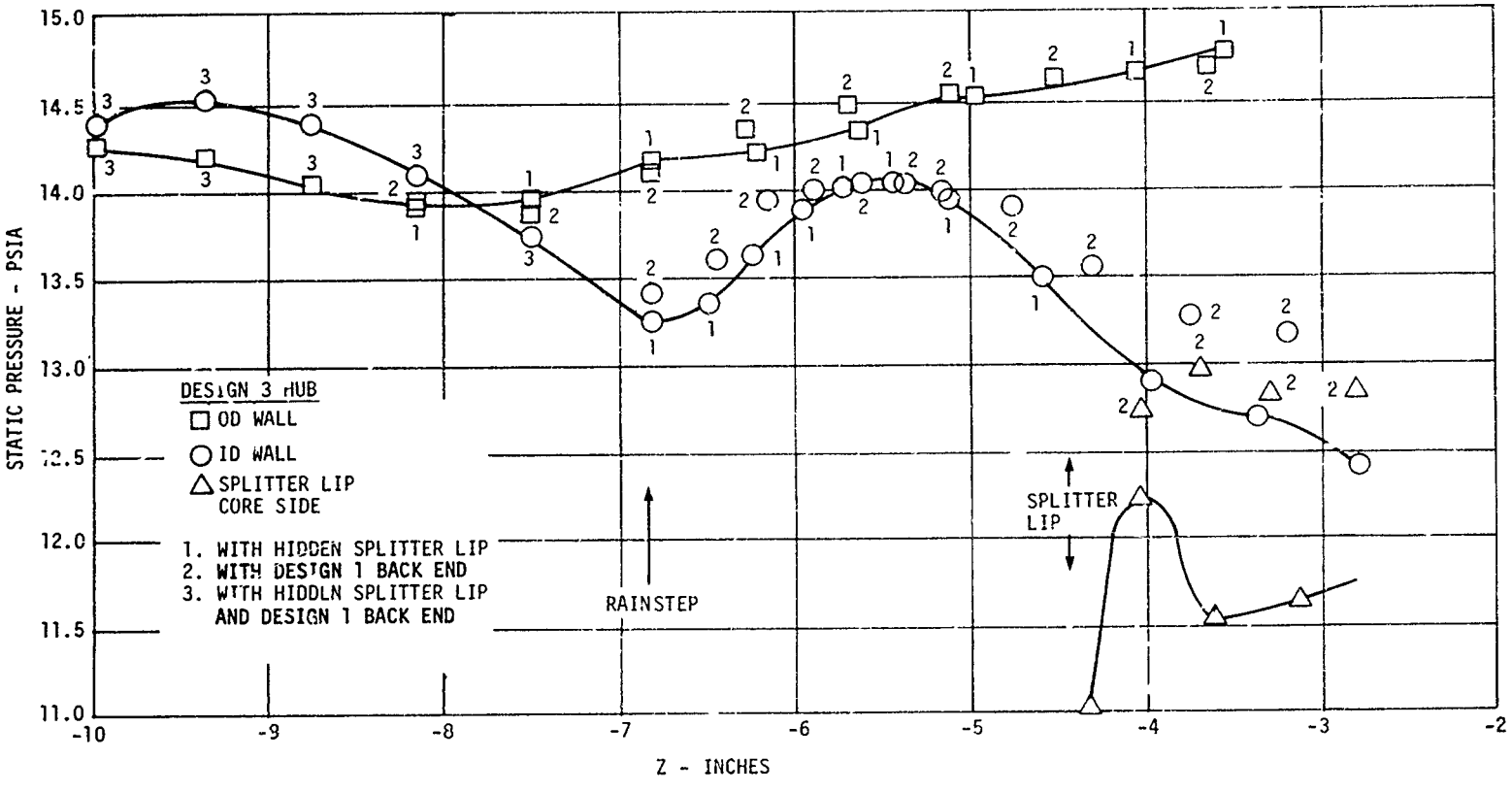

Figure 15. 5 Lb/Sec Model Predicted Wall Static Pressures.

The scroll separator design al o can be adapted to other configurations, such as would result from reversing the locations of the gearbox and oil tank.

Anti-icing is less of a problem with the scroll separator than the T700 types since there are no swirl or scavenge vanes and only one set of struts. It is estimated that proper location of oil tubing plus an integral oil tank will provide sufficient anti-icing capability.

Aerodynamic Losses for Inlet Scroll Separator

A preliminary assessment was made of the total pressure loss through the 2 lb/sec scroll separator. It was found that the design presented in Figures 16 and 17 had a pressure loss of about 13.5 inches of water.

The losses can be assigned to three primary sources:

1. Friction throughout the system.

2. Turning through the inlet to the scroll.

3. Turning through the scroll and into the core.

The latter is both the largest, as shown in Figure 18, and due to a lack of directly applicable data, the most uncertain.

Losses due to both the inlet turn into the scroll and the turning through the scroll and into the core were modeled as offset bends. The bends had R/d ratios which varied from 1.0 to 1.5 and duct Mach numbers which varied from 0.25 to 0.30. Those losses were interpolated from the data presented in Figure 19. Friction losses were based on Prandtl's universal law of friction for smooth pipes as shown in Figure 20. The losses due to turning and friction are shown broken down in Figure 18. It shows that the variation of total pressure loss with percentage design is a compromise between frontal area and pressure loss, since an increase in duct size tends to increase frontal area but decreases duct Mach number and, therefore, losses.

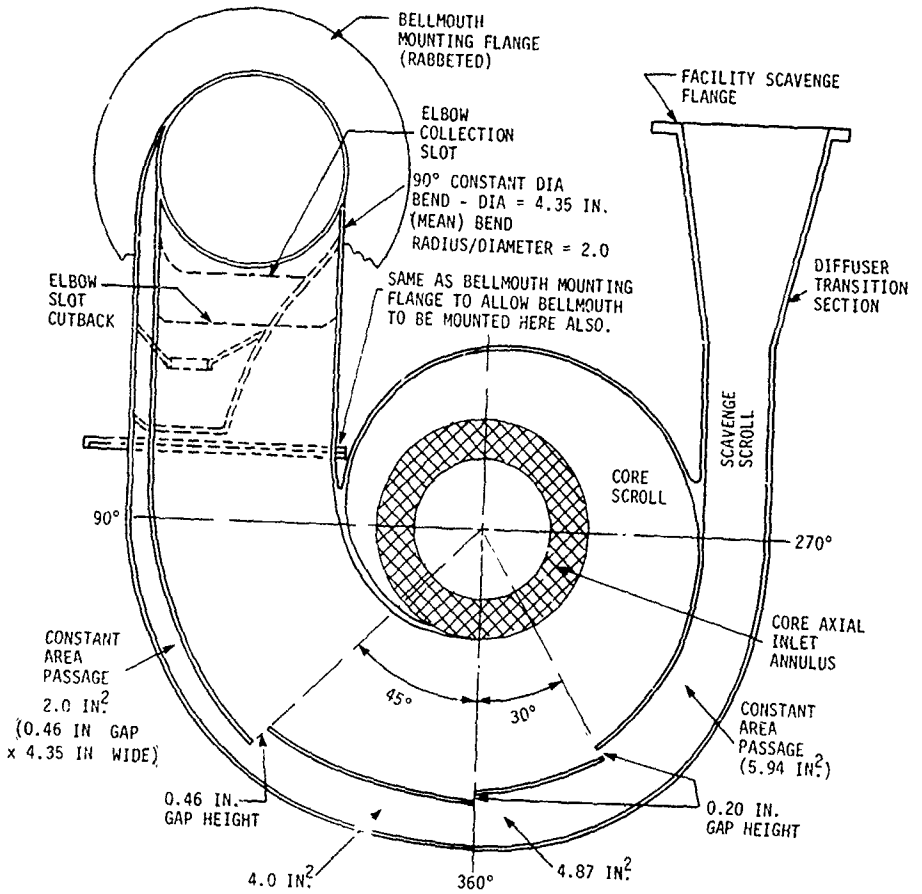

Figure 16. 2 Lb/Sec Scroll Separator Model (Reference Figure 17).

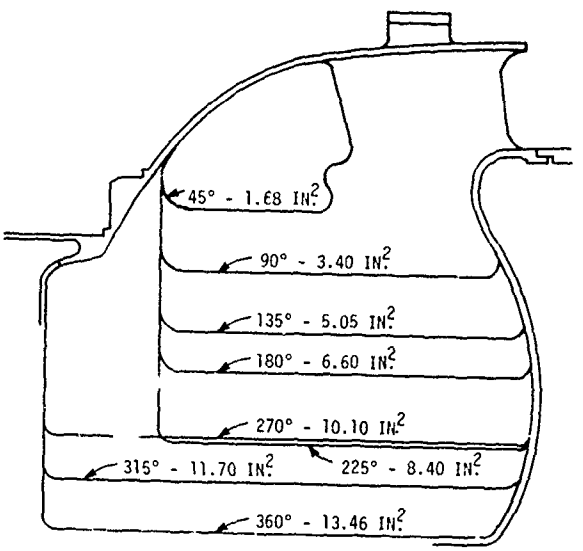

Figure 17. 2 Lb/Sec Scroll Separator Cross Section.

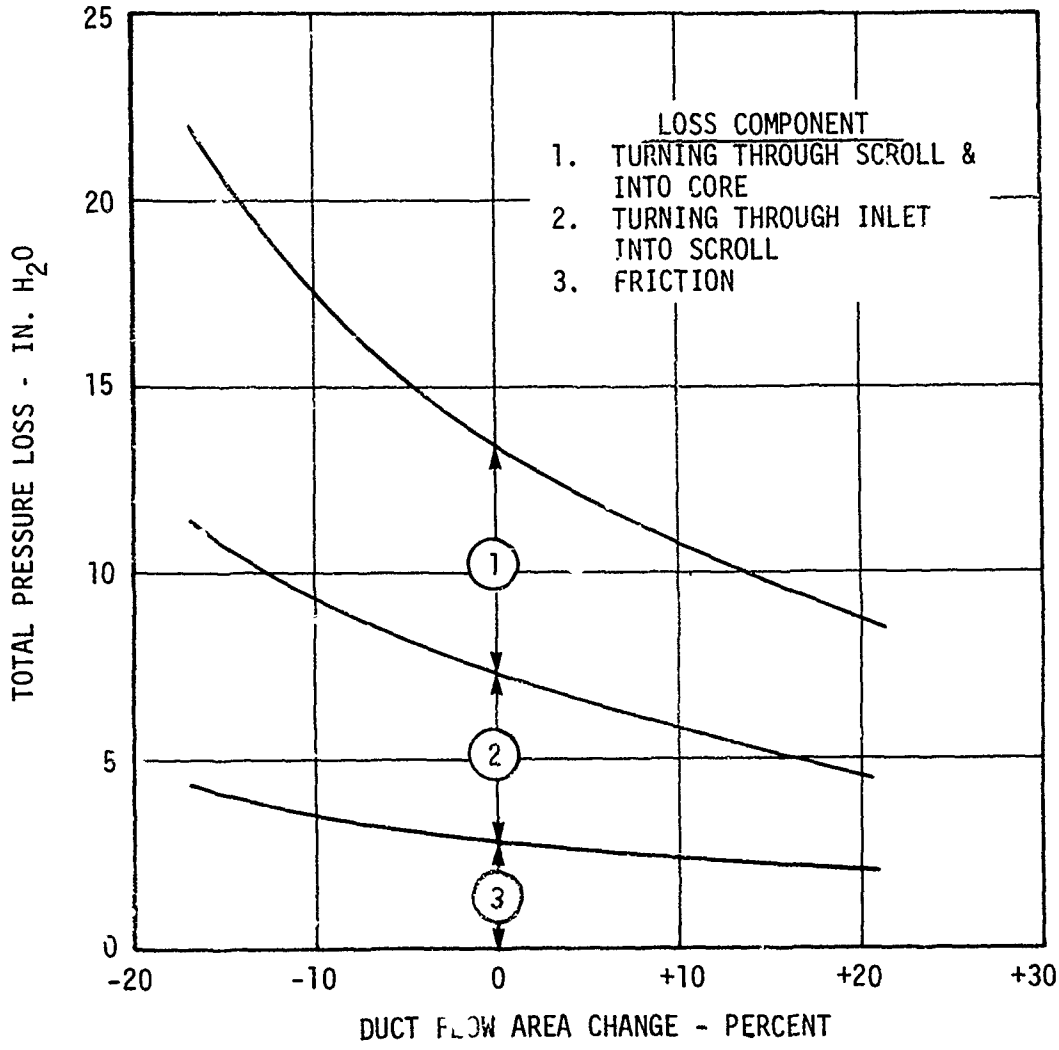

Figure 18 Scroll Separator Pressure Loss Variation With Flow Area.

DATA TAKEN FROM SAE AEROSPACE APPLIED
THERMODYNAMICS MANUAL-SECOND EDITION, PAGE 62

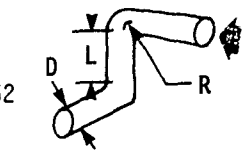

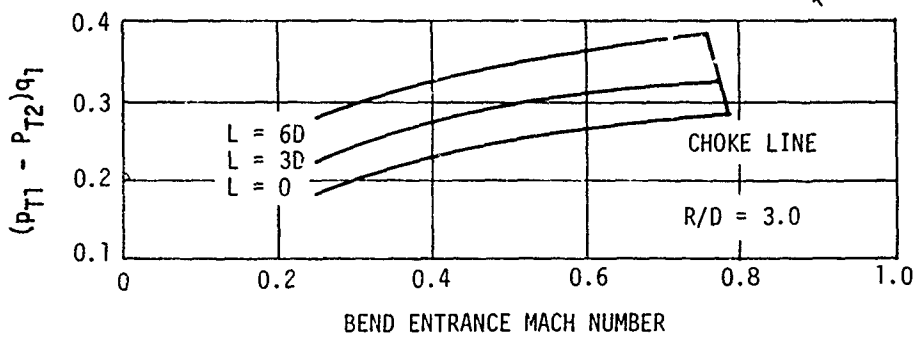

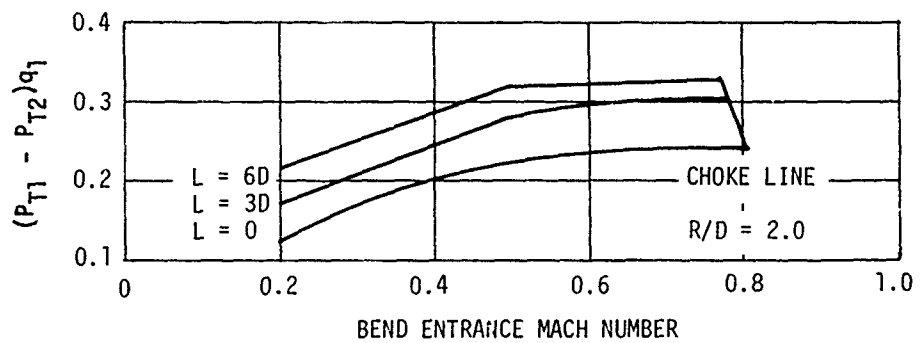

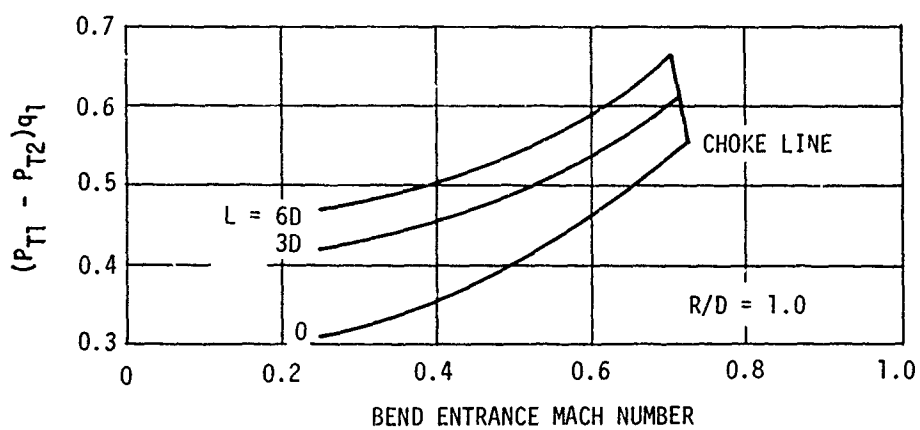

Figure 19. Total Pressure Loss Through Offset Bends.

TAKEN FROM SCHLICHTING, BOUNDARY LAYER THEORY
McGRAW-HILL BOOK COMPANY, 1968, PAGE 562

$\Delta P/q = \lambda\ L/d$

PRANDTL's UNIVERSAL LAW OF FRICTION FOR SMOOTH PIPES
$1/\sqrt{\lambda} = 2.0\ \text{LOG}\ (\text{RED}\ \sqrt{\lambda}) - 0.8$

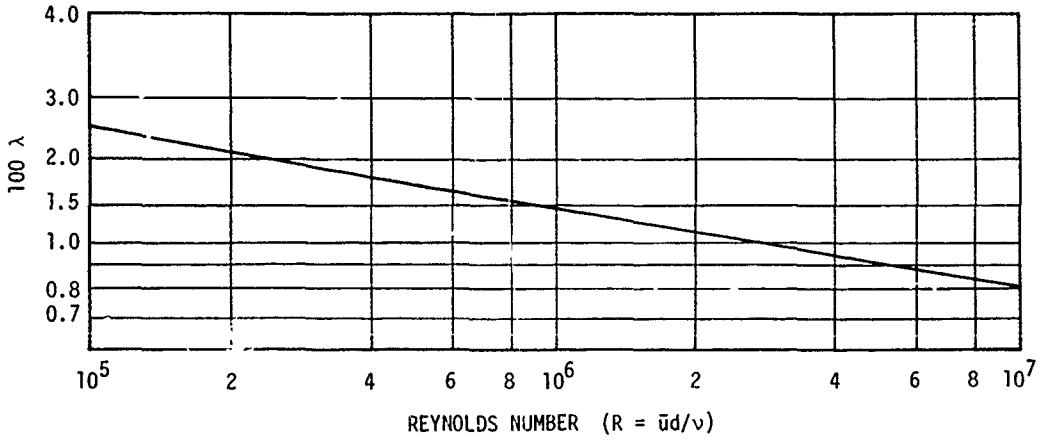

Figure 20. Frictional Resistance In a Smooth Pipe.

5 LB/SEC SEPARATOR DESIGN

Mechanical Design

The 5 lb/sec integral separator is almost a direct scale-down of the T700 separator. The flow path, however, incorporates these changes:

1. The splitter lip is hidden behind the inner flow path wall.

2. The scavenge air vanes are increased to approximately 80% scale of T700 separator to obtain sufficient internal area for porting oil and structural strength. This reduces tne number of scavenge vanes from 15 to 14.

3. There is a slight increase in size of PTO strut over the directly scaled strut.

Other changes to the 5 lb/sec engine are:

1. Increase in size of gearbox and accessories to a larger size than direct scale.

2. Increase in volume of oil tank required to store oil to a larger capacity than direct scale.

3. Increase in amount of supplemental cooling required from air due to the relatively higher percentage of oil flow required for a 5 lb/sec over a T700 engine.

The flow path for the model is shown in Figure 21. Because of the large beneficial effect found in the 2 lb/sec vaneless model when it was tested with a "hidden" splitter lip, the hidden splitter lip was also incorporated into the 5 lb/sec model. The vaneless flow path forward of the rainstep is called the "design 3" flow path. The design of the core flow path aft of the rainstep was directed toward prevention of large adverse wall static pressure gradients. Figure 15 shows that the pressure gradients are reasonable and that they should not cause large total pressure losses. As a comparison, Figure 22 shows the pressure distribution calculated for the 2 lb/sec model with hidden splitter lip. That configuration was tested only to evaluate its effect on separation efficiencies. The large adverse pressure gradient on the hub wall aft of the rainstep (indicated by Figure 22) is the probable reason for an 11.2 in. H_2O core total pressure loss. The large gradient caused by hiding the splitter lip on the 2 lb/sec model was eliminated on the 5 PPS model, and relatively low loss resulted.

The swirl vane for the 5 lb/sec model is shown in Figure 23 as design 3A. It is the same design 3, tested during Phase II in the 15 lb/sec model, except that its thickness was reduced in an effort to produce a beneficial effect on swirl frame loss.

The scroll separator design was considered for this size of engine, and several design studies were initiated. The studies were stopped, however, when they indicated that the frontal area and separator size would be larger for this design than for a scaled T700 separator.

Aerodynamic Design

For the 5 lb/sec design, which is almost a direct scale of the T700, the ratio of scrubbed area to flow area is virtually unchanged from the T700 value. Therefore, the only first-order factor which causes the loss to be different from the T700 is the friction coefficient, which is inversely proportional to Reynolds number raised to the 0.2 power. On this basis the 5 lb/sec separator has 3.7 in. H_2O friction loss. Summation of turning and friction losses yields the overall inlet pressure loss, which is 9.3 in. H_2O. This compares with the 9.1 in. H_2O loss for the T700 separator. Second-order effects of size have been left out of this estimate since they are sufficiently small that their impact will be indistinguishable from model construction and surface finish effects. The breakdown of losses can be found in Table 4. During the Phase V tests, a core loss of 8.3 in. H_2O was achieved.

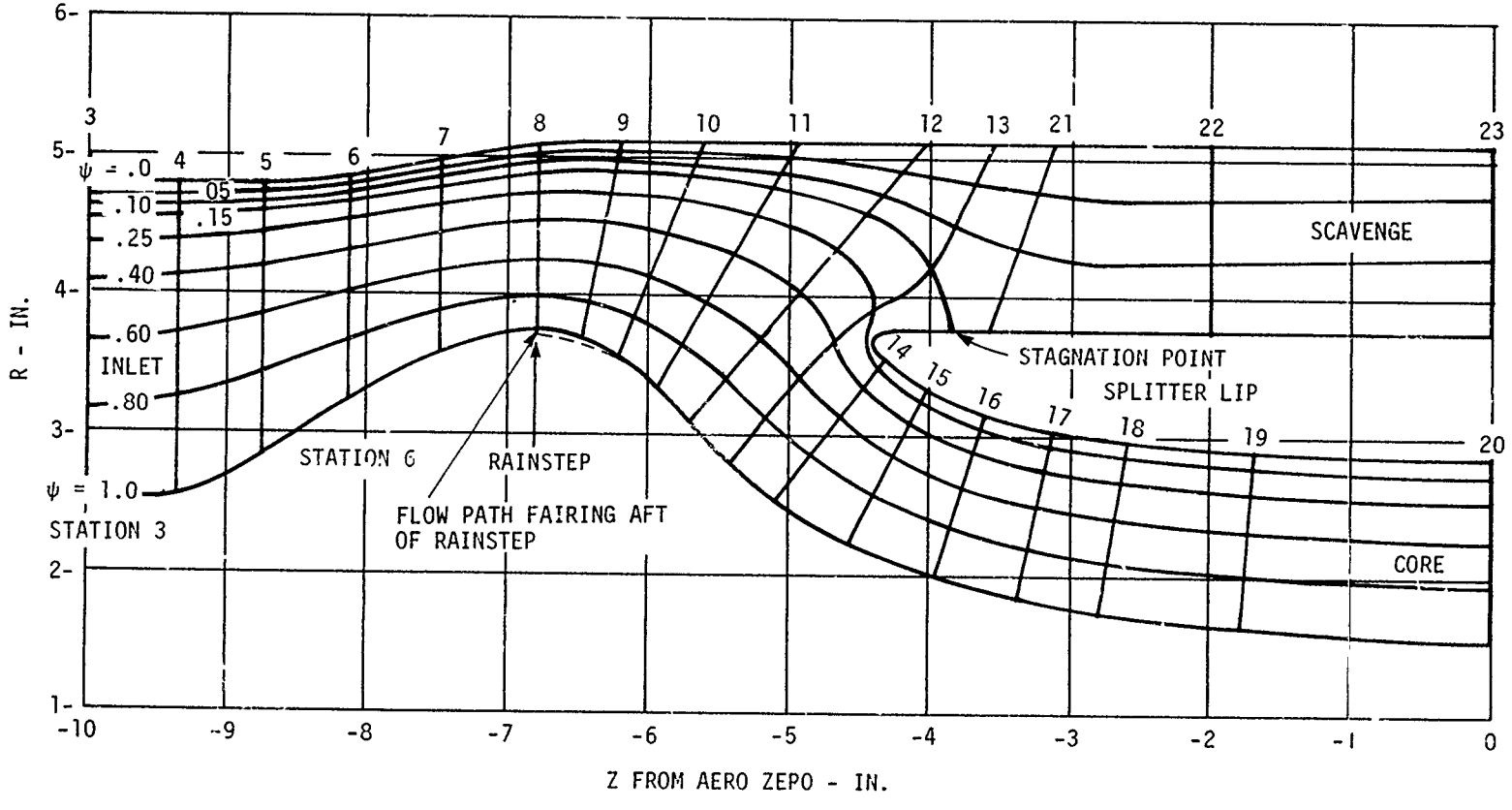

Figure 21. Aero Analysis of 5 Lb/Sec Flow Path, Showing Stations.

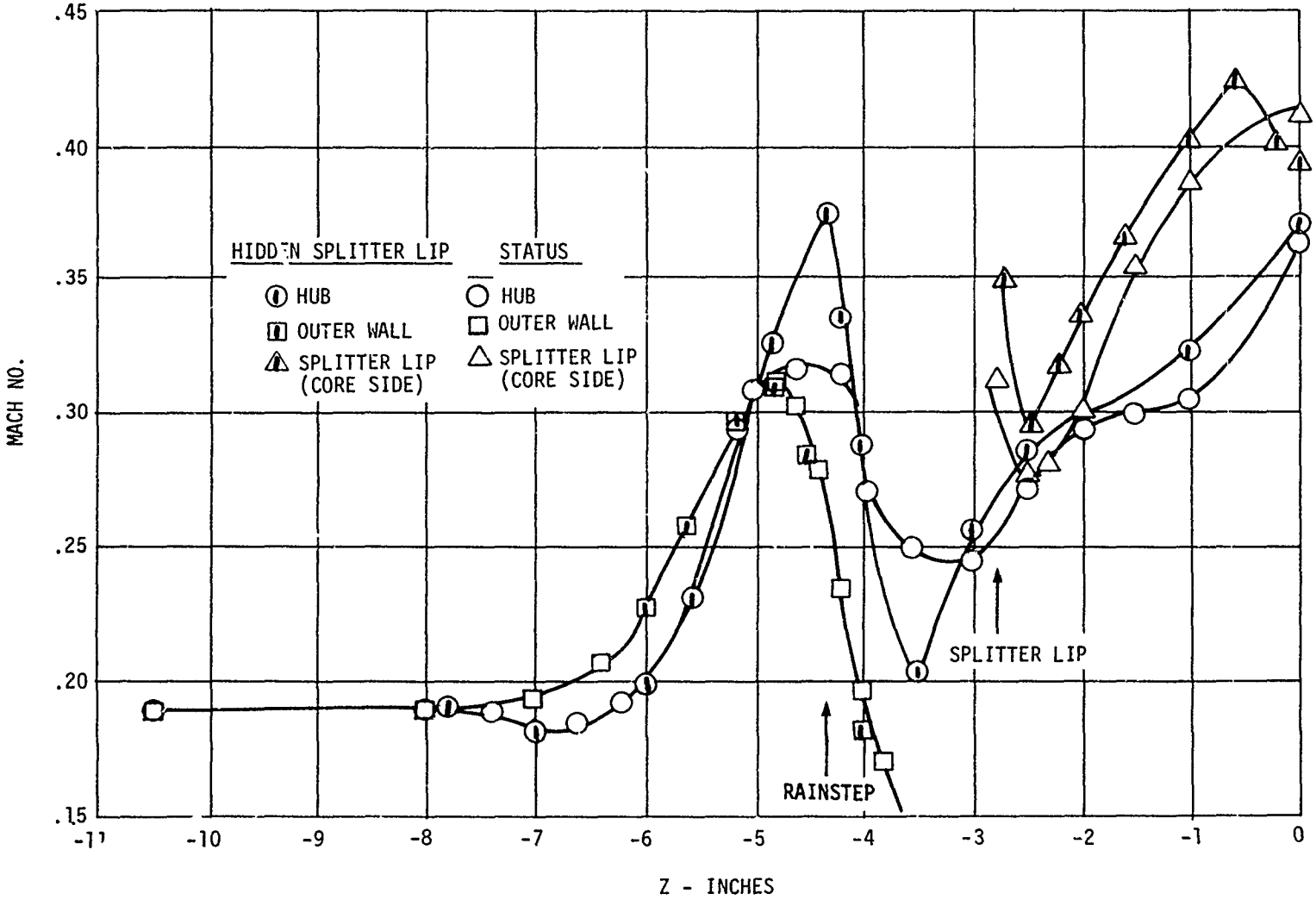

Figure 22. 2 Lb/Sec Separator Predicted Wall Mach Number.

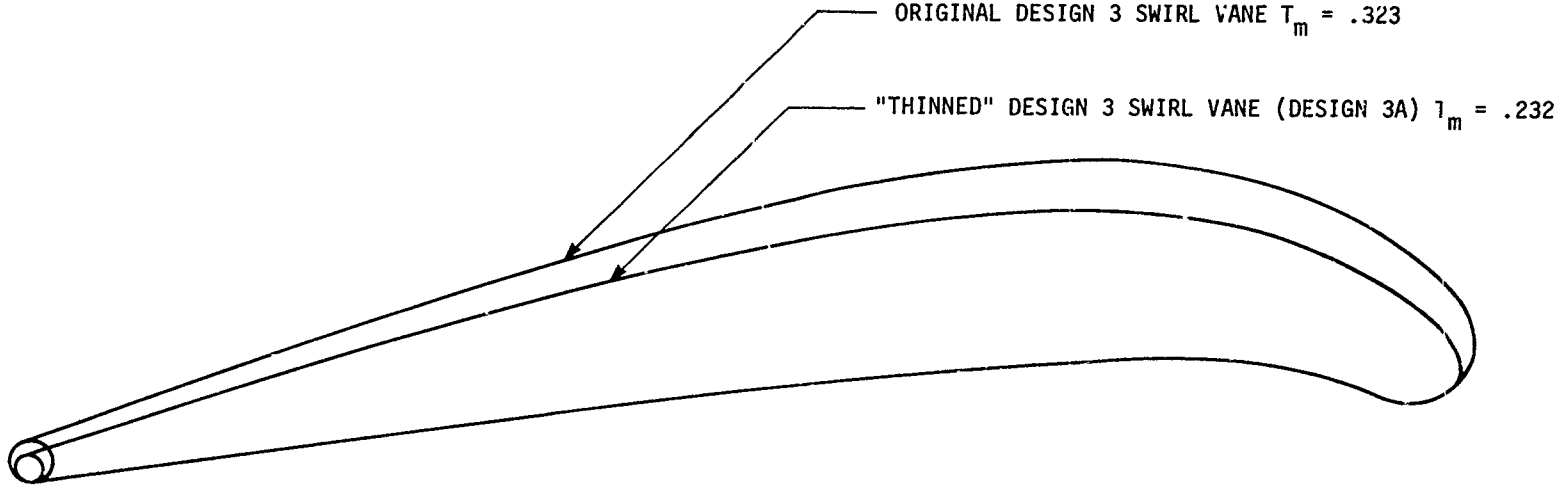

Figure 23. 5 Lb/Sec Thinned Design 3 Vane.

15 LB/SEC SEPARATOR DESIGN

Mechanical Design

The first design studies on the scaled T700 separator were made for the 15 lb/sec engine because the larger separator was most directly scalable. The initial studies included a scaling up of flow path dimensions, with the only change being to move the scroll scavenge vanes forward to maintain the same spacing to the splitter lip as for the T700 separator. The T700 engine was then photographically enlarged, and the engine separator flow path was compared with the flow path obtained by actually drawing the T700 flow path to the scaled-up dimension. Comparison of the flow paths was excellent, and the conclusion was reached that the 15 lb/sec separator design could be scaled directly from the T700 separator. The only changes to the flow path of the separator were:

1. Scavenge air vanes were moved forward to maintain the same distance from the inner leading edge of the vanes to the leading edge of the splitter lip as for the T700 design.

2. Bumping of the flow path in the compressor inlet duct for the PTO bearing is necessary in the T700, but it is not necessary for the 15 lb/sec engine.

Other minor changes are:

1. Oil tank volume and oil flow can be reduced below that indicated by a direct scale-up from the T700.

2. Accessories and AGB can be reduced below that indicated by a direct scale-up from the T700.

The scroll separator design was not evaluated for this size engine because its overall size was estimated to be excessive in comparison to a scaled T700 separator design.

Aerodynamic Design

For the 15 lb/sec design, which scaled directly from the T700, the ratio of scrubbed area to flow area is unchanged from the T700 value. Therefore, the only first-order factor which causes the loss to be different from the T700 is the friction coefficient, which is inversely proportional to Reynolds number raised to the 0.2 power. Summation of turning and friction losses yields the overall inlet pressure loss of 8.9 in. H_2O. This compares with the 9.1 in. H_2O loss for the T700 separator. Second-order effects of size have been left out of this estimate since they are expected to be sufficiently small that their impact will be indistinguishable from model construction and surface finish effects. The breakdown of losses can be found in Table 4. During Phase V tests, a core loss of 8.6 in. H_2O was achieved.

15 Lb/Sec Model Features (Figure 24)

The basic construction was modular with the same number of units and flexibility of assembly as the 2 lb/sec model. Because of the increased size, the 15 lb/sec model had more extensive use of fiberglass and less aluminum, but all vanes and the splitter lip were aluminum. The fiberglass used in sand bearing areas of bellmouth, bulletnose, and scroll cover was hard-coated to reduce erosion. The coating used was a carbide-filled epoxy.

Design 3 Swirl System for the 15 Lb/Sec Separator

Based on the test results and analysis of Phases II and III, the swirl system for the Phase V 15 lb/sec model was redesigned.

Features of the redesigned swirl system, called design 3, are:

1. Increased swirl vane pressure side slope near the vane leading edge. Figure 25 shows the pressure side slope, defined as the angle between the pressure side surface and the engine centerline, of four different swirl vane designs. The T700 design 1 had 1.5% better C-Spec efficiency and 3.5% better AC Coarse efficiency than the T700 design 2 vane at the same swirl levels. This led to the design 3 vane, also shown in Figure 23.

2. Improved solidity camber and angle of attack selection. The T700 design 2 separator has about 1 in. H_2O less loss than the T700 design 1 separator at the same swirl angle, and the T700 design 1 swirl vane has the highest ratio of deviation angle to camber angle of any of the swirl systems tested. Aerodynamic differences between these two cascades are:

   a. T700 design 1 has a much lower solidity than the T700 design 2. The T700 design 1 12-vane cascade has the lowest solidity tested.

   b. T700 design 1 has a -12° angle of attack versus 0° to +5° for the T700 design 2.

   c. T700 design 1 has the highest camber angle of any cascade tested.

   For a swirl angle at the rainstep of 36°, the design 3 solidity was chosen as 2.10 at the I.D., varying to 1.30 at the OD. Camber angle was chosen as a constant 38.2° compared with camber angles as high as 64° for the T700 and 53° for the 15 lb/sec Phase II swirl systems. Angle of attack for the design 3 vane was chosen as +4° at the 36° swirl level setting.

INLET HUB FLOWPATH	
Z FROM AERO "0"	R_1
- .000	2.669
- .078	2.669
- 1.759	2.685
- 1.985	2.704
- 2.204	2.728
- 2.400	2.753
- 2.719	2.811
- 3.284	2.916
- 3.769	3.017
- 4.294	3.144
- 4.799	3.283
- 5.305	3.433
- 5.810	3.592
- 6.062	3.675
- 6.315	3.759
- 7.013	4.031
- 7.325	4.130
- 7.578	4.222
- 7.831	4.325
- 8.083	4.438
- 8.336	4.560
- 8.588	4.711
- 8.841	4.875
- 9.094	5.036
- 9.346	5.248
- 9.599	5.441
- 9.851	5.632
- 10.104	5.813
- 10.420	6.018
- 10.736	6.185
- 11.051	6.317
- 11.367	6.407
- 11.683	6.481
- 11.784	6.494
- 11.784	6.517
- 11.998	6.503
- 12.569	6.410
- 13.201	6.264
- 13.832	6.069
- 14.464	5.854
- 15.095	5.582
- 15.727	5.270
- 16.358	4.945
- 16.990	4.646
- 17.621	4.435
- 17.930	4.414

INLET SPLITTER FLOWPATH	
Z FROM AERO "0"	R_2
- .086	4.955
- .202	4.955
- .330	4.975
- .436	4.996
- .678	5.051
- 1.320	5.106
- 1.759	5.161
- 2.204	5.216
- 2.450	5.245
- 2.690	5.276
- 3.536	5.403
- 3.769	5.451
- 4.105	5.513
- 4.421	5.579
- 4.736	5.646
- 5.052	5.721
- 5.357	5.805
- 5.684	5.884
- 5.999	5.979
- 6.315	6.086
- 6.587	6.184
- 7.044	6.346
- 7.272	6.488
- 7.452	6.624
- 7.574	6.740
- 7.694	6.934

INLET OUTER FLOWPATH	
Z FROM AERO "0"	R_3
- .000	—
- 9.796	9.220
- 9.922	9.220
- 10.179	9.206
- 10.427	9.169
- 10.680	9.107
- 10.933	9.054
- 11.185	8.986
- 11.436	8.929
- 11.690	8.846
- 11.784	8.840
- 11.938	8.806
- 12.569	8.664
- 13.201	8.549
- 13.832	8.451
- 14.464	8.367
- 15.095	8.321
- 15.727	8.304
- 16.358	8.304
- 16.990	8.304
- 17.621	8.304
- 17.930	8.304

	BULLET NOSE	BELLMOUTH
L FROM SEPARATOR INLET	R_4	R_5
.000	4.414	8.304
8.304	4.414	8.304
9.00	4.396	8.323
9.50	4.368	8.362
10.00	4.321	8.421
10.50	4.257	8.501
11.00	4.175	8.604
11.50	4.074	8.730
12.00	3.955	8.883
12.50	3.809	9.063
13.00	3.640	9.274
13.50	3.443	9.522
14.00	3.212	9.812
14.50	2.939	10.154
15.00	2.611	10.566
15.50	2.203	11.077
16.00	1.658	11.761
16.50	.709	12.950
16.608	.000	13.840

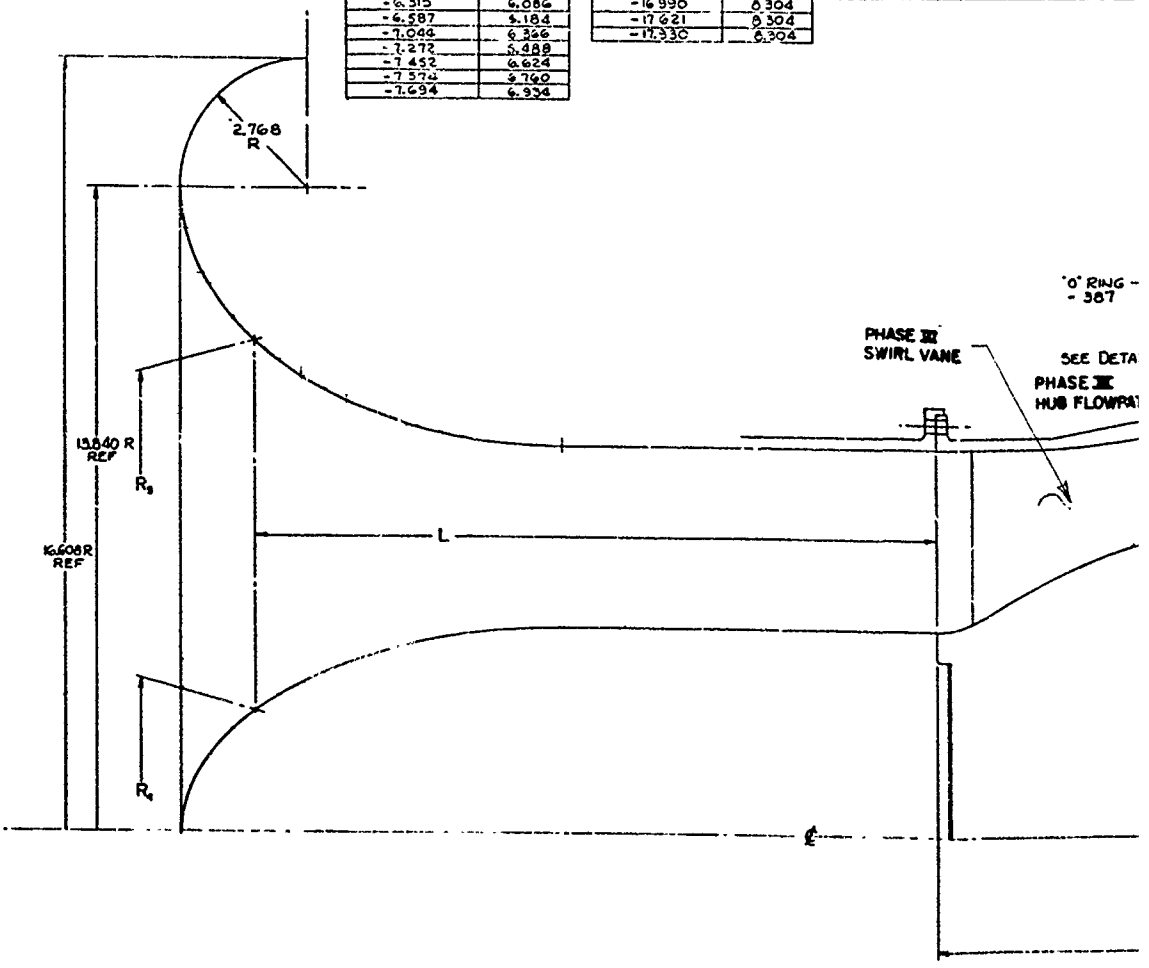

Figure 24. 15 Lb/Sec Separator Model.

BELLMOUTH	
	R_3
	8.304
	8.304
	8.323
	8.362
	8.421
	8.501
	8.604
	8.730
	8.883
	9.065
	9.274
	9.522
	9.812
	10.154
	10.566
	11.077
	11.761
	12.950
	13.840

COLLECTOR SCROLL		
ANGULAR LOCATION	B	C
30°	1.360	2.400
45°	1.720	"
60°	2.040	
75°	2.410	
90°	2.720	
105°	3.120	"
120°	3.450	2.400
135°	"	2.934
150°		3.540
165°		3.107
180°		3.375
195°		3.769
210°		4.005
225°		4.051
240°		4.270
255°		4.504
270°		4.738
285°		4.972
300°		5.209
315°		5.439
330°		5.673
345°		5.907
360°	3.450	6.140

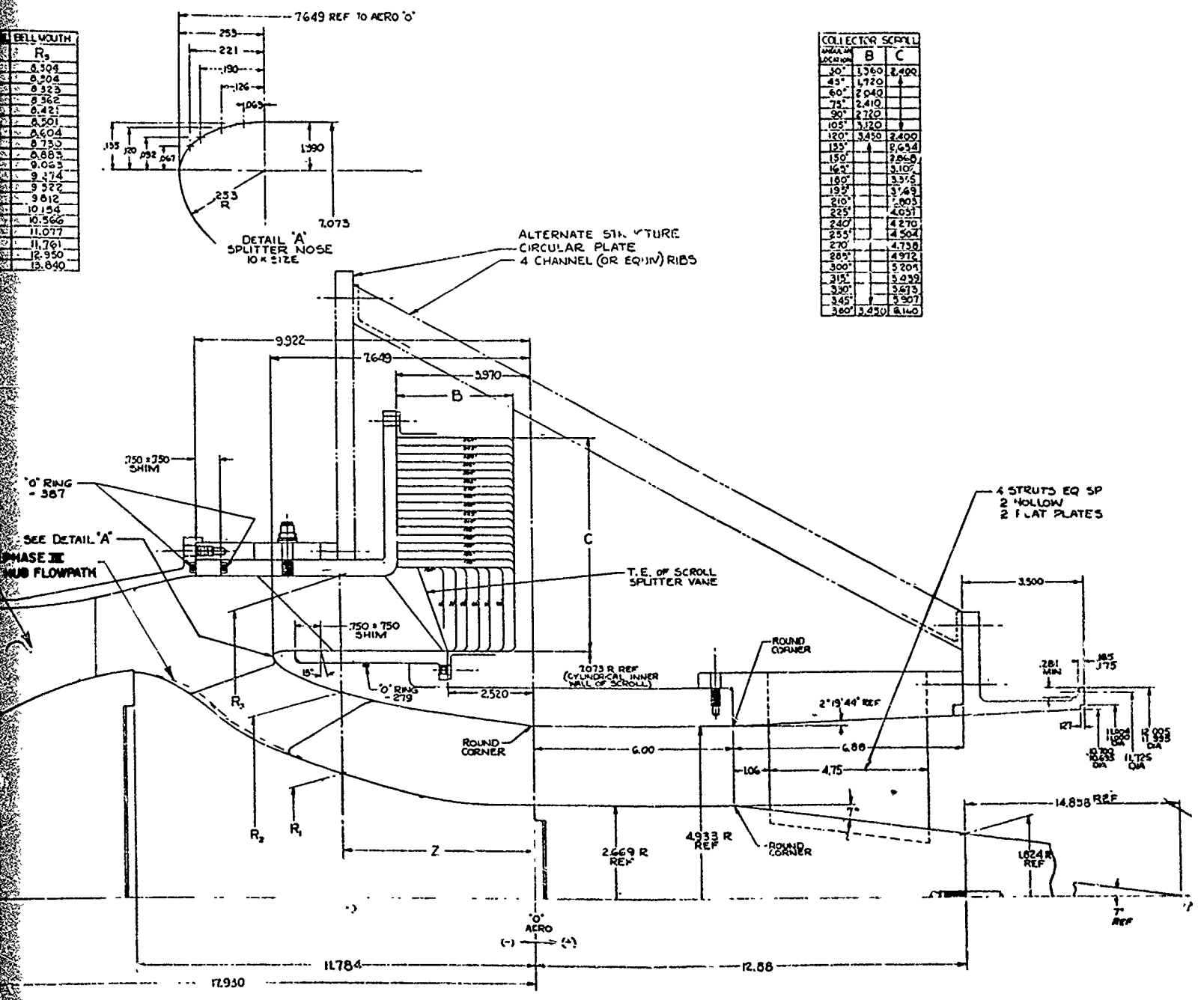

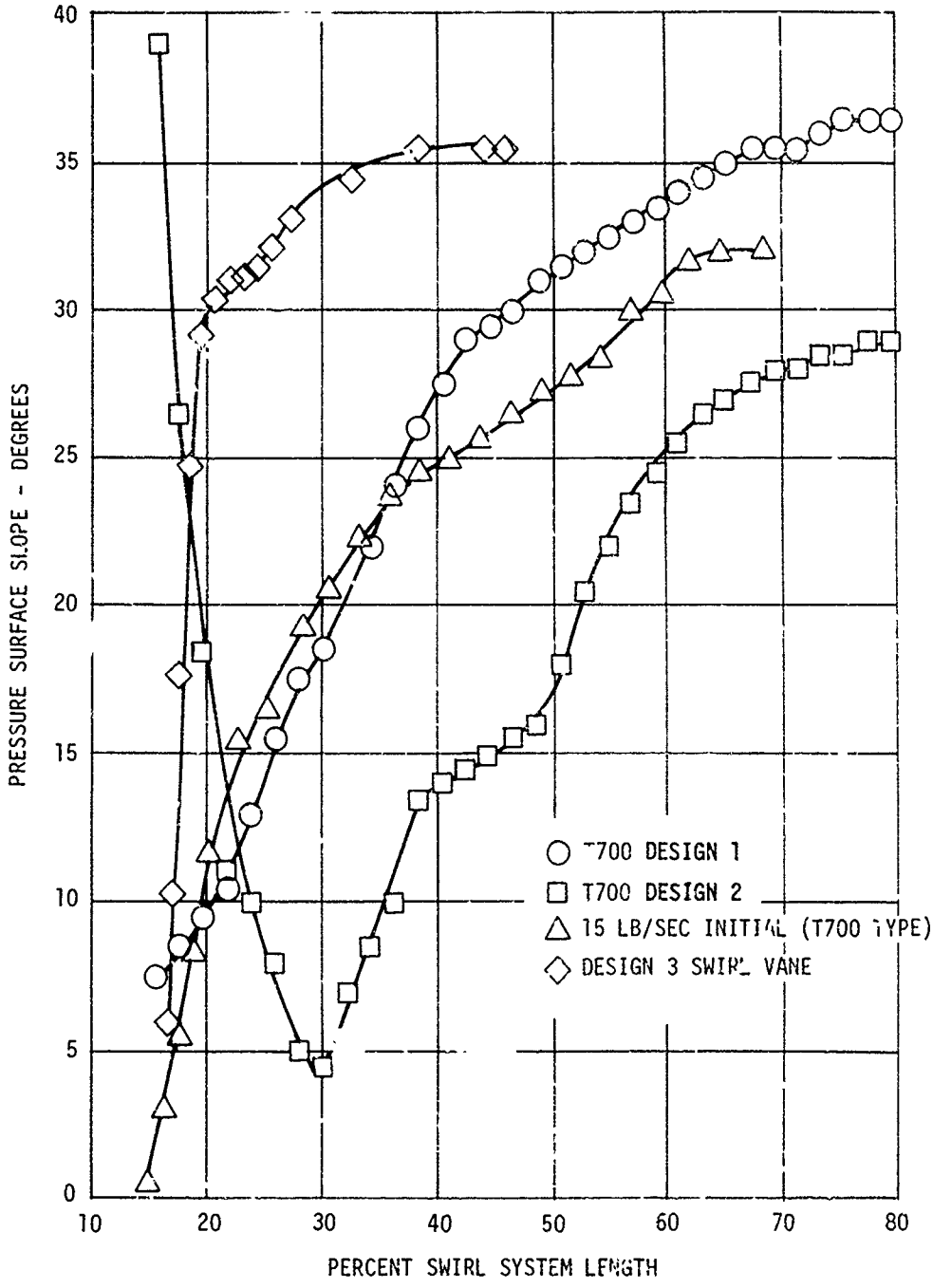

Figure 25. Vane Pressure-Side Slope.

3. Reduced vane chord and area ruled flow path. Pressure drop was reduced 2.6 in. H_2O in the 15 lb/sec model when 12 swirl vanes were removed from the 24-vane cascade. A similar result occurred in the T700 separator, although a swirl level reduction accompanied the swirl cascade solidity reduction. This pressure loss decrease is not explained by a reduction in swirl vane skin friction alone. To identify the reason for loss reduction, an analysis was made of the loss due to diffusion and mixing of the swirl vane wakes between the swirl vanes and the deswirl vanes. The result of the analysis for the T700 separator is that a difference of 1.8 in. H_2O results from this diffusion/mixing process. The 1.8 in. H_2O reduction plus the 0.5 in. H_2O reduction in basic cascade loss gives a computed 2.3 in. H_2O pressure drop reduction, versus a measured 2.9 in. H_2O reduction. Based on this analysis, swirl vane axial length was made 62% of the T700 design 1 vane length, and the flow area aft of the vane was designed with less diffusion than the T700 design 1 vane. The increased axial distance between the design 3 vane trailing edge and the rainstep provided better mixing of the vane wakes prior to diffusion aft of the rainstep.

The design 3 flow path shape is shown in Figure 26. The effects of vane blockage and turning angle were considered in the flow path design, which was chosen to give a constant or accelerating area through the cascade. As shown in Figure 26, a constant area flow path would give too large a local slope at the rainstep, probably causing excessive separation aft of the rainstep. For this reason, the compromise flow path was chosen to lower the rainstep slope and give an area diffusion of 4.8% just ahead of the rainstep. No change was made to the outer wall of the flow path. Capability existed in the 15 lb/sec model to shift the outer wall axially if necessary to improve separation efficiency.

Table 5 lists the geometric parameters of the T700 design 1 swirl cascade, which is the cascade that was extrapolated for the 15 lb/sec Phase II model. Table 6 lists the same parameters for design 3. The table shows that the design 3 vane has constant camber, chord, stagger, and thickness, thus making it a practical vane shape that can be easily controlled in manufacturing. The design 3 maximum thickness was chosen to allow the vane to be cast if desired.

Prediction of separator performance for design 3 was based largely on Phase II performance of the 15 lb/sec model. Pressure loss was expected to be reduced somewhat from that of the original Phase II configuration because of similarity to the T700 design 2, which achieved the lowest losses in the T700 size.

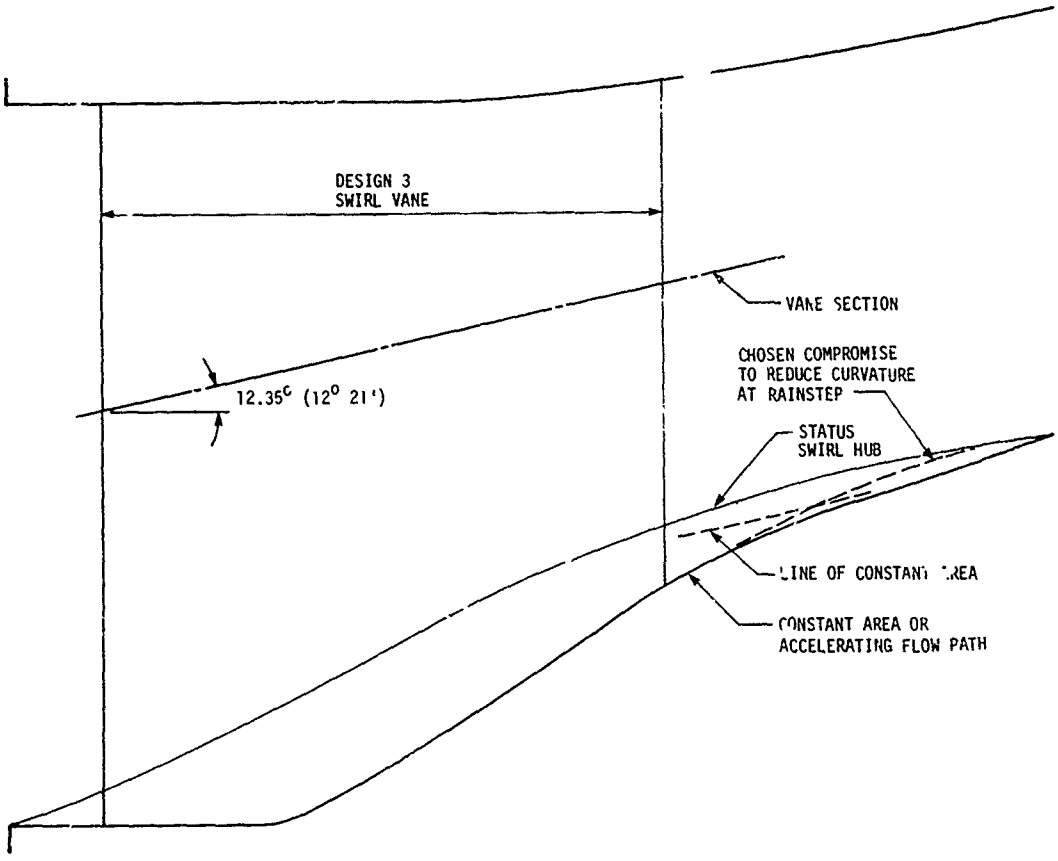

Figure 26. Design 3 Separator Swirl System.

TABLE 5. T700 SWIRL VANES - CASCADE SECTION PROPERTIES

	Section Radius (in.)							
Parameter	3.5	4.0	4.5	5.0	5.5	6.0	6.5	7.0
Chord - in.	1.807	2.352	2.856	3.274	3.644	3.966	4.237	4.511
Stagger Angle - deg min	36°02'	33°02'	30°50'	28°27'	26°53'	25°21'	24°09'	23°13'
Thickness (max) - in.	.206	.220	.250	.277	.298	.315	.317	.318
Leading Edge - in.	.103	.105	1.06	.106	.107	.107	.108	.109
Trailing Edge - in.	.045	.050	.048	.048	.047	.047	.046	.046
Solidity	1.97	2.25	2.42	2.50	2.53	2.52	2.79	2.76
$T_{m/c}$	.114	.094	.089	.085	.082	.079	.075	.071
Camber - deg	64°	58°	59.5°	54.5°	51.0°	52.°	52.0°	53.0°

TABLE 6. DESIGN 3 SWIRL VANE - T700 SIZE

Parameter	Hub	Pitch	Tip
Radius - in.	4.000	5.536	6.575
Camber - deg	38.2°	38.2°	38.2°
Stagger Angle - deg	33.1°	33.1°	33.1°
LE Angle of Attack - deg	4.0°	4.0°	4.0°
Chord - in.	2.978	2.978	2.978
Thickness (max) - in.	.436	.436	.436
$T_{m/c}$	14.6%	14.6%	14.6%
Solidity	2.13	1.54	1.30

TEST FACILITY AND EQUIPMENT

FACILITY

The separators were tested at General Electric, Lynn, Mass., in a facility having electric-motor-driven fans to supply separately controlled main and scavenge airflows. Figure 27 shows the test cell.

SAND FEEDING EQUIPMENT

As illustrated in Figure 27, typical sand feeding equipment was used for the tests. The sand was poured into a high-capacity feeder hopper, where it was weighed. The auger feed system can be adjusted by controlling the variable-speed motor to provide the desired sand concentration.

The sand from the hopper is dumped into a feeder funnel, where it is entrained by shop air and transported to the ingestion nozzles. The nozzles are fixed to provide localized or uniform sand ingestion.

PRESSURE MEASURING EQUIPMENT

All pressure measurement probes were manufactured as specialty equipment for the model. These probes were connected to water manometer panels which were continually monitored. When data was taken, a visual reading was made and recorded on a log sheet. The manometer panel in the separator facility supplied a total of 36 measurement points plus 4 reference points.

INSTRUMENTATION

The following instrumentation was used for all tests:

1. Airflow Measurement
    a. Inlet Bellmouth - measures total airflow
        (1) Four OD Statics
    b. Scavenge Orifice - measures scavenge airflow
        (1) Upstream Static (1)
        (2) Downstream Static (1)
    c. Sling psychrometer - for wet and dry bulb temperature.

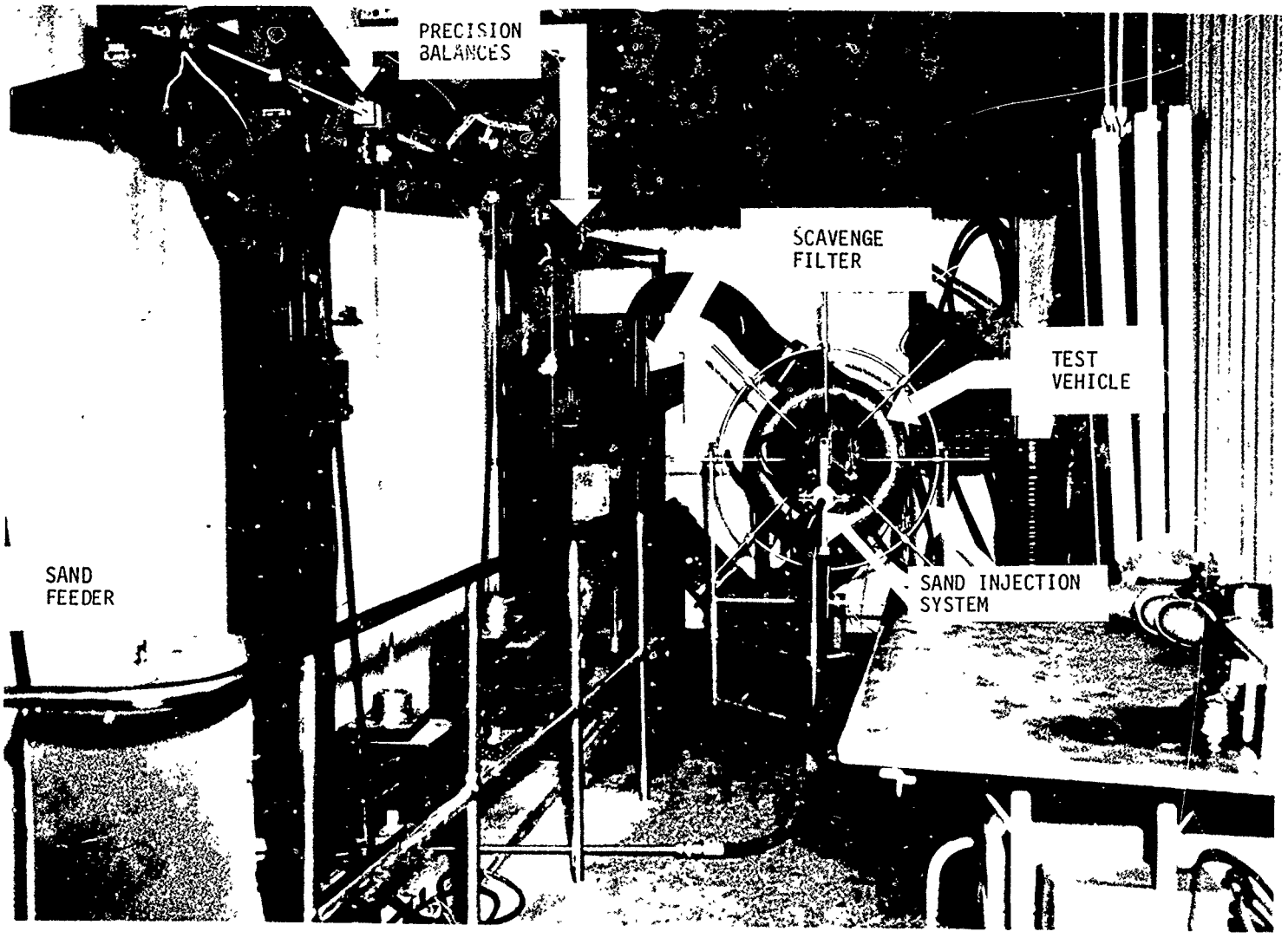

Figure 27. Inlet Separator Test Cell.

2. Internal Aerodynamic Measurement

a. Cobra Probe - measures swirl angle and total pressures

(1) Swirl Cascade Discharge - radial traverse capability
(2) Core Inlet

(a) Radial traverse capability
(b) Circumferential traverse capability

b. Kiel Probe (Measures Total Pressure)

(1) Used at any location which accepts the cobra probe

c. Separation Efficiency

(1) Scavenge sand was collected by barrier filter
(2) Feeder for sand to be ingested
(3) Ormond beam balance to weigh both feeder and filter

Separation efficiency can be defined in different ways, two of which are commonly used. The definition based on weight is

$$\eta_w = (\text{WEIGHT OF SAND SCAVENGED})/(\text{WEIGHT OF SAND AT SEPARATOR INLET}) \quad (7)$$

The second definition recognizes a penalty for scavenge airflow. It is

$$\eta_c = 1 - (\text{SAND CONCENTRATION AT IGV})/(\text{SAND CONCENTRATION AT SEPARATOR INLET}) \quad (8)$$

where concentration is (Sand Flow)/(Airflow). The two efficiencies are related by the equation

$$\eta_c = \eta_w - (1 - \eta_w)\ (\text{SCAVENGE AIRFLOW})/(\text{COMPRESSOR AIRFLOW}) \quad (9)$$

TEST PROCEDURE

The following tests were conducted with all models:

1. Vaneless Flow Path Evaluation (without swirl or deswirl vanes)

    a. Measure core pressure drop.
    b. Measure pressure drop at rainstep.
    c. Measure C-Spec efficiency.
    d. Measure AC Coarse efficiency.

2. Swirl Vane Evaluation (without deswirl vanes)

    a. Measure swirl angle and total pressure loss at the rainstep over an extent of 40°.
    b. Measure AC Coarse efficiency.
    c. Measure C-Spec efficiency.

3. Deswirl Vane Evaluation

    a. Measure core pressure drop.
    b. Measure AC Coarse efficiency.
    c. Measure C-Spec efficiency.
    d. Photograph dye traces of separator flow path.

4. Model Tuning - Review test results from 3 and modify model if necessary to improve model performance. Modifications were:

    a. Swirl vane solidity changes and restagger.
    b. Deswirl vane solidity changes and redesign.
    c. Flow path changes.
    d. Scavenge vane solidity changes.

Tests 1 through 4 were run at maximum airflow and 16.5% scavenge flow. All tests had swirl angle data obtained with a cobra probe. A Kiel probe was used to obtain pressure drop at the scroll exit and core inlet.

The tuned configurations which were established by this test program were tested at 15 different airflow combinations. Measurements were made at 100%, 90%, 80%, 60% and 40% flow with about 20%, 16.5% and 10% scavenge flow.

TEST RESULTS

2 LB/SEC AXIAL SEPARATOR

The results of the Phase II test program are given in Table 7. Because of the relatively high separator pressure loss through the 2 lb/sec model, several modifications of it were tested. The main results seen in Table 7 are:

1. In the change from Configuration II to V, Configuration V had good AC Coarse separation efficiency, but C-Spec efficiency dropped about 4.7%.

2. When the splitter lip was moved forward (Configuration III), core pressure loss increased about 4 in. H_2O, but separation efficiency on C-Spec improved only 1%.

3. The vaneless Configuration VII had 5.6 in. H_2O pressure drop, indicating that the basic vaneless core flow path of the 2 lb/sec model accounts for over half the core pressure drop found in Configuration I and nearly half of the loss in Configuration II.

4. Since trajectory analysis work showed the importance of closed line of sight relative to the core inlet, the 2 lb/sec axial separator was modified as shown in Figure 28 to hide the splitter lip. This new splitter lip was run in a vaneless configuration, and the results are shown in Table 7, Configuration VIII. Separation efficiency on C-Spec sand increased from 66.2 to 78.9%. On AC Coarse dust, separation efficiency increased from 15.3 to 58.2%. These large increases in efficiency came at the expense of a 5.6 in. H_2O increase in core pressure loss.

5. For Phase V tests the flow path was redesigned to reduce diffusion on the inner core wall. The off-design tests were conducted on Configuration X of Table 7. Results of the Phase V off-design tests on the 2 lb/sec axial separators are given in Table 8, which shows that the redesigned model had losses consistent with design predictions and excellent separation performance due primarily to the hidden splitter lip.

   In addition to off-design testing, foreign object ingestion tests were run on the 2 lb/sec model. Listed in Table 9 are the 48 items ingested.

TABLE 7. 2 LB/SEC SEPARATOR TESTING SUMMARY

Configuration No.	Configuration 2 lb/sec Separator Modifications	Swirl Angle (deg)	Pressure Loss ΔP_T* (in. H_2O)	Pressure Loss Core Flow (%)	Pressure Loss ΔP_T** (in. H_2O)	Pressure Loss Scav (%)	AC Coarse Sand Core Flow (lb/sec)	AC Coarse Sand Scav (%)	AC Coarse Sand η_w (%)	AC Coarse Sand η_c (%)	C-Spec Sand Core Flow (lb/sec)	C-Spec Sand Scav (%)	C-Spec Sand η_w (%)	C-Spec Sand η_c (%)
	STATUS TEST	32.5	33.3	14.6	15.8	15.2	2.06	14.8	76.7	73.3	2.06	15.0	88.0	86.2
	MODIFICATION TESTS													
I	50% Reduction in Swirl Cascade (13 Vane)	31.5	19.3	17.2	10.1	17.6	--	--	--	--	2.00	16.2	85.0	82.6
II	13 Vane Swirl at +5°	35.5	27.0	16.2	13.6	16.3	2.04	15.2	80.3 80.0	77.3 77.8	2.03	15.6	86.5	84.5
III	II + Splitter 0.34 in. Forward	35.5	25.0	16.9	17.7	16.9	2.01	16.4	81.0	77.9	2.01	16.4	87.4	85.3
IV	II + Scroll Vanes 0.5 in. Aft	35.5	24.8	16.5	--	--	2.06	16.5	81.6	78.6	2.04	16.4	86.2	83.9
V	II + 50% Reduction in. Scroll Vanes	35.5	17.7	17.3	13.3	17.2	2.03	16.7	80.6	77.4	2.04	15.7	82.7	79.8
VI	V + Increased Scavenge	35.5	19.6	26.2	18.4	31.6	2.04	18.6	82.1	78.8	2.02	19.3	86.7	84.1
VII	Basic Flow Path (no vanes)	0	12.8	17.2	5.6	18.0	2.00	17.8	27.9	15.3	2.01	17.4	71.2	66.2
VIII	Vaneless - Reduced Splitter Lip Radius	0	--	--	11.2	18.6	1.97	17.0	64.3	58.2	1.96	17.6	82.1	78.9
	PHASE V TESTS													
IX	VIII + 13 Swirl Vanes, Redesigned Flow Path and No Deswirl Vanes	31.5	--	--	9.3	16.9	1.67	16.8	84.8	82.2	1.66	17.5	93.6	92.5
X	IX + 26 Deswirl Vanes	31.5	--	20.2	13.6	17.3	2.03	16.7	85.5	83.1	2.03	16.7	94.5	93.6
XI	X With 13 Deswirl Vanes	31.5	--	--	11.1	15.6	--	--	--	--	--	--	--	--

* Corrected to 0.33 lb/sec scavenge flow.
** Corrected to 2 lb/sec core flow.

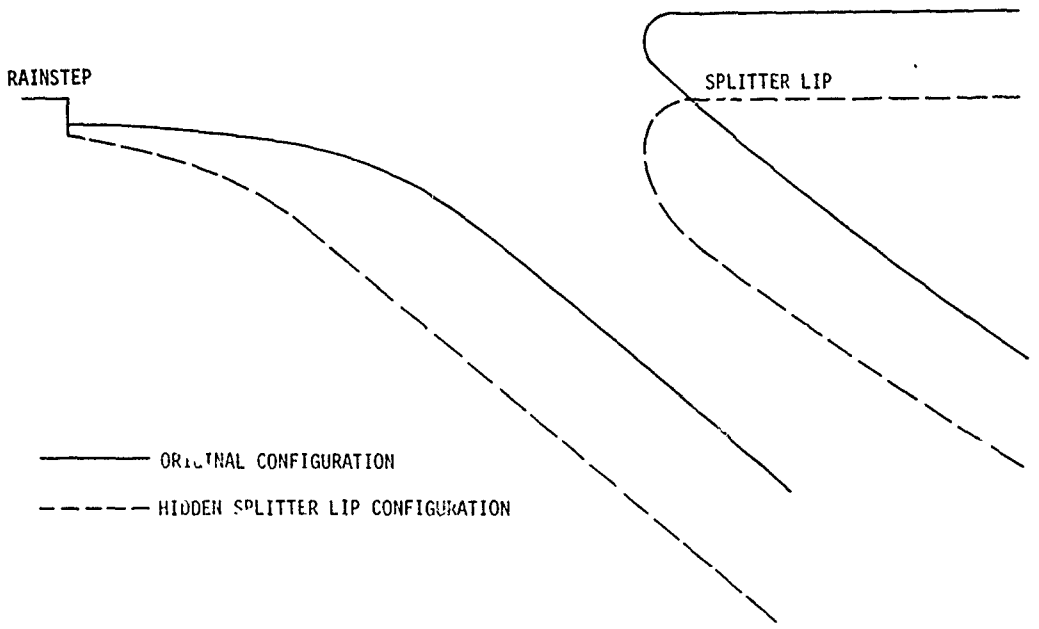

Figure 28. 2 Lb/Sec Hidden Splitter Modification.

Of the items listed in Table 9, one 1/4-in. nut was not separated from the core airstream by the 2 lb/sec separator. All other items were either trapped on the swirl vanes, trapped on the scroll vanes, or completely separated and lodged in the facility filter. As a result of this test, it is obvious that some changes to the FOD test procedure must be made when testing separators in the 2 lb/sec size range. During testing done at design point airflow, it was necessary to stop during the tests and clear the scroll vanes of lodged material in order to maintain design point scavenge flow.

Tests which simulated ingesting FOD during engine start-up were also conducted. The items ingested are also listed in Table 9. All items placed in the model bellmouth were scavenged. All items placed on the top of the model bullet nose passed into the core airstream. It should be noted that it is very unlikely that a foreign object will inadvertently balance itself on the top of a 2 lb/sec engine bullet nose.

An attempt was made to evaluate the performance of the separator in removing water. Because of difficulties in accounting for water that evaporates during a water ingestion test, 2 pounds of water was poured directly into the separator at design point core flow and zero scavenge flow. Very little of the water went into the scavenge system.

TABLE 8. 2 LB/SEC INLET SEPARATOR TEST RESULTS - PRESSURE LOSS AND AC COARSE EFFICIENCY

Run No.	Scroll Pressure Loss			Core Pressure Loss			AC Coarse			
	Core Flow (lb/sec)	Scav Flow (% Core)	ΔP_T (in. H_2O)	Core Flow (lb/sec)	Scav Flow (%)	ΔP_T (in. H_2O)	Core Flow lb/sec)	Scav (%)	η_w (%)	η_c (%)
1	1.99	20.6	22.974	1.99	21.1	13.667	1.99	20.6	85.5	83.7
2	1.98	17.2	20.231	1.97	17.3	13.604	2.03	16.7	85.5	83.1
3	1.97	11.7	18.059	1.96	11.7	12.952	2.00	10.0	81.2	79.3
4	1.77	22.0	18.860	1.78	21.9	10.262	1.73	20.8	86.9	84.2
5	1.77	18.6	16.231	1.79	17.9	10.380	1.81	16.6	84.1	81.5
6	1.78	11.2	14.288	1.78	11.8	10.281	1.776	11.5	81.9	79.8
7	1.59	20.8	14.288	1.57	21.7	7.990	1.61	21.1	87.0	84.3
8	1.56	18.6	12.687	1.57	19.1	7.852	1.59	18.2	84.7	81.9
9	1.58	10.8	10.744	1.585	11.0	7.936	1.58	11.1	81.8	79.8
10	1.20	20.0	8.001	1.19	21.8	4.218	1.177	22.3	87.9	85.2
11	1.21	16.5	7.087	1.26	12.7	4.484	1.197	17.8	85.1	82.8
12	1.15	13.0	5.601	1.15	12.2	3.944	1.166	12.3	80.9	78.6
13	0.78	23.1	3.886	0.76	25.0	1.538	0.769	23.5	88.3	85.6
14	0.79	19.0	3.543	0.79	20.3	1.871	0.836	18.4	85.4	82.7
15	0.80	8.8	2.858	0.772	11.4	1.926	0.87	11.5	78.4	75.9

TABLE 9. FOREIGN OBJECT INGESTION TEST RESULTS - 2 LB/SEC MODEL

Item	Number Ingested at Design Pt	Number Ingested at Start-Up
#10 Nut, 9610MP01 or equivalent (P08, P19, P28)	10	6
1/4 in. Nut, 9610M50P02 or equivalent (P09, P29)	10	6
#10 Bolt, J643P05 (0.438 in. shank)	10	5
Lockwire 0.032 in. Dia (two strands twisted together 1 in. long)	10	9
1/4 in. Socket (normal socket head from a socket wrench)	3	2
1/8 in. Allen Wrench	3	4
Rag, 12 in. x 12 in. Cotton, Wool or Linen	2	0

Grass was ingested during the FOD evaluation, with the result that the majority of the grass clogged the model swirl vanes.

2 LB/SEC INLET SCROLL SEPARATOR

Summary

The 2 lb/sec scroll separator tests evaluated the basic design concept of the scroll configuration plus five modifications. Test results listed in Table 10 indicate that the scroll design concept (shown in Figure 16) has potential. The 84.9% separation efficiency on C-Spec sand and the 78% efficiency on AC Coarse establish the feasibility of the scroll design. Testing of design modifications highlighted important performance effects and pointed the way to improving the basic separation efficiency levels. Scroll separator pressure drops listed in Table 10 are two to three times axial separator losses. Approximately 35% of this loss is computed to be in the duct between the separator exit at station zero and the ΔP_T measuring plane. This large duct loss is due to the swirling flow in the duct, and indicates that installation of deswirl vanes could make the scroll separator pressure losses similar to axial separator pressure losses. The table shows that a drop of 10.9% on C-Spec sand occurred when the 90° inlet elbow was removed to make Configuration II. The next separator modification, Configuration III, was to remove the larger of the two internal scavenge vanes, forming a 4.5-in. collection slot. Although this had potential, it allowed particles to bounce back into the core airstream and probably starved the elbow collector of much of its share of the scavenge flow. The net effect was a performance decrease of 11.6% on C-Spec sand from the original system.

For Configuration IV, all internal scavenge slots were closed so that all of the scavenge air (except for some leakage) was drawn from the elbow scavenge slot. This approach with 27.1% decrement in C-Spec separation efficiency does not appear to be fruitful.

Configuration V returned the scavenge circuit to the original design and had a substantial modification (shown in Figure 29) to the core inlet in an effort to reduce the pressure loss. The goal of reduced pressure drop was achieved with a 21.4 in. H_2O improvement at the expense of 9.9% in AC Coarse dust separation efficiency. It may be possible to regain the lost efficiency by rotating the inlet elbow 90° to make its rotation in the same direction as the basic scroll. The basis for a modification of this kind is that the inlet elbow tended to force sand into the area where core inlet modification removed what had been a barrier.

TABLE 10. 2 LB/SEC SCROLL SEPARATOR TESTING SUMMARY

Configuration	Test Point					AC Coarse				C-Spec			
	Core Flow (lb/sec)	Scav (%)	ΔP_T (in. H_2O)	Residual Swirl (Deg)	ΔP_T* (in. H_2O)	Core Flow (lb/sec)	Scav (%)	η_w (%)	η_c (%)	Core Flow (lb/sec)	Scav (%)	η_w (%)	η_c (%)
No. 2 LB/SEC SCROLL SEPARATOR MODIFICATIONS													
I Basic Scroll + 90° Inlet Elbow	1.32	16.7	18.8	55.0	45.2	1.30	16.5	81.1	78.0	1.29	16.0	87.0	84.9
II Basic Scroll Only	1.29	16.3	14.9	55.5	34.2	1.39	15.8	75.4	71.5	1.38	15.7	77.5	74.0
III Scroll and Elbow With Large Scavenge Vane Removed	-	-	-	-	-	1.34	16.4	71.1	66.4	1.33	16.6	77.1	73.3
IV Scroll and Elbow With Scroll Scavenge Ports Closed	-	-	-	-	-	-	-	-	-	1.32	15.9	63.6	57.8
V Configuration I With "Bathtub Drain" Rework of Core Inlet	1.33	16.5	10.5	54.5	23.8	1.37	16.1	72.6	61.8	-	-	-	-
VI V + Cutback Scavenge Slot in Elbow	1.31	16.8	13.1	52.1	30.5	1.33	16.5	74.6	70.4	1.32	16.7	82.8	79.9

*Extrapolated to 2 lb/sec.

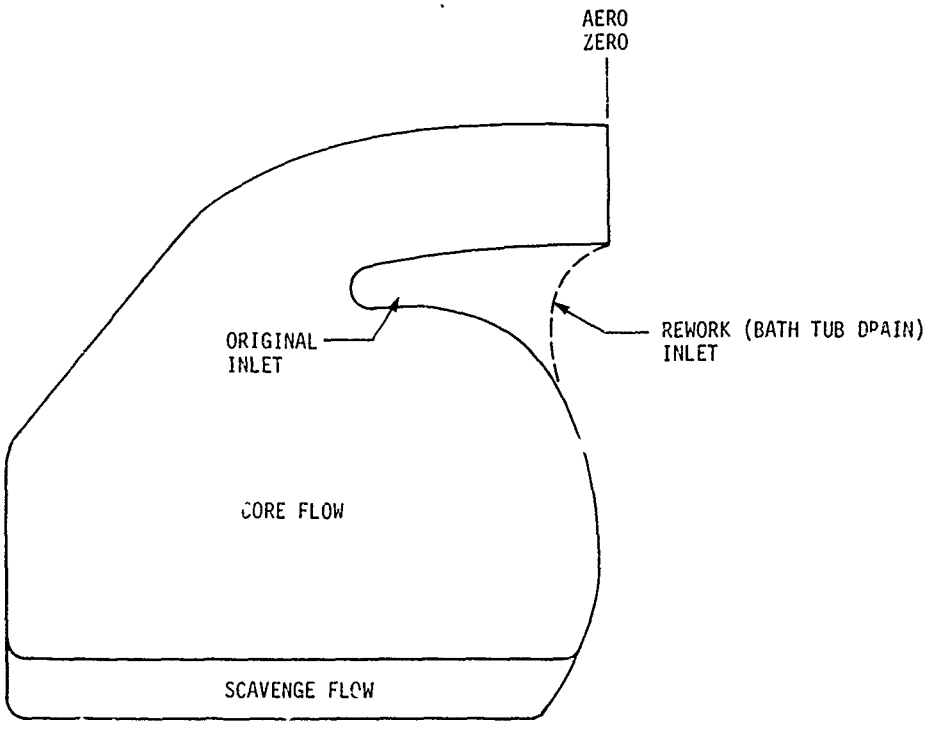

Figure 29. 2 Lb/Sec Scroll Separator Inlet Rework.

After testing Configuration V, the bathtub drain core inlet shown in Figure 29, an elbow collection slot cutback was tested. Figure 16 shows the collection slot cutback, which is Configuration VI. Configuration VI, compared with Configuration V, had a 25% increase in pressure drop, a 2.3% increase in AC Coarse efficiency, and a C-Spec efficiency of 79.9%. The C-Spec efficiency reflects the net impact of the bathtub drain and the cutback elbow slot. Because the bathtub drain provides a more open path to the core inlet, it decreased C-Spec efficiency relative to Configuration I.

The Configuration VI calculated loss downstream of station zero was 0.8 in. H_2O less than Configuration V due to the reduction in residual swirl angle. On this basis the increased elbow slot added 3.4 in. H_2O pressure loss to the Configuration V level. The large loss due to the elbow slot is a result of the slot to main passage area ratio which is considerably larger than the scavenge flow ratio. Since the slot lips in the scroll separator did not have very large leading edge radii, each slot probably contributed to the overall pressure loss. As can be seen in Figure 30, the cutback slot raised pressure losses across the entire annulus, and the bathtub drain caused a major improvement in the center annulus loss when compared to Configuration I. This suggests that a large portion of the loss is caused by separation due to the collection slot, which is mixed by the time it reaches the measuring plane. The core

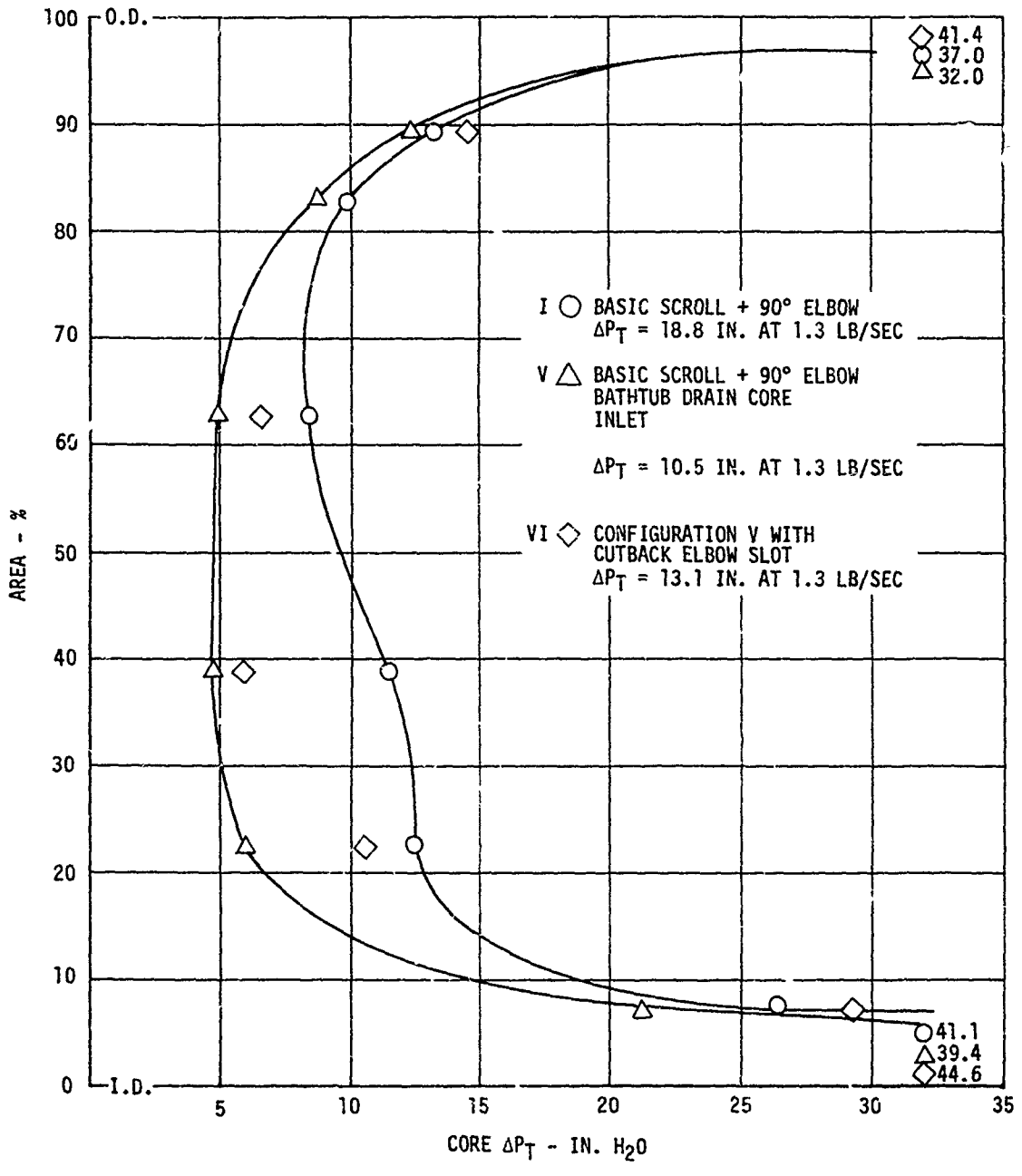

Figure 30. 2 Lb/Sec Scroll Separator Core ΔP_T Profiles.

inlet bathtub drain reduced the entrance loss by increasing the entrance radius of curvature and also by increasing the flow effective area in the entrance region.

Phase IIB, the scroll inlet portion of the program, demonstrated feasibility of a scroll type separator in the 2 lb/sec size. The test results indicate that a redesigned 2 lb/sec scroll separator should be about 24% larger in flow area than the present configuration to achieve an acceptable 5 to 8 in. H_2O pressure loss. With no improvements, efficiency levels would be 85-90% on C-Spec. and 80-85% on AC Coarse. With design improvements suggested by Phase IIB results, higher collection efficiency levels could be achieved.

Trajectory analysis activity carried out under Phase III essentially matched test results from the vaneless axial type separators. With some modification, the trajectory analysis program could be adapted to analyze the scroll separator geometry. At present, the trajectory analysis treats axisymmetric flow paths with swirl vanes. The scroll separator is not axisymmetric, but could be modeled as axisymmetric over several short intervals. Using the modified trajectory analysis, scroll collection slot geometry and location could be changed to improve collection efficiency.

At present, the scroll entrance elbow is in a plane perpendicular to the scroll plane. Turning the elbow to be in the same plane as the scroll, with the turn rotation the same as the scroll rotation, would improve the collection efficiency. The sand would enter the elbow uniformly, migrate to the outside of the elbow, and continue along the outside of the scroll. The present elbow orientation is such that sand leaving the elbow is concentrated to the rear of the scroll, not the OD of the scroll where the scavenge slots are located. Present model geometry does not allow this elbow change without significant model modification.

A suggested program for future improvement of the scroll concept for a 2 lb/sec separator is:

1. Modify trajectory analysis program to analyze the scroll separator.

2. Analyze the scroll with the turned elbow at 1.3 lb/sec and 2 lb/sec airflows.

3. Change the existing model by reorienting the entrance elbow, relocating the collection slots, and changing the slot contours in sequence to assess the impact of each change.

4. Measure the pressure drop and collection efficiency of each change.

5. For the best configuration tested - design, build, and test a set of deswirl vanes at both 1.3 lb/sec and 2.0 lb/sec airflows.

5 LB/SEC SEPARATOR

The 5 lb/sec model had the highest swirlless separation efficiencies achieved during the program, while the swirlless core total pressure loss was equal to the lowest. This shows that the hidden splitter lip design need not have a large pressure loss penalty. Figure 21 shows the 5 lb/sec model flow path which included a hidden splitter lip in conjunction with a design 3 forward flow path.

Installation of swirl vanes in the 5 lb/sec separator, Configuration II, Table 11, produced little improvement in separation efficiency over the performance of the vaneless flow path. Table 11 shows a C-Spec increase from 90.0 to 92.8% and an AC Coarse improvement from 74.2 to 77.4% at the expense of a core pressure loss increase from 3.7 to 7.0 in. H_2O.

The reduced diameter outer wall of the 5 lb/sec separator adversely affected the vaned separator efficiency, and a similar result was obtained from the 15 lb/sec model, Configurations IX and X, Table 12. In the 15 lb/sec separator the penalties for the change were 9.0% on C-Spec and 4.8% on AC Coarse dust. The reduced diameter outer wall flow path was utilized in the 5 lb/sec separator in an effort to keep the core pressure loss low.

During the 5 lb/sec Phase V tests, an anomaly was noted in the test data. Testing at the design point gave 79.8% efficiency on AC coarse dust, which was inconsistent with the 10% and 20% scavenge flow result at 100% core airflow. It was found that the batch of AC Coarse sand used at the design point airflow was different from that used for all other flow conditions. When the sand batch used for the off-design conditions was run at the design conditions, the efficiency increased from 79.8 to 81.3%. This indicates that a variation of at least 1.5% in AC coarse can result from using different batches of AC coarse sand that are within AC coarse specification limits. Listed in Table 13 is the size distribution from both the sand that gave 79.8% efficiency and the sand that gave 81.3% efficiency.

The Phase V off-design tests were conducted on Configuration IV of Table 11. The results are given in Table 12.

Trajectory analysis of the 5 lb/sec separator hidden splitter lip configuration indicated almost 100% separation efficiency. Since the swirlless model test results were 70.7% on AC coarse dust and 89% on C-Spec, it seemed possible that some of the inefficiency was due to sand bouncing off the scroll vanes. Therefore, the scroll vanes were moved aft 4 in. from their original axial location so that any sand that did bounce would have much less chance of bouncing into the core stream. Test results of the 4 in. aft configuration gave 65.5% on AC coarse and 86.7% on C-Spec, which was a significant drop in efficiency rather than an improvement.

TABLE 11. 5 LB/SEC SEPARATOR TESTING SUMMARY

Configuration 5 lb/sec Separator No.	Modifications	Swirl Angle (deg)	Pressure Loss ΔP_T* (in. H_2O)	Core Flow (%)	ΔP_T** (in. H_2O)	Scav (%)	AC Coarse Sand Core Flow (lb/sec)	Scav (%)	η_w (%)	η_c (%)	C-Spec Sand Core Flow (lb/sec)	Scav (%)	η_w (%)	η_c (%)
	MODIFICATION TESTS													
I	Vaneless Flow Path Test	0	-	-	3.7	17.9	5.02	15.6	77.7	74.2	4.99	16.7	91.4	90.0
II	Design 3A Swirl Vanes and No Deswirl Vanes	30.1	-	-	7.0	17.4	4.92	16.9	80.7	77.4	5.00	17.8	93.9	92.8
III	II + Deswirl Vanes	30.1	-	-	10.7	16.3	5.24	16.2	82.6	79.8	5.24	16.2	94.4	93.5
IV	III + Moved Out Outer Flow Path	30.1	11.6	16.4	10.9	16.1	4.94	17.8	84.1	81.3	4.94	17.8	96.4	95.8
V	IV + ½ Swirl Vanes + Scaled T700 Swirl Hub (i.e., 9 Swirl Vanes + 9 Deswirl)	-	-	-	8.3	17.6	5.03	17.3	84.3	81.6	4.99	17.2	96.6	96.0
VI	V With No Swirl and No Deswirl	-	-	-	8.7	18.1	4.94	17.4	75.0	70.7	4.85	17.5	90.6	89.0
VII	VI + Scroll 4.0 in. Aft	-	-	-	-	-	4.99	17.6	75.0	65.5	4.98	17.5	88.7	86.7
VIII	IV & ½ Deswirl Vanes (i.e., 9 Deswirl Vanes)	-	-	-	9.0	19.2	-	-	-	-	-	-	-	-

* Corrected to 0.33 lb/sec scavenge flow.
** Corrected to 2 lb/sec core flow.

TABLE 12. 5 LB/SEC INLET SEPARATOR TEST RESULTS - PRESSURE LOSS AND AC COARSE EFFICIENCY

	Scroll Pressure Loss			Core Pressure Loss			AC Coarse			
Run No.	Core Flow (lb/sec)	Scav Flow (% Core)	ΔP_T (in H_2O)	Core Flow (lb/sec)	Scav Flow (%)	ΔP_T (in H_2O)	Core Flow (lb/sec)	Scav (%)	η_w (%)	η_c (%)
1	5.25	18.7	11.788	4.95	19.8	10.730	5.04	19.4	85.9	83.2
2	5.24	16.4	11.581	4.91	18.1	10.551	4.94	17.8	84.1	81.3
3	5.45	10.1	13.339	4.95	11.[illegible]	9.999	5.00	10.0	80.2	78.2
4	4.61	20.4	8.996	4.53	21.4	9.671	4.50	20.0	84.8	81.8
5	4.45	17.5	8.065	4.47	18.1	8.975	4.51	16.4	82.7	79.9
6	4.44	10.4	8.375	4.46	11.0	8.214	4.55	9.9	78.5	76.4
7	3.97	20.9	6.618	3.92	22.4	7.373	4.03	19.9	83.8	80.6
8	3.94	16.8	6.307	4.00	18.3	6.828	3.99	16.5	80.9	77.7
9	3.94	10.4	6.307	3.96	11.1	6,506	4.03	9.9	76.8	74.5
10	3.11	20.6	3.929	2.88	21.5	3.879	2.94	20.7	82.3	78.6
11	2.99	17.1	3.516	2.93	16.7	3.293	2.91	16.8	80.7	77.5
12	2.98	10.7	3.516	2.94	10.5	3.439	2.91	10.5	77.2	74.8
13	1.955	21.2	1.551	2.48	19.2	2.076	1.905	20.7	83.0	79.5
14	2.01	16.9	1.551	1.95	16.9	1.704	1.997	16.2	79.6	76.3
15	1.98	10.1	1.551	1.97	10.2	1.697	1.999	10.1	74.1	72.1

TABLE 13. AC COARSE SIZES			
	Batch Test Results		
Size Range (microns)	79.8%	81.3%	AC Coarse Spec
0-5	13.8%	13.7%	12±2%
5-10	10.2	10.2	12±3
10-20	12.6	13.5	14±3
20-40	24.4	22.9	23±3
40-80	30.5	28.8	30±3
80-200	7.9	10.6	9±3

TABLE 14. FOREIGN OBJECT INGESTION TEST RESULTS - 5 LB/SEC MODEL			
Object	No. Ingested	No. Separated at 5 lb/sec	No. Separated at 2 lb/sec Idle)
#10 Nut	10	10	4
1/4 in. Nut	10	10	6
#10 Bolt	10	9	9
Lockwire	10	7	8
1/4 in. Socket	3	3	2
1/8 in. Allen Wrench	3	2	1

The reduced performance when the scroll vanes were moved aft 4 in. was probably due to lower velocities in the scavenge stream at the splitter lip. Also, the splitter lip stagnation streamline moved aft 2 to 3 in. (as measured by a handheld tuft wand). The reverse flow forward of the stagnation point and around the splitter lip leading edge may have carried with it sand that had already been separated. The conclusion is that the reverse flow forward of the stagnation point or lower scavenge inlet velocities when the scroll vanes are 4 in. aft causes a larger inefficiency than the bouncing of particles off the scroll vanes into the core when they are in their normal location.

When the 5 lb/sec separator without deswirl vanes was tested with and without swirl vanes, swirl angle and wall static pressure were measured. They are compared with design prediction. in Figures 31, 32, 33 and 34. Wall static pressures for the vaneless model are shown in Figure 31. The prediction agrees with test results to within 10% of a velocity head except at Z = 5.4 on the inner wall of the flow path. The larger deviation of 22.5% of a velocity head which occurs there is probably caused by slight separation in the diffusing region aft of the rainstep. Measured inner wall static pressures are lower than predicted due to friction losses which were not accounted for in the potential flow aerodynamic design computer program. Figure 32 shows wall static pressures for the model with swirl vanes and without deswirl vanes. Agreement is within 10% of a velocity head for all points. Both Figures 31 and 32 show that the predicted static pressures along the walls are in good agreement with the measured test results.

Swirl angle at the rainstep axial location is presented in Figure 33. The trend of the test results is in very good agreement with predictions, but the absolute level is high by about 2 deg. The higher measured swirl level may be due to the inaccuracies in hardware construction. A large boundary layer on the outer flow path caused by the adverse pressure gradient and the conservation of angular momentum results in a larger measured swirl or hooking over of the curve in the region near the outer wall.

Figure 34 shows a comparison of swirl angles at the core measuring station. Agreement is within 1 degree except at the hub. The high measured swirl in the tip region is probably caused by losses. The hub measured swirl indicates that angular momentum is not conserved along the hub flow path.

Foreign object ingestion test results on configuration VII of Table 11 are listed in Table 1'.

During the Idle Foreign Object Test, 13 of the items not separated also did not go into the core. These items laid on the bottom of the model outer wall since there was not enough air velocity to drag the items into the scroll. Grass ingested during these tests passed through the vaneless separator into the core, causing no change in separator pressure loss. The grass probably would have accumulated on the IGV's of an engine's compressor.

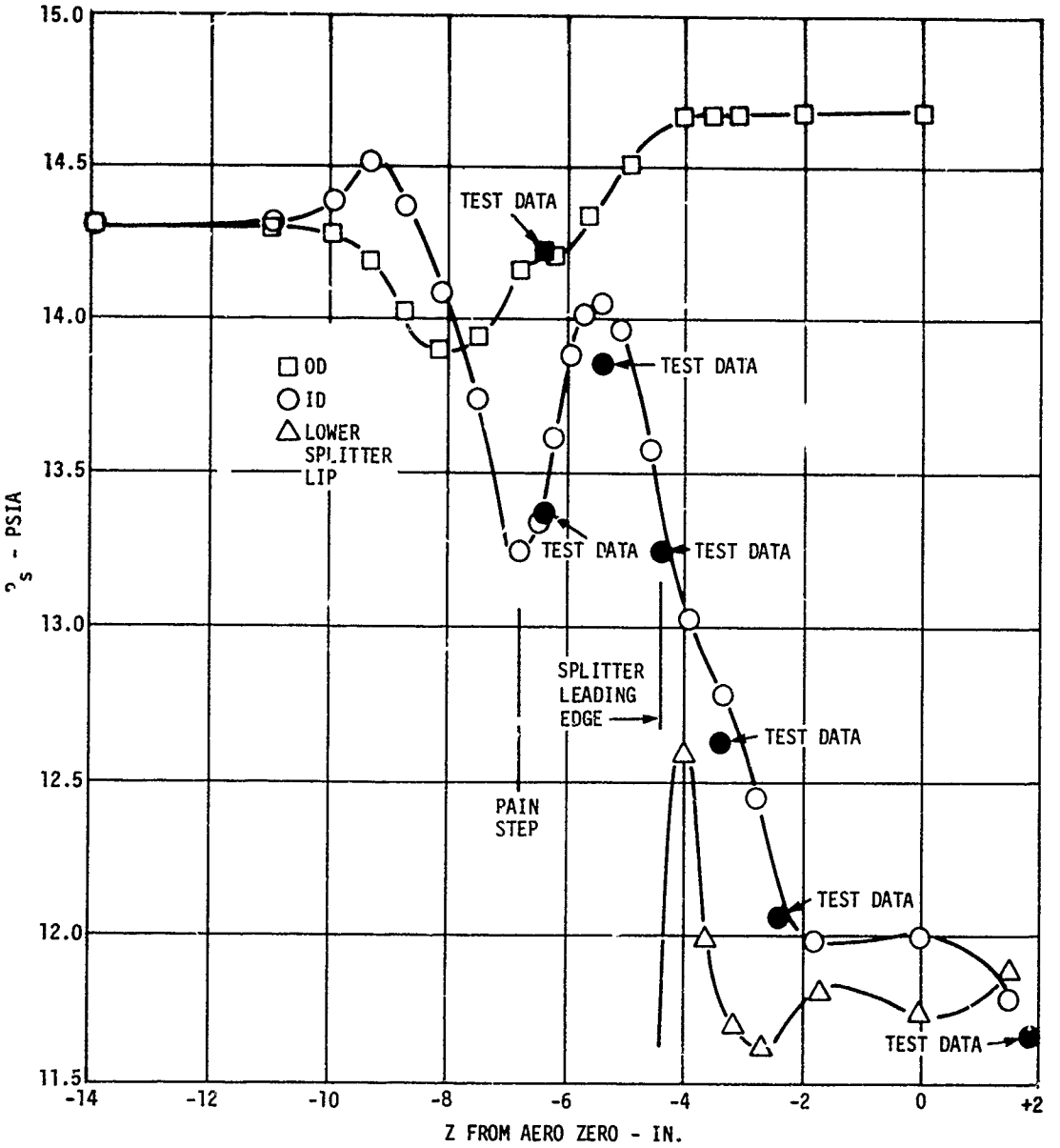

Figure 31. Wall Static Pressure for 5 Lb/Sec Separator Model - Vaneless.

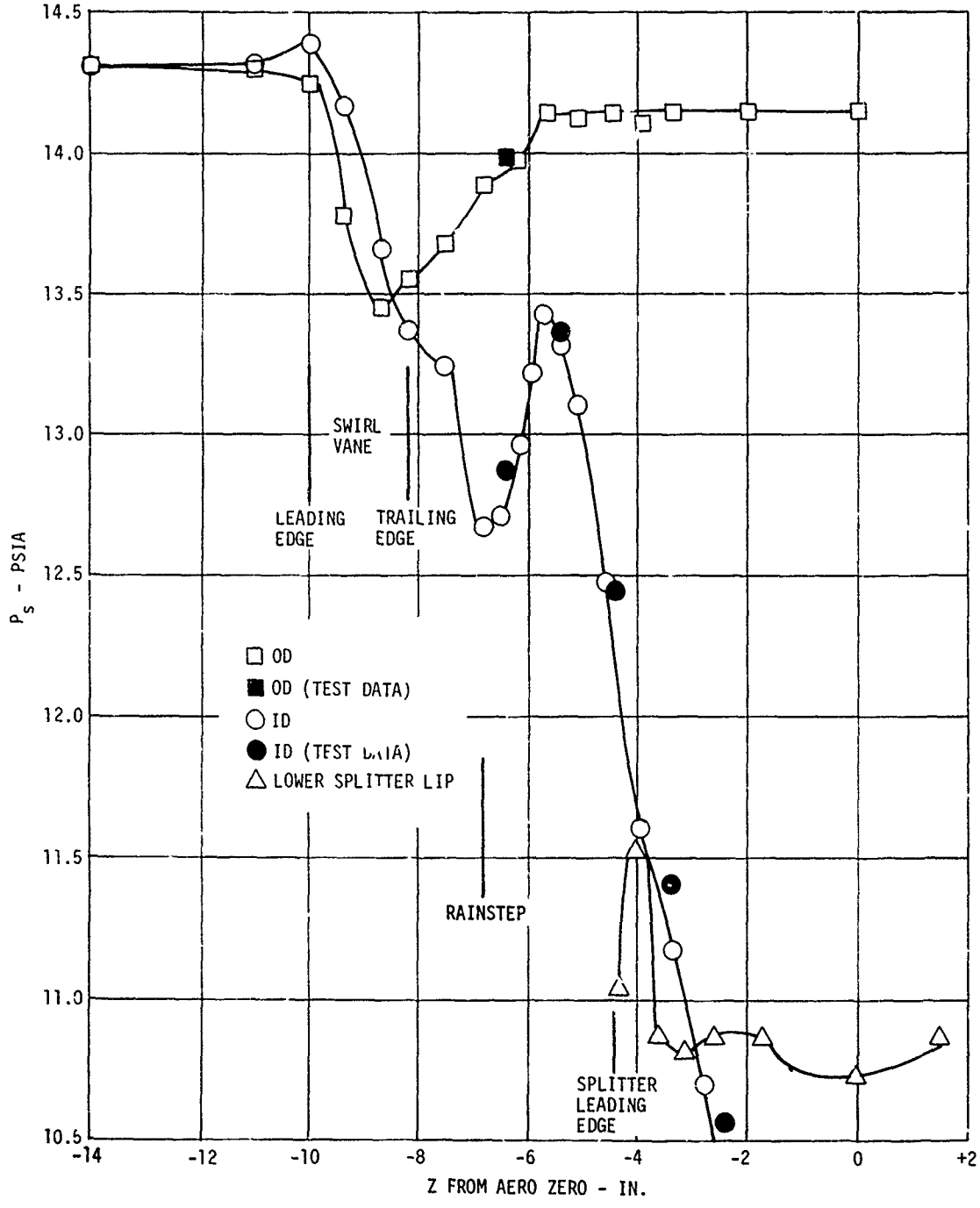

Figure 32. 5 Lb/Sec Separator Model Wall Static Pressure With Swirl Vanes.

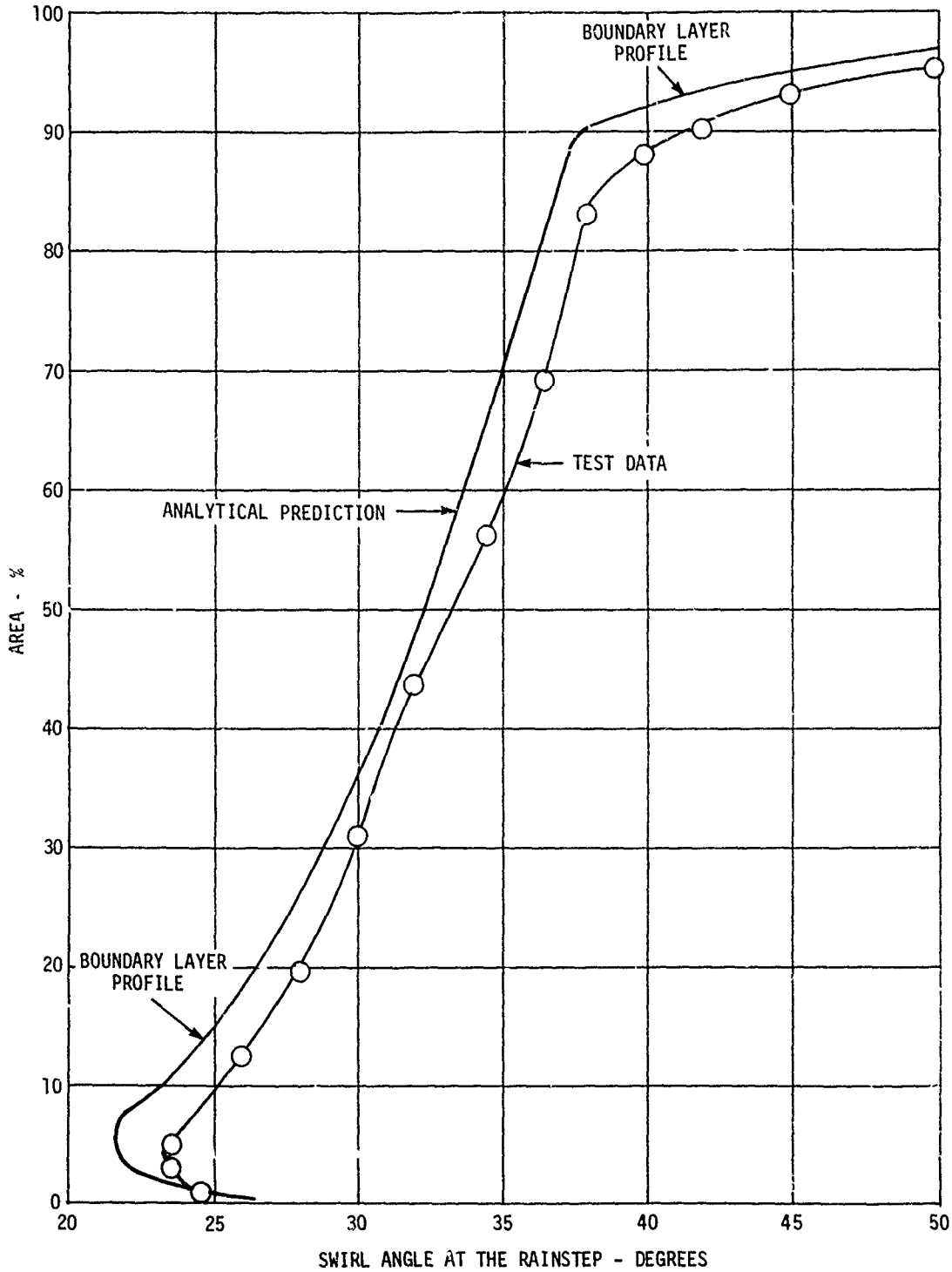

Figure 33. Comparison of Rainstep Swirl Angle Prediction With Test Data.

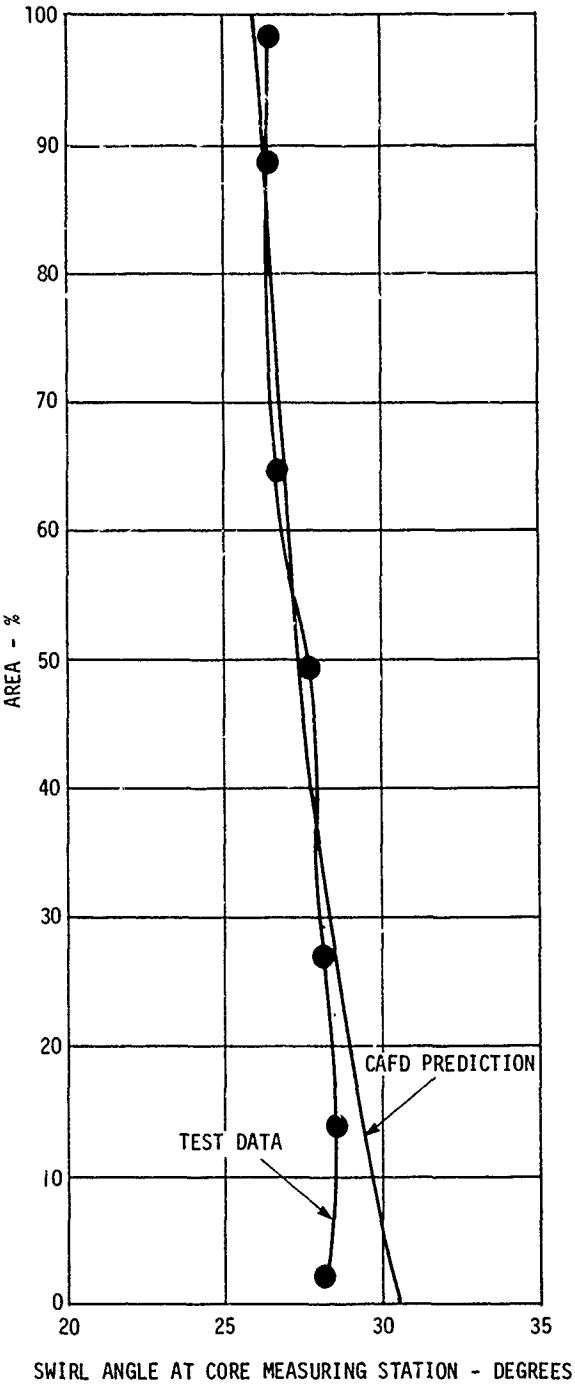

Figure 34. Core Swirl Angle With No Deswirl Vanes.

TABLE 15. 15 LB/SEC SEPARATOR TESTING SUMMARY

Configuration No.	15 lb/sec Separator Modifications	Swirl Angle (deg)	Pressure Loss ΔP_T* (in. H_2O)	Pressure Loss Core Flow (%)	Pressure Loss ΔP_T** (in. H_2O)	Pressure Loss Scav (%)	AC Coarse Sand Core Flow (lb/sec)	AC Coarse Sand Scav (%)	AC Coarse Sand η_w (%)	AC Coarse Sand η_c (%)	C-Spec Sand Core Flow (lb/sec)	C-Spec Sand Scav (%)	C-Spec Sand η_w (%)	C-Spec Sand η_c (%)
	STATUS TESTS	31.5	19.7	15.6	8.3	15.2	14.9	16.3	78.6	75.1	14.9	16.4	95.2	94.4
	MODIFICATION TESTS													
I	50% Reduction in Swirl Cascade Solidity (12 Vane)	31.5	--	--	5.7	11.0	15.0	16.4	79.4	76.1	15.1	16.4	92.9	91.8
II	I + 6° Increase in Swirl Vane Stagger Angle	36.5	20.4	16.3	8.3	16.2	15.0	16.2	78.5	75.0	14.9	16.1	93.8	92.8
III	Status Vaneless Flow Path	0	--	--	4.3	16.1	15.2	16.0	64.2	55.8	14.8	16.6	83.3	80.5
IV	Status and Design 5 Deswirl Hub (Vaneless)	0	--	--	3.9	16.5	15.1	16.3	60.3	53.8	14.8	16.8	80.3	77.0
V	IV With .75 in. Reduction in Rainstep-to-Splitter Lip Length (Vaneless)	0	--	--	3.7	16.1	15.1	15.6	58.1	51.6	15.1 15.0	15.4 16.2	79.2 80.4	76.0 77.2
VI	Status Deswirl a Design 3 Swirl (Vaneless)	0	--	--	3.8	16.6	15.0	16.3	60.8	54.4	14.9	16.5	83.0	80.2
VII	Design 3 Swirl System	37.4	--	--	9.3	15.5	15.2	16.0	81.0	78.0	15.2	15.9	95.6	94.9
VIII	Design 3 - 6° Stagger Angle	31.7	--	--	7.0	16.5	15.0	16.4	77.5	73.8	15.0	16.6	94.9	94.1
IX	VIII + Filled Outer Flow Path	31.7	--	--	6.8	16.2	--	--	--	--	15.1	16.4	87.1	85.0

* Corrected to 0.33 lb/sec scavenge flow
** Corrected to 2 lb/sec core flow.

TABLE 15. - Continued

Configuration No.	15 lb/sec Separator Modifications	Swirl Angle (deg)	Pressure Loss ΔP_T* (in. H_2O)	Core Flow (%)	ΔP_T** (in. H_2O)	Scav (%)	Coarse Sand Flow (lb/sec)	Coarse Sand Scav (%)	Coarse Sand η_w (%)	Coarse Sand η_c (%)	C-Spec Sand Core Flow (lb/sec)	C-Spec Sand Scav (%)	C-Spec Sand η_w (%)	C-Spec Sand η_c (%)
MODIFICATION TESTS - Continued														
X	VIII + Outer Flow Path Step Diffuser	31.7	--	--	6.8	16.6	15.0	16.2	73.3	69.0	15.0	16.4	87.3	85.2
XI	VIII + OD Boundary Layer Trip	31.7	--	--	7.3	16.0	--	--	--	--	--	--	--	--
XII	VIII + OD and ID Boundary Layer Trips	31.7	--	--	7.3	16.2	--	--	--	--	--	--	--	--
	A. ½ Pitch (15°)	31.7	--	--	6.8	16.4	--	--	--	--	--	--	--	--
	B. ¼ Pitch (30°)	31.7	--	--	7.2	16.1	--	--	--	--	--	--	--	--
	C. 3/4 Pitch (15°)	31.7	--	--	6.8	16.2	--	--	--	--	--	--	--	--
	D. 5/8 Pitch (12.5°)	31.7	--	--	6.7	16.4	--	--	--	--	--	--	--	--
XIV	Design 3 - 6° Stagger Angle and Status Swirl Hub	38.1	--	--	8.6	16.0	15.1	16.3	81.2	78.1	15.2	16.0	96.0	95.4
XV	Design 3 - 9° Stagger Angle and Status Swirl Hub	32.1	--	--	6.9	16.0	15.0	17.0	78.4	74.7	15.0	16.8	95.7	95.0
XVI	XV + Triangular Extension to Trailing Edge of Swirl Vane	32.8	--	--	7.5	16.6	14.9	17.3	80.2	76.8	14.9	17.3	96.6	96.0
XVII	Scaled 5 lb/sec Hidden Splitter Lip (Same as 5 lb/sec Configuration VI)	--	--	--	5.3	17.2	15.0	16.4	67.8	62.5	15.6	16.6	90.9	89.4

* Corrected to 0.33 lb/sec scavenge flow.
** Corrected to 2 lb/sec scavenge flow.

15 LB/SEC SEPARATOR

Swirlless 15 Lb/Sec Model

Four vaneless flow paths were tested. The status flow path, Configuration III, had the best efficiency and also the highest total pressure loss. Table 15 Configuration IV, shows that the design 5 hub, which was contoured to minimize hub separation just aft of the rainstep, reduced total pressure losses and decreased separation efficiency. When the splitter lip was moved forward relative to the rainstep, Configuration V, the impact was quite different from a similar test with the vaned 2 lb/sec model. In that case, pressure drop increased by 30% and efficiency improved by 1.0 and 0.5 points for C-Spec and AC Coarse dusts, respectively. The 15 lb/sec model performance showed negligible change in pressure drop and in C-Spec efficiency and a 2.2-point decrease in AC Coarse efficiency. Neither of these configurations showed strong evidence that appreciable performance gains could be achieved through changes in the deswirl region. Therefore, the status deswirl flow path was reinstalled when the design 3 swirl section flow path was used. This combination had 12% less pressure loss, equivalent C-Spec separation efficiency and 4% poorer AC Coarse efficiency than the original swirlless status flow path.

Figure 35 is a comparison of core, radial pressure drop profiles for the status and the status plus design 3 swirl flow paths. Also included for reference are the status systems with 24 and 12 swirl vanes. Figure 35 shows that both the hub and tip total pressure losses improved substantially in both swirlless configurations. The swirlless profiles are essentially flat at about 2 in. H_2O ΔP for the center 70% of the channel and have boundary layers which cover about 15% of the flow at both the outer and inner walls. When vanes are installed in the status flow path, the 55-60% area shows little additional loss, but the hub and tip losses increase by 5 - 8 in. H_2O.

Design 3 Swirl System Test Results

The 15 lb/sec model was run with the complete design 3 swirl system at both nominal and 6° open stagger angles. The results are listed in Table 15. Figure 36 shows that the model's performance on C-Spec sand was substantially better (1.9 points) than that of the 12-vane status system at a given swirl level. Its performance was almost equal to that of the 24-vane status system. Figure 37 shows that the best efficiency demonstrated on AC Coarse in the 15 lb/sec size was achieved with the design 3 swirl system at nominal stagger angle. The pressure drop of these swirl vanes with the status deswirl vanes is halfway between the 24- and 12-vane status swirl cascade performance. The design 3 swirl cascade produces a different swirl profile from the status cascade. Therefore, it was probably mismatched with the deswirl cascade, so a deswirl cascade redesign could be expected to move the design 3 performance toward the 12-vane status levels shown in Figure 38.

Utilizing the 15 lb/sec model's capability for rapid inexpensive design changes, twelve different configurations were tested aimed at improving and understanding separator pressure loss.

As shown in Table 15, the first configurations tested involved a filled outer flow path and a step diffuser flow path as shown in Figure 39. The theory of these two configurations was to delay and control separation on the outer wall of the separator. After running the entire configuration shown in Figure 39, the 1.8-in. ring was removed and the test was rerun with just the step diffuser. Neither configuration lowered pressure loss significantly, but as can be seen in Table 15, a drastic reduction in separation efficiency occurred as a result of the change.

The next two configurations involved putting boundary layer trip wires at the separator entrance along the ID and OD. These trips were meant to create turbulence in the boundary layers and thus lower the swirl section losses. The test results show that the trips actually raised the pressure loss.

A series of tests was run with the swirl vanes "reclocked" relative to the deswirl vanes. These tests were most encouraging since a net pressure loss reduction of 0.3 in. H_2O was realized. Figure 40 shows that the total variation in loss was 0.5 in. H_2O for this 18-vane system.

Figures 41 and 42 show that the installation of the design 3 swirl vanes in the status flow path improved separation efficiency as a function of pressure loss. One effect of this change was the "high gain" of the swirl system. The higher velocity through the cascade caused higher swirl levels at constant swirl vane stagger angle. This caused an increase in core pressure loss. The stagger angle of the swirl vanes were, therefore, reduced to return the separator to the same absolute level of pressure loss.

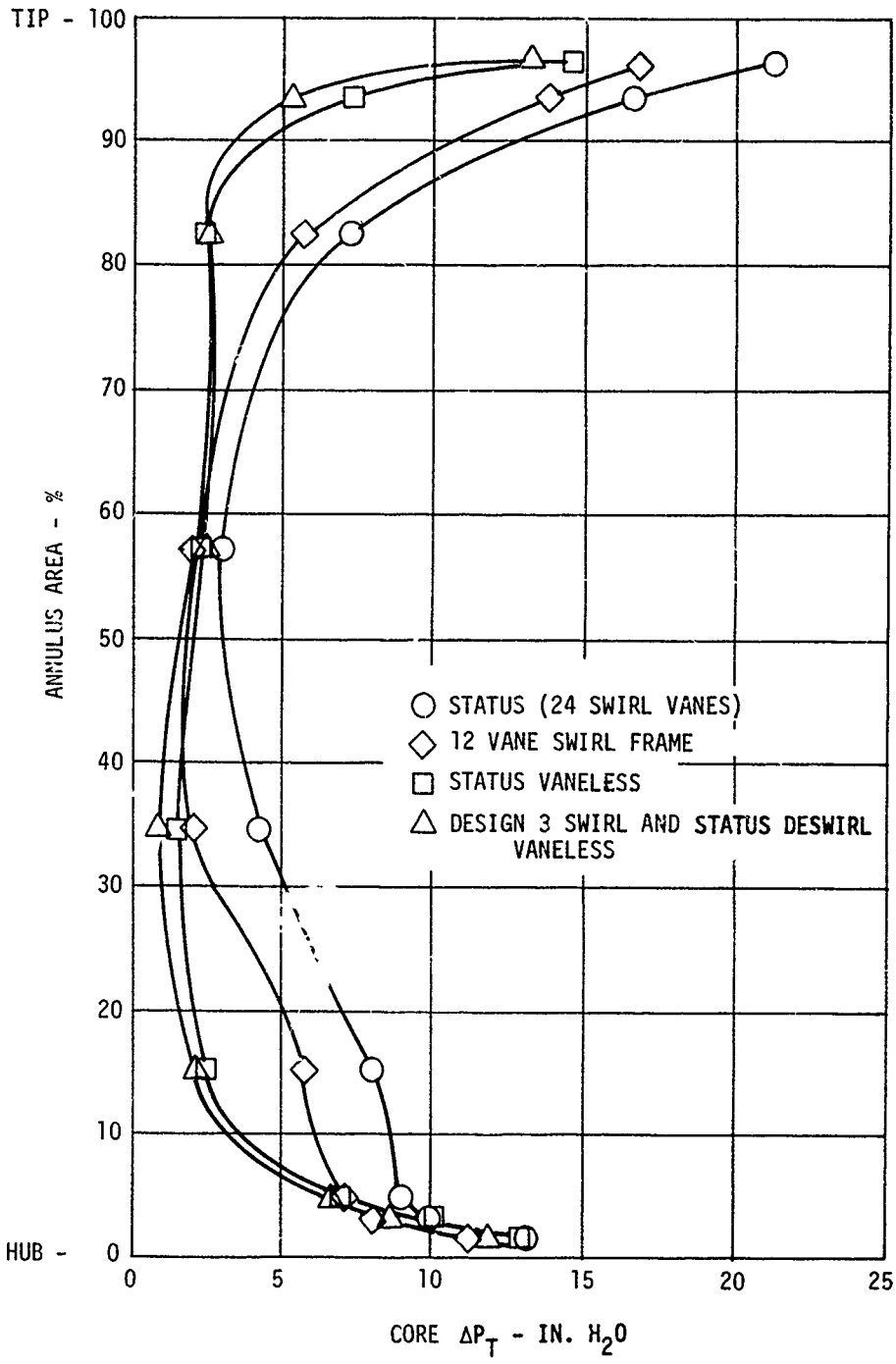

Figure 35. 15 Lb/Sec Separator Exit Radial Profiles at Design Airflows.

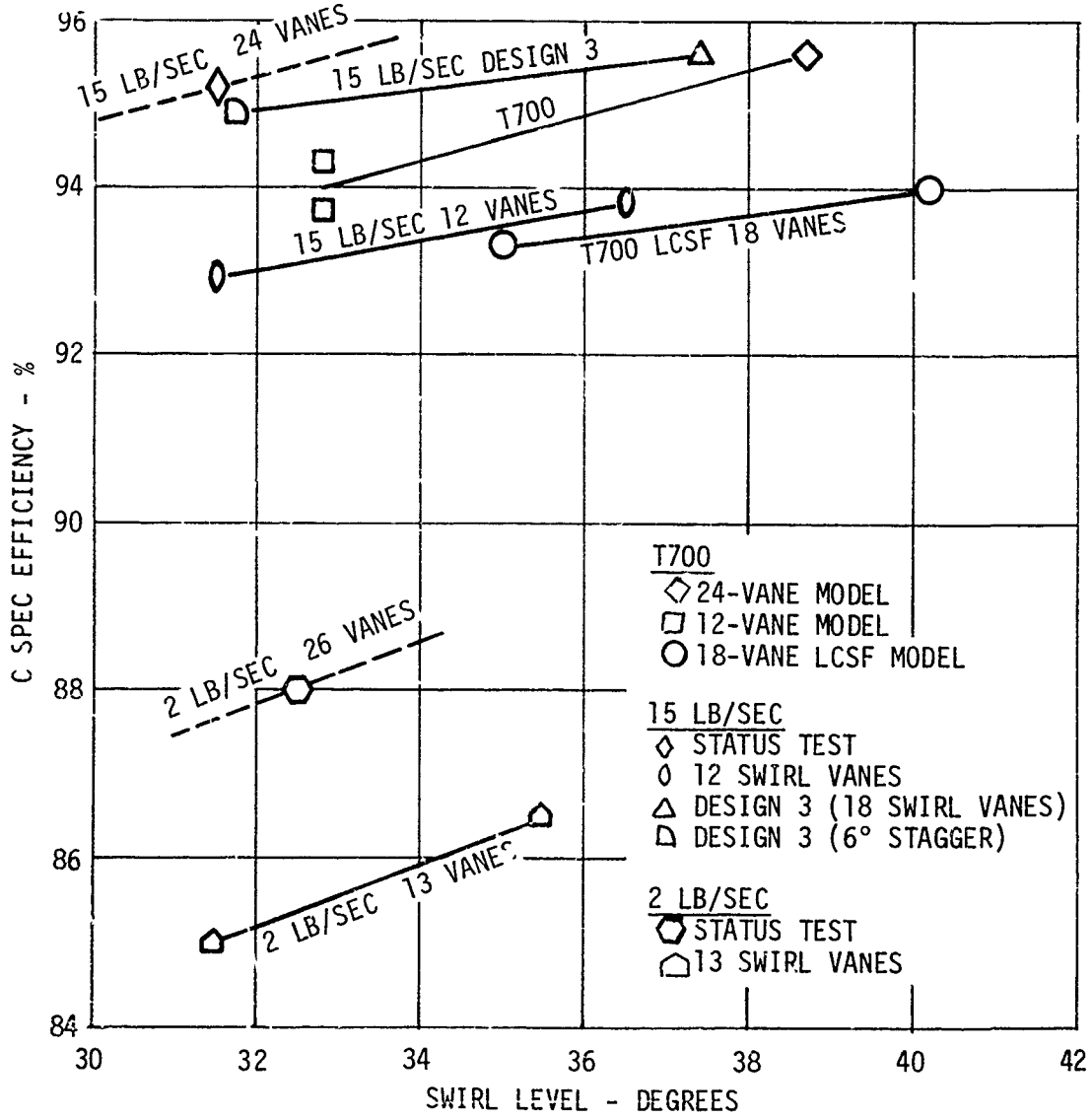

Figure 36. C-Spec Efficiency vs Swirl Level.

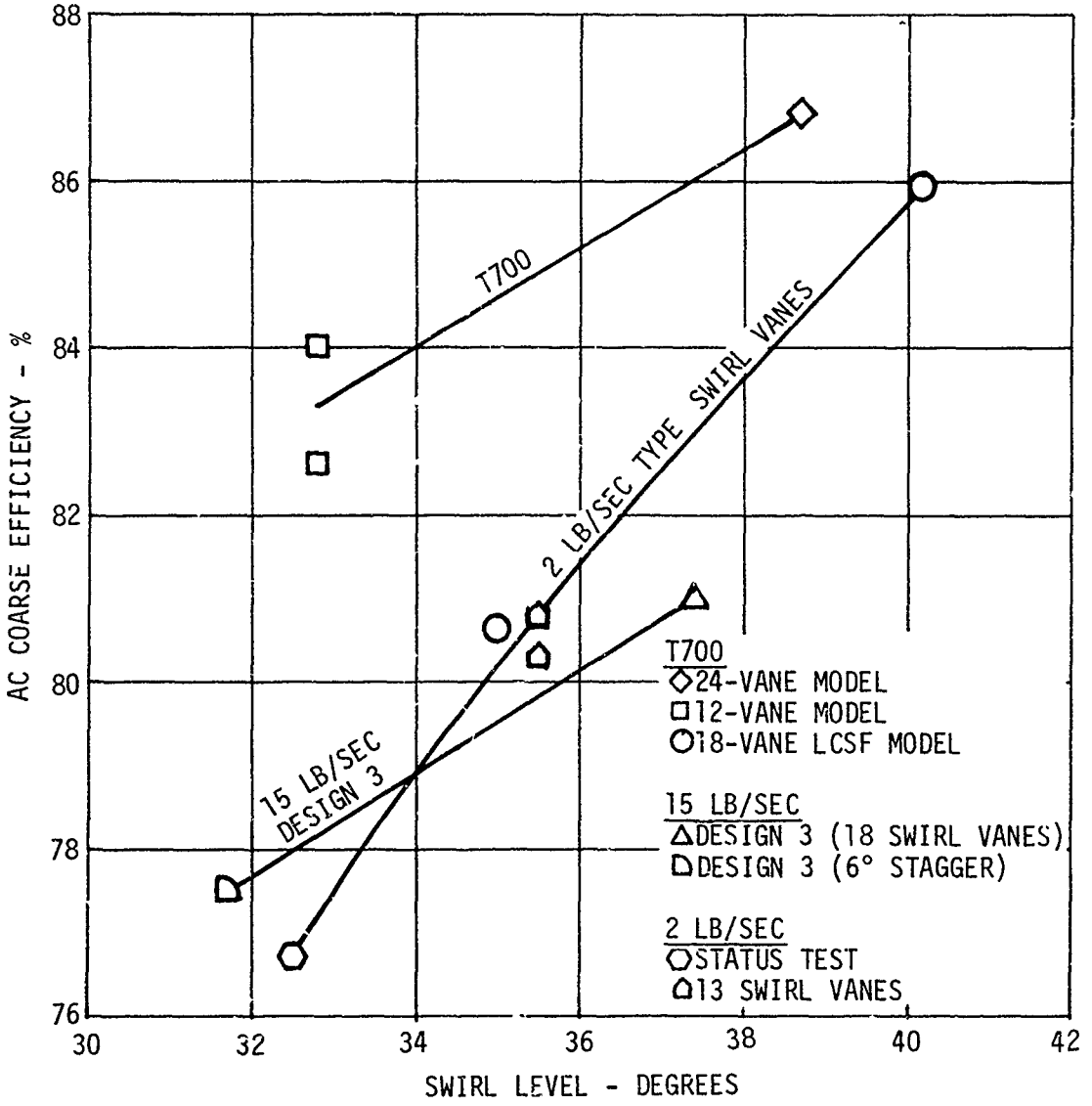

Figure 37. AC Coarse Efficiency vs Swirl Level.

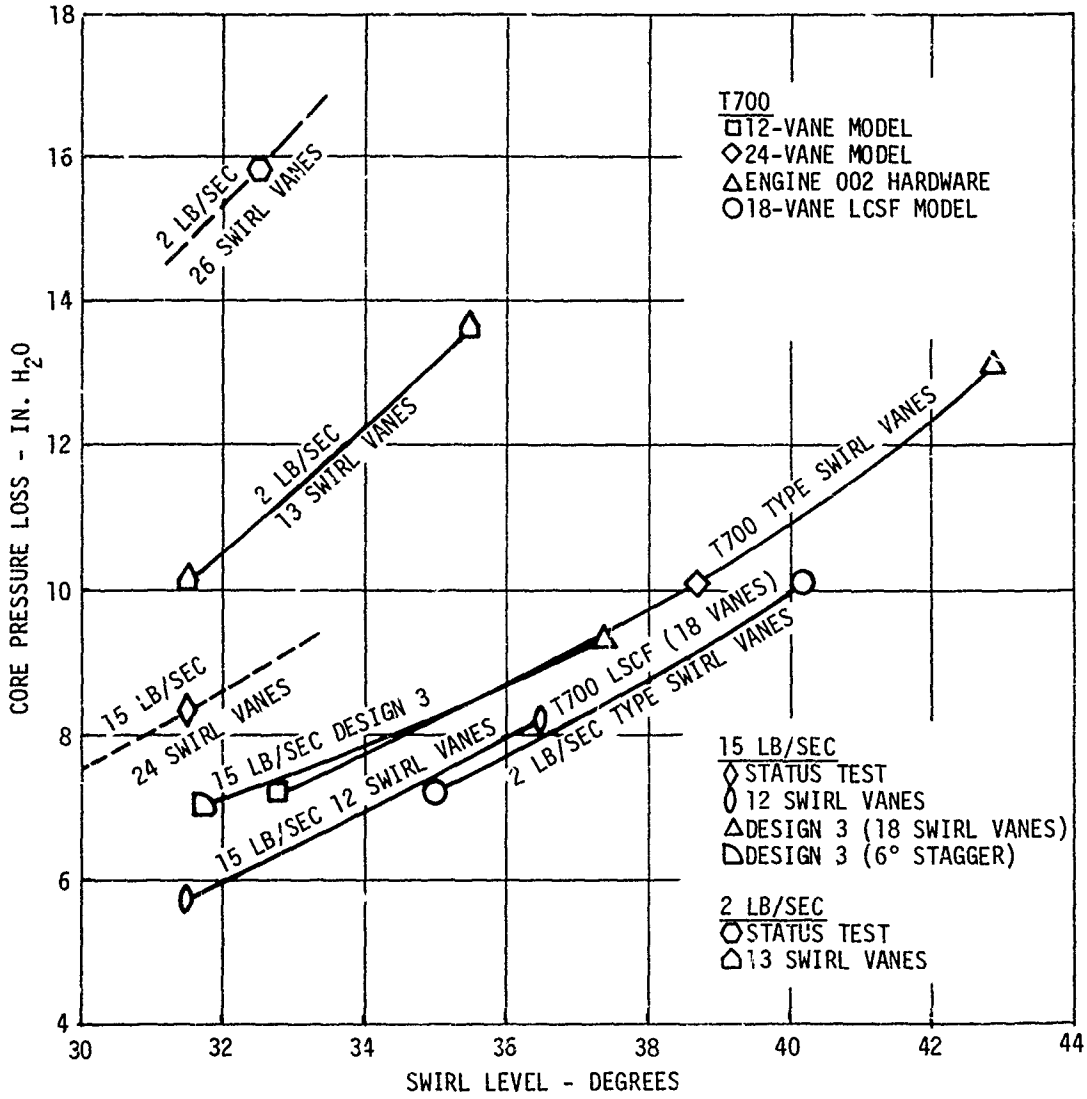

Figure 38. Core Pressure Loss vs Swirl Level.

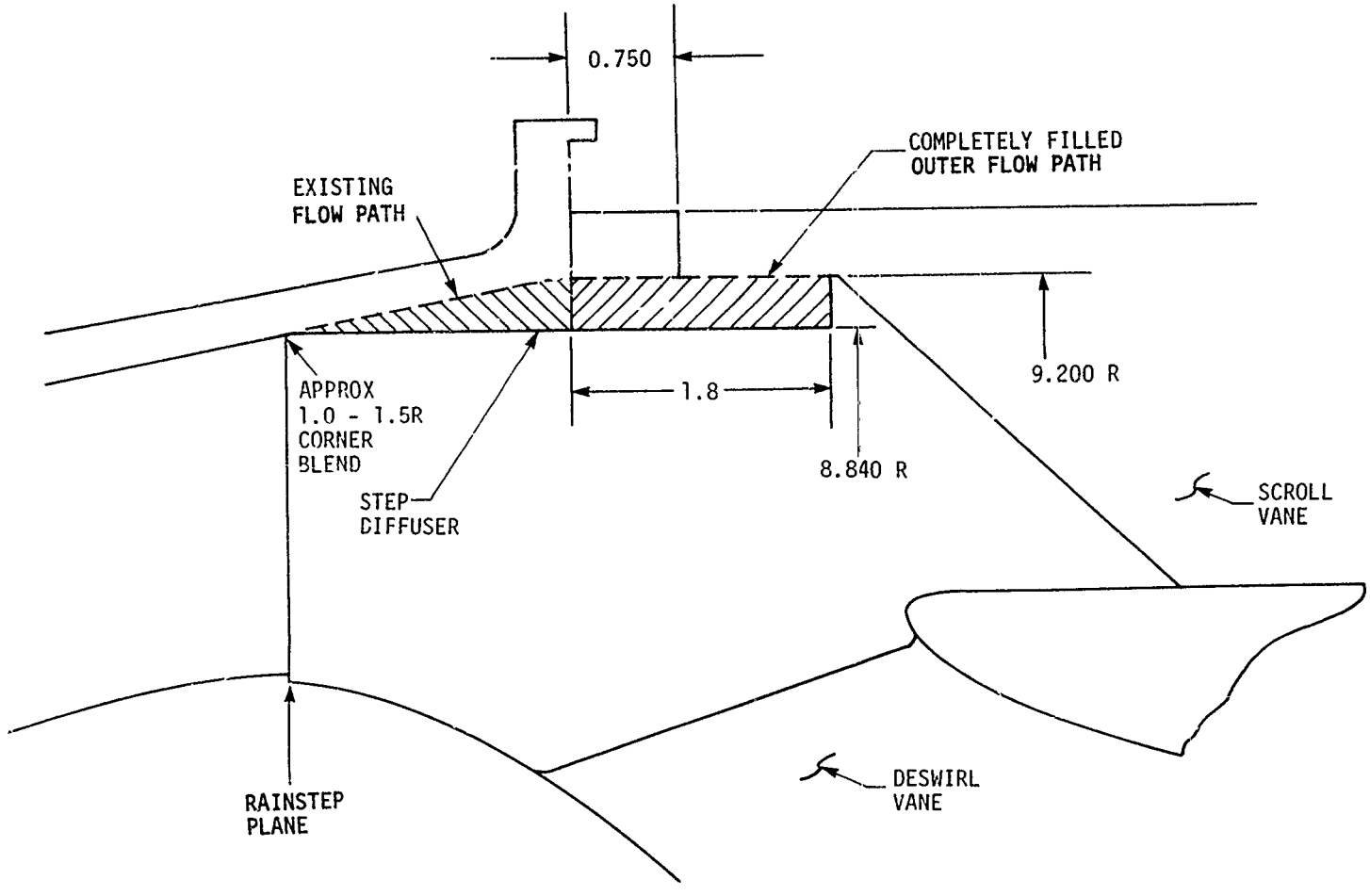

Figure 39. 15 Lb/Sec Model Flow Path Modification.

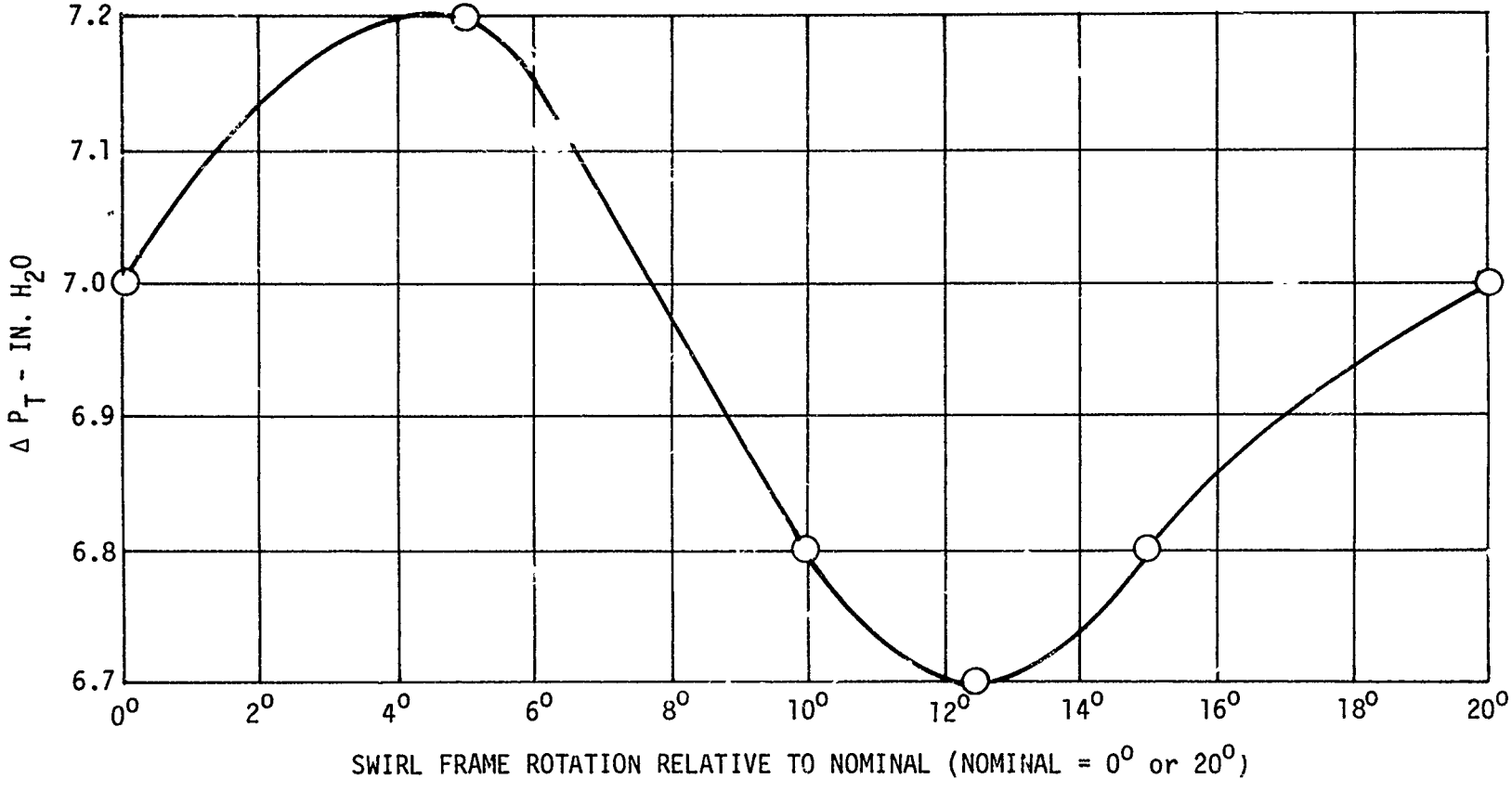

Figure 40. Swirl Vane Clocking Relative to Deswirl Vanes.

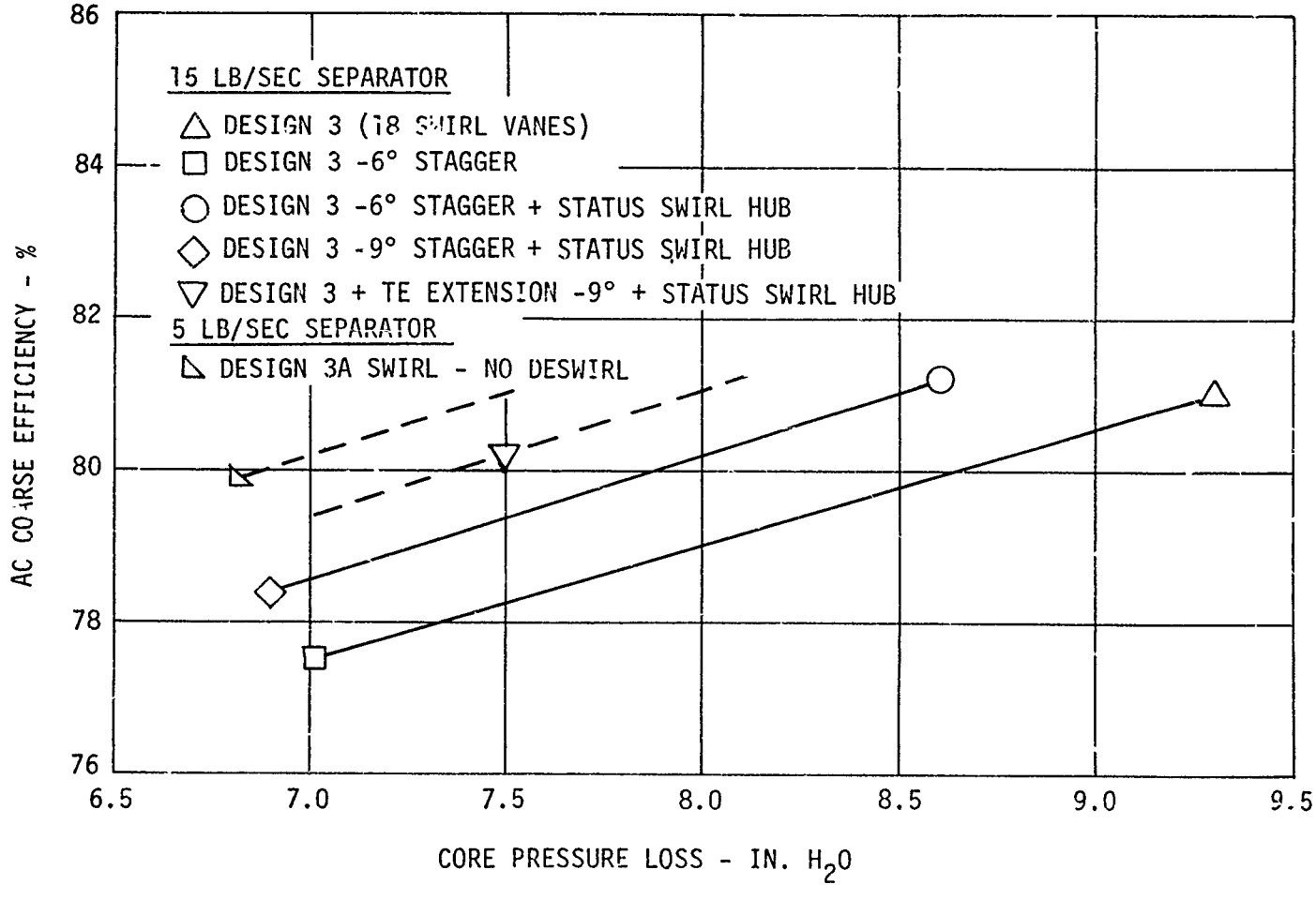

Figure 41. AC Coarse Separation Efficiency vs Pressure Loss.

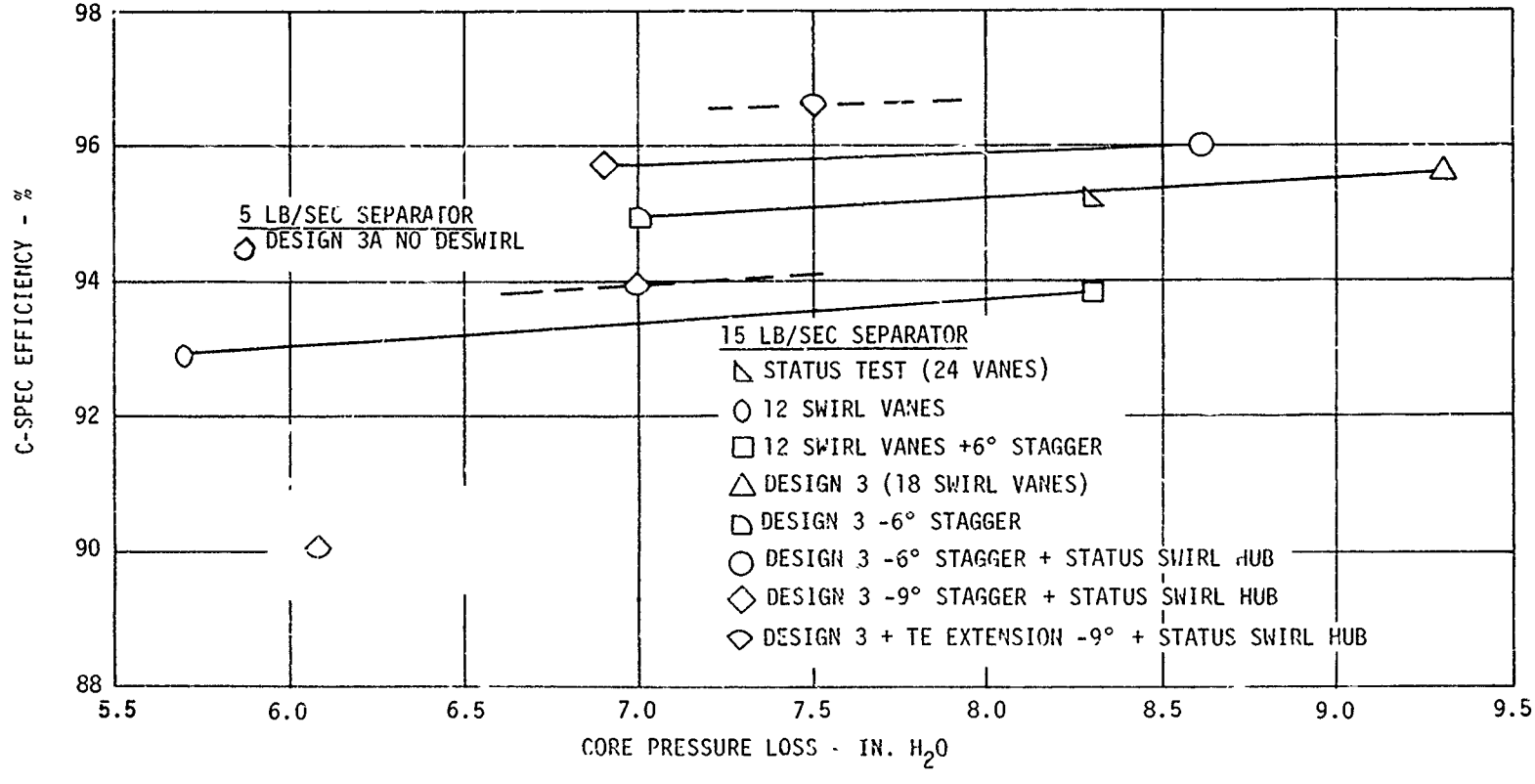

Figure 42. C-Spec Efficiency vs Pressure Loss.

Figure 43 shows the triangular trailing-edge extension to the swirl vane which resulted in an improvement of 0.8 point in the separation efficiency of both C-Spec and AC Coarse dusts at constant pressure drop. Unlike the flow path change, the trailing-edge modification resulted in no significant change in swirl level, as shown in Table 15.

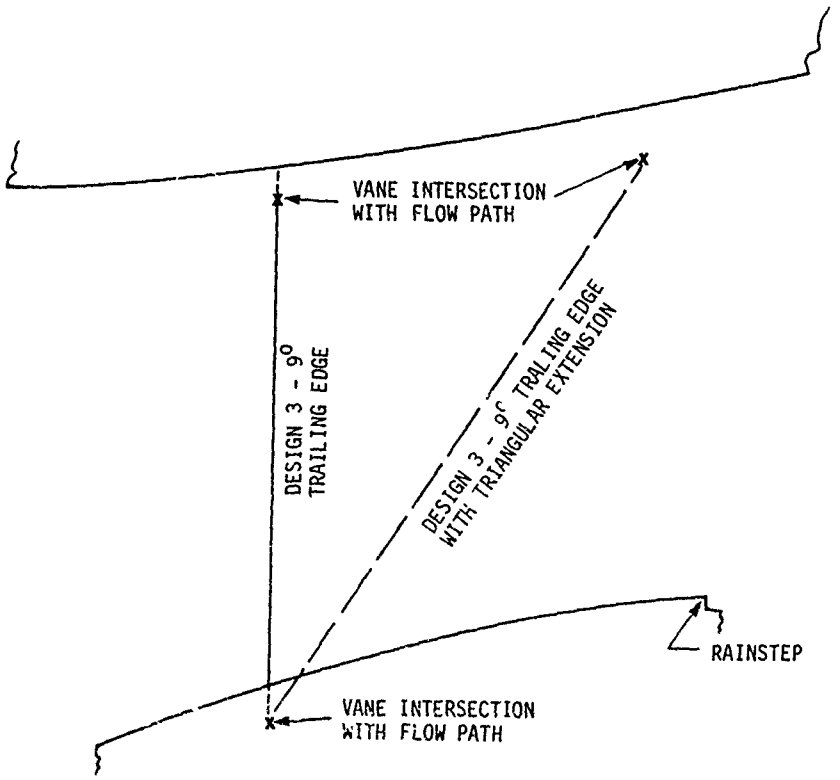

Figure 43. 15 Lb/Sec Design 3 Trailing-Edge Extension.

The 15 lb/sec model was finally tested in a swirlless configuration with a hidden splitter lip. Results, listed in Table 15, show a 8.9% increase in C-Spec efficiency due to the hidden splitter lip at a 1.0 in. H_2O pressure loss penalty. AC Coarse efficiency improved 4.1% due to the hidden splitter lip. These improvements, found by comparing Configuration III to XVII in Table 15, are greater than the normal trade-off of pressure loss for efficiency achieved by swirl vane stagger angle change.

Foreign object ingestion results are listed in Table 16 for the swirlless hidden splitter lip configuration.

TABLE 16. FOREIGN OBJECT INGESTION TEST RESULTS - 15 LB/SEC MODEL

Item	No. Ingested	No. Separated at 15 Lb/Sec	No. Separated at 6 Lb/Sec (Idle)
#10 Nut	10	7	9
1/4 in. Nut	10	9	9
#10 Bolt	10	9	10
Lockwire	10	8	9
1/4 in. Socket	3	3	3
1/8 in. Allen Wrench	3	3	1

Off-Design Testing

Required parametric off-design tests were carried out on Configuration VII of Table 15. Results are listed in Table 17 and plotted in Figures 44 and 45. Figure 44 shows increasing efficiency with increasing scavenge flow. The rate of gain, however, diminishes as the scavenge flow approaches 20% of the core flow. This indicates that there is a trade-off of efficiency against scavenge power for levels of about 20% scavenge flow. The lines of constant core flow appearing in Figure 44 show decreasing separation performance with decreasing flow. This is to be expected since the g-field created by the swirl system decreases with reduced velocity.

Figure 45 shows the effect of varying core flow on the core total pressure loss for three different levels of scavenge flow. While there appears to be about a 1 to 1.3 in. H_2O penalty in going from 10 to 16.5% scavenge flow at constant core flow, the change from 16.5 to 20% seems to have only a small (<0.3 in. H_2O) penalty. Therefore, for operation between 16.5 and 20% scavenge flow, the results of these tests indicate that scavenge flow should be based primarily on a trade-off of separation efficiency vs scavenge power requirements.

TABLE 17. 15 LB/SEC SEPARATOR TEST - PRESSURE LOSS AND AC COARSE EFFICIENCY

Run No.	Pressure Loss Scroll Pressure Loss Core Flow (lb/sec)	Scav Flow (% Core)	ΔP_T (in. H_2O)	Core Pressure Loss Core Flow (lb/sec)	Scav Flow (%)	ΔP_T (in. H_2O)	AC Coarse Core Flow (lb/sec)	Scav (%)	η_w (%)	η_c (%)
1	14.75	18.0*	25.0	14.90	17.2	9.82	14.92	19.2	82.1	78.7
2	14.95	16.7	23.9	15.10	16.5	10.3	15.15	16.3	81.1	78.0
3	14.93	10.3	18.1	14.80	10.8	8.59	15.03	10.1	77.8	75.6
4	13.46	20.0	20.7	13.30	21.9	9.05	13.79	19.3	80.7	77.0
5	13.60	16.5	18.2	13.52	16.9	8.03	13.50	16.7	80.4	77.1
6	13.33	10.3	13.3	13.57	10.2	6.80	13.43	10.2	76.9	74.5
7	12.01	20.3	16.1	12.02	20.6	6.55	11.96	19.98	80.6	76.7
8	12.07	16.8	13.9	11.96	16.6	6.39	12.07	16.0	79.8	76.6
9	12.22	10.1	10.7	12.00	10.0	5.13	11.91	10.4	75.2	72.6
10	9.04	20.0	8.5	8.80	21.0	3.85	9.03	19.6	80.5	76.7
11	9.23	16.5	7.7	8.89	17.5	3.60	9.05	16.6	78.7	75.2
12	9.02	10.9	6.2	8.92	11.0	2.91	8.99	11.2	74.7	71.9
13	6.22	19.9	3.7	6.21	20.4	2.08	6.16	20.1	78.4	74.1
14	6.09	17.4	3.5	5.86	15.2	1.59	6.09	16.51	77.1	73.3
15	15.97	9.7	2.8	5.87	10.4	1.48	6.09	10.8	73.0	70.1

*Facility Scavenge Flow Limit

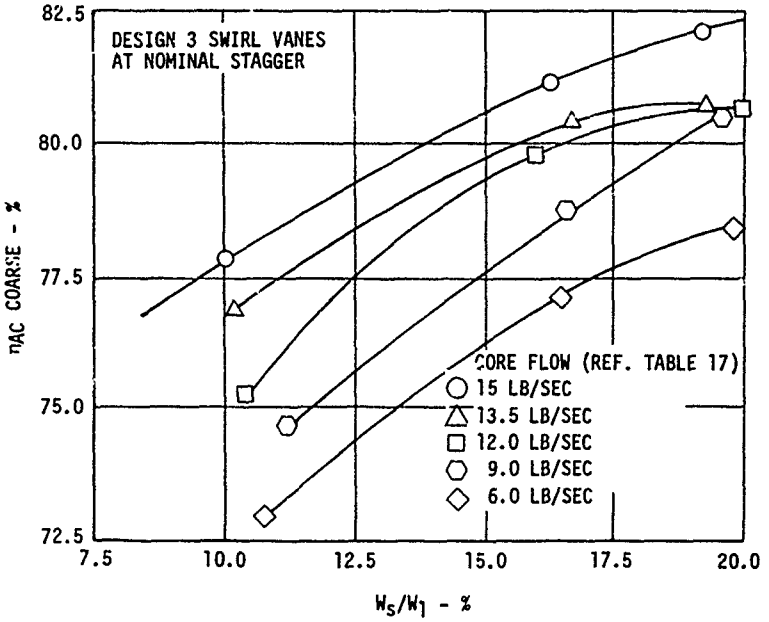

Figure 44. AC Coarse Efficiency vs Scavenge Flow Ratio - 15 Lb/Sec Model.

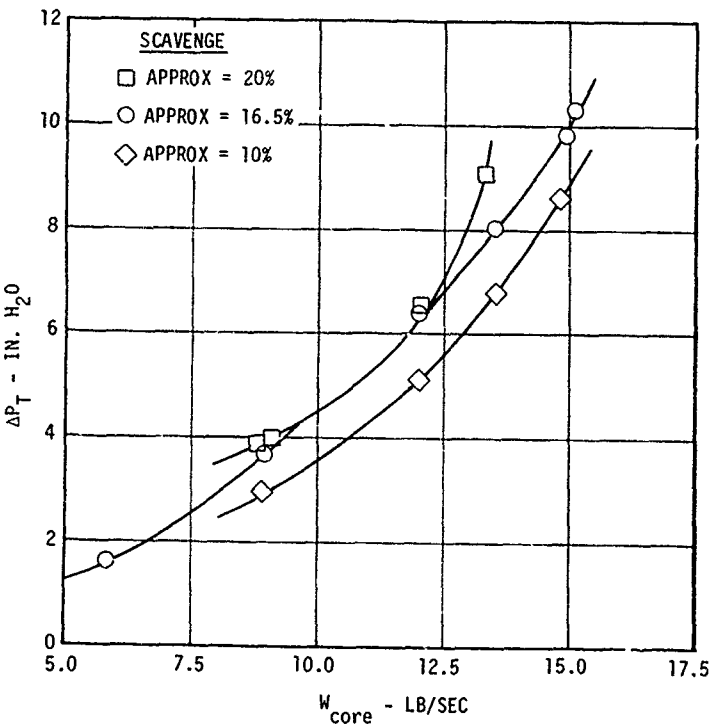

Figure 45. 15 Lb/Sec Core Pressure Loss.

SEPARATOR PERFORMANCE COMPARISON

PRESSURE LOSS

Figures 45, 46, and 47 show the core pressure loss as a function of core flow and scavenge flow for the 15, 2, and 5 lb/sec separators respectively. Core loss increased appreciably with the core flow for each separator. Scavenge flow affected loss insignificantly for the 2 and 5 lb/sec separators. For the 15 lb/sec separator, core loss increased as the scavenge flow increased from 10% to 16.5%. Core loss increased less as scavenge flow increased from 16.5% to 20%.

The scroll pressure losses for the 2, 5, and 15 lb/sec models are shown on Figures 48, 49, and 50 respectively. The figures show that there is a difference in trend between the 5 lb/sec separator and the trend for the 2 and 15 lb/sec separator. In the 2 lb/sec and 15 lb/sec separators the scroll total pressure loss increases with increasing scavenge flow. Pressure loss in the 5 lb/sec separator, however, remains essentially unchanged when scavenge flow increases at constant core flow.

Figure 51 shows the core pressure loss radial profile of the various 2 lb/sec configurations tested. A 50% reduction in swirl cascade solidity, shown as squares, resulted in a general decrease in core total pressure loss with respect to the status profile. With a 5° stagger increase in the swirl cascade, the profile remained generally below status levels. Forward movement of the splitter lip generated a change in shape of the profile, with the hub and tip experiencing greater deterioration than midstream. Since it caused only small (+1 point in C-Spec or +0.5 point in AC Coarse) efficiency improvements, this change was not considered further. Running of a vaneless flow path indicated that the greatest impact of blading on losses occurs in the tip region. These losses are probably partly due to hub losses which show up downstream at the tip due to secondary flows in the deswirl cascade. They are probably also caused by the scavenge entrance - splitter lip - deswirl vane tip portion of the flow path.

OFF-DESIGN PERFORMANCE

Figure 52 shows AC coarse efficiency as a function of scavenge flow ratio for the 2 and 5 lb/sec separators. The 2 lb/sec model with 1.5 degrees greater swirl and a higher g-field due to its smaller size consistently gave higher separation efficiency than the 5 lb/sec model. At scavenge levels above 20%, the 2 lb/sec separator showed little difference in separation efficiency between 100% and 40% core flow. The 5 lb/sec model did not demonstrate this characteristic and had at least a 3-point difference

over the same range of core flows, with the highest core flow showing the highest efficiency.

Figure 52 shows that the separation efficiency of the 5 lb/sec model increases with increasing scavenge flow. The rate of gain, however, diminishes as the scavenge flow approaches 20% of the core flow. This indicates that there is a trade-off of efficiency against scavenge power for levels of scavenge flow above 20%. The lines of constant core flow appearing in Figure 52 show decreasing separation performance with decreasing flow. The reason is probably that the g-field created by the swirl system decreases with reduced velocity.

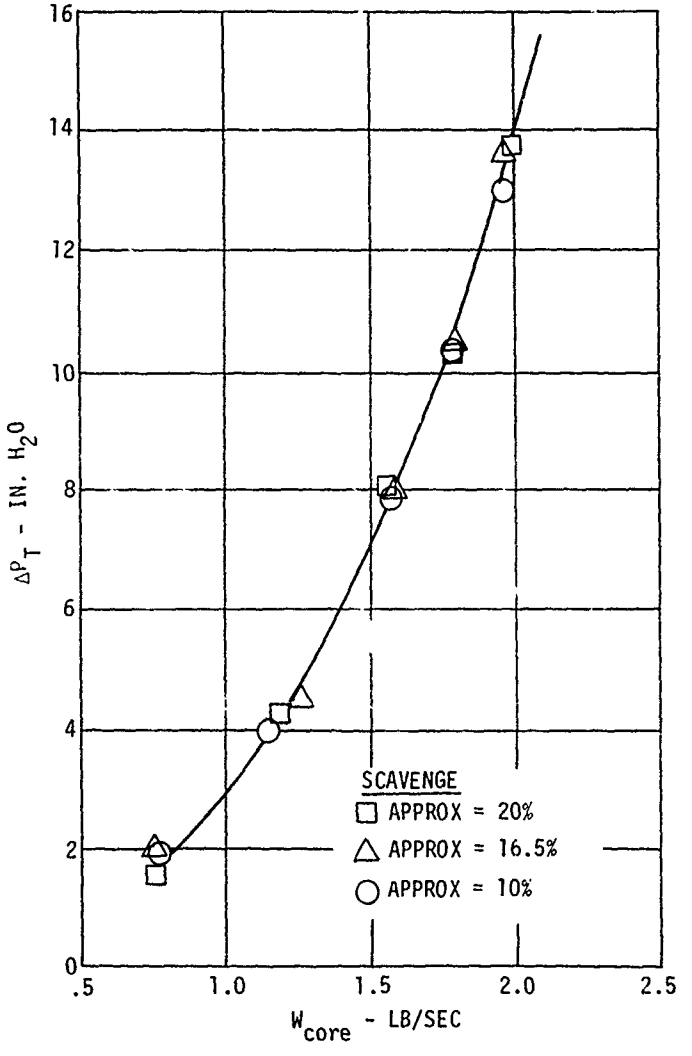

Figure 46. 2 Lb/Sec Core Pressure Loss.

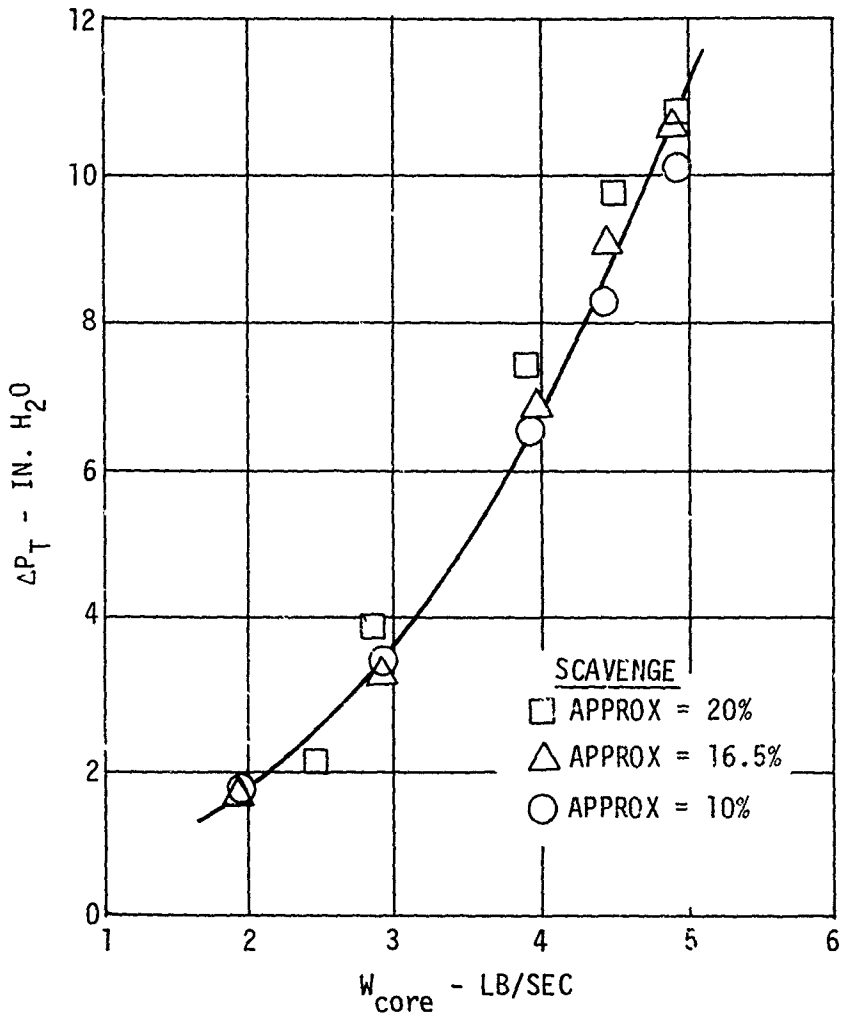

Figure 47. 5 Lb/Sec Core Pressure Loss.

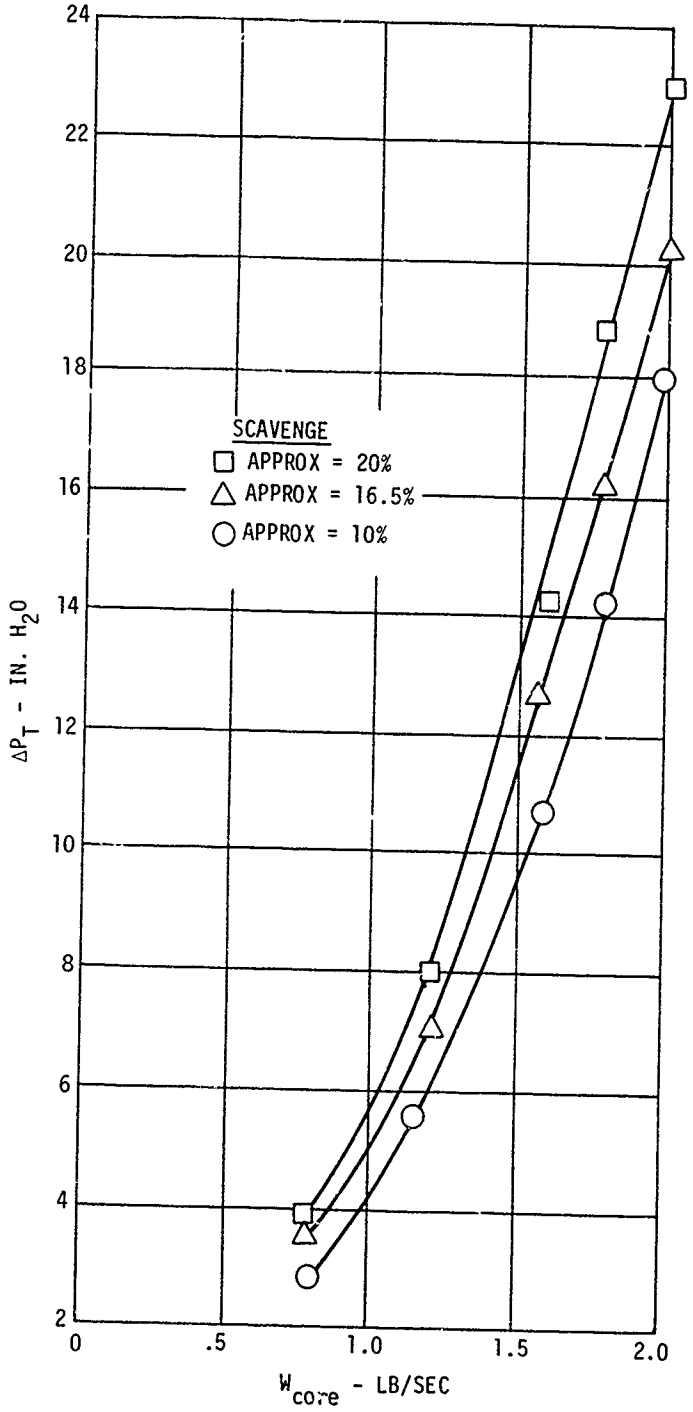

Figure 48. 2 Lb/Sec Scroll Pressure Loss.

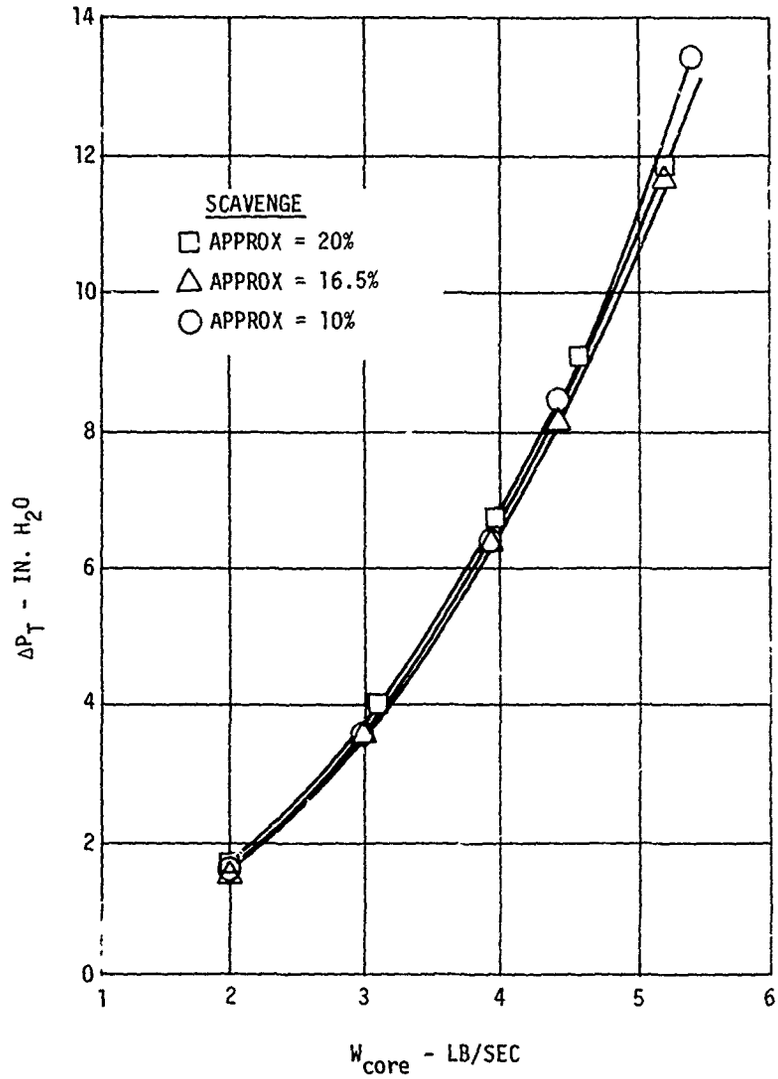

Figure 49. 5 Lb/Sec Scroll Pressure Loss.

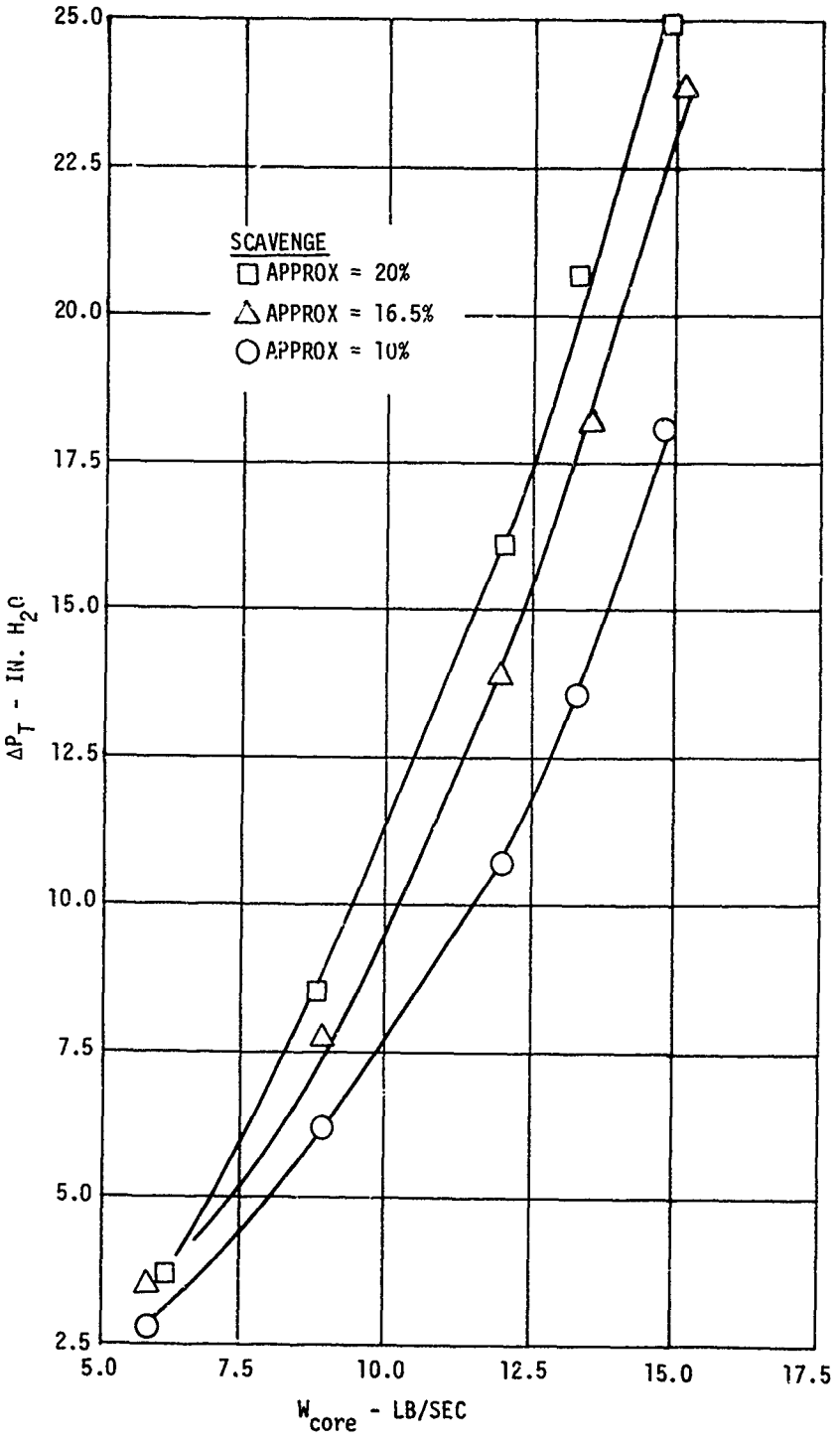

Figure 50. 15 Lb/Sec Scroll Pressure Loss.

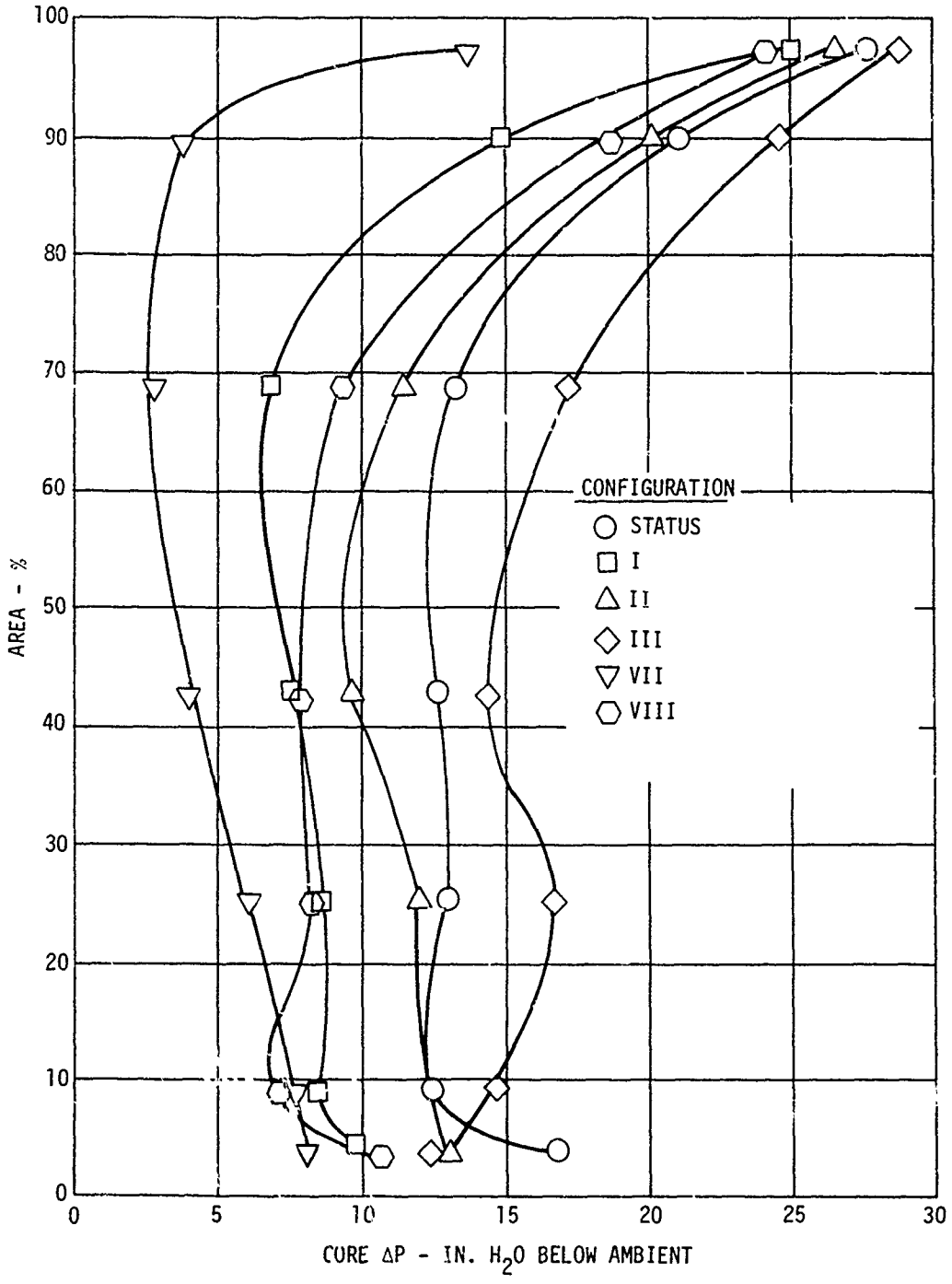

Figure 51. Separator Exit Radial Profiles at Design Airflow.

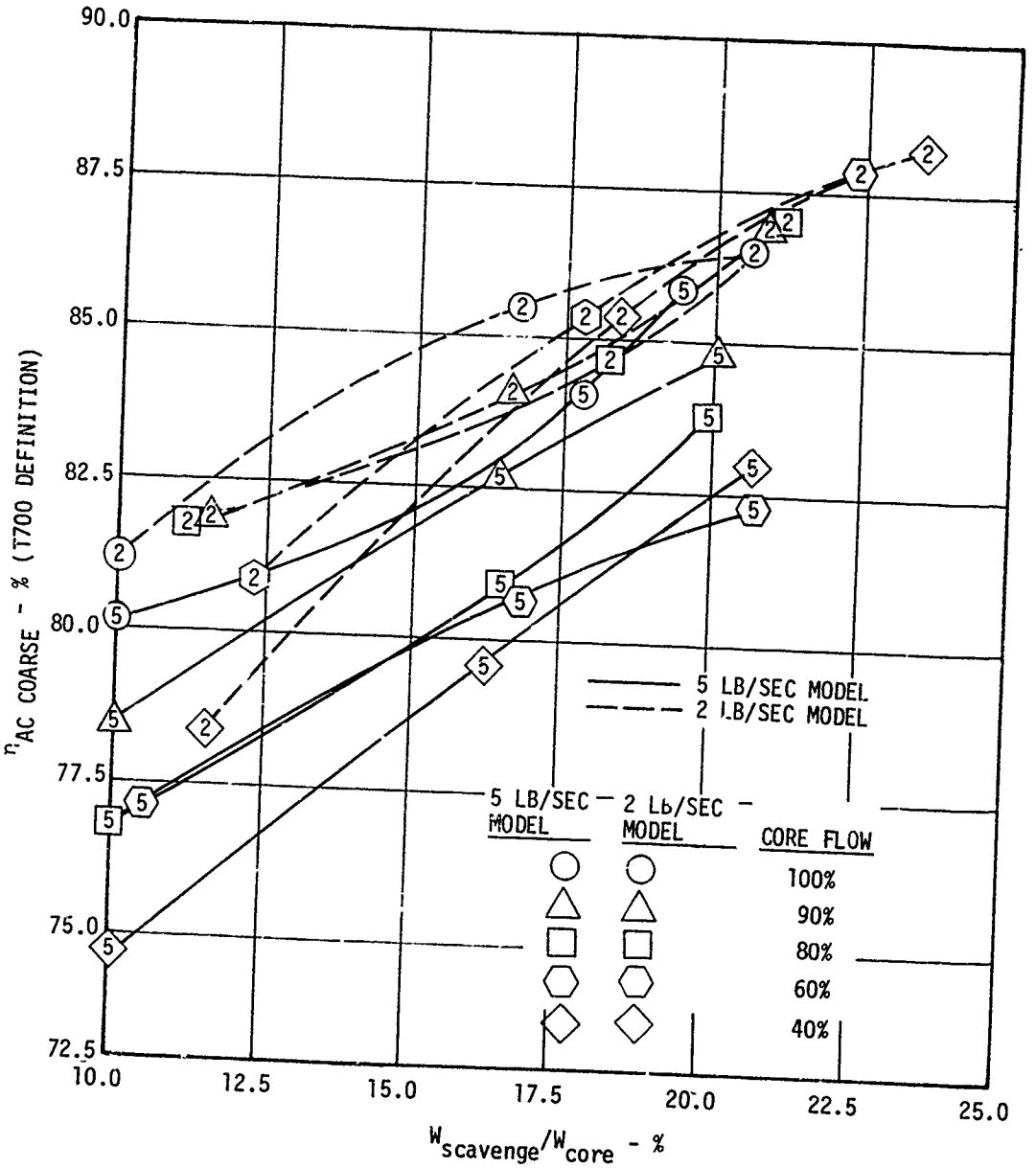

Figure 52. AC Coarse Collection Efficiency vs Scavenge System Airflow.

CONCLUSIONS

1. The program established the feasibility of swirlless inlet particle separators. More development is required to achieve their potential.

2. The 80% separation efficiency goal of the program was exceeded by the 5 and 2 lb/sec models by about 1.5% and 3%. The 15 lb/sec model, which has a lower g field than the smaller models, had about 78% separation efficiency.

3. Sand concentrations of Specification MIL-E-5007C are lower than those found around operational helicopters.

4. Sand size distributions for operational helicopters lie between Specification MIL-E-5007C and AC Coarse distributions.

5. The method of injecting sand into a separator inlet can have a strong effect on separation efficiency.

6. The program established the feasibility of inlet scroll separators.

RECOMMENDATIONS

Continue to conduct a development program that makes use of the existing separator models. Systematically vary the following features to obtain improvements in separator performance:

1. Improve collection efficiency and reduce collector scroll pressure loss by varying the separator outer wall shape.

2. Improve collection efficiency and reduce collector scroll pressure loss by systematically varying scroll vane solidity, twist, and camber.

3. Improve collection efficiency and reduce scavenge flow requirements for swirlless separator configurations by varying the ratio of inner flow path maximum diameter to splitter lip diameter while outer flow path and scavenge vane designs remain fixed.

4. Investigate the inlet parameters of sand injection to determine their influence on collection efficiency; to establish engine installation design rules and to develop appropriate component test sand injection techniques.

LIST OF SYMBOLS

$\bar{a}$	acceleration, ft/sec^2
A	area, ft^2
c	chord length, in.
c_o	local sand concentration, mg/ft^3
c_s	average sand concentration, mg/ft^3
C	parameter - $\pi C_d \rho V/8\rho_p ZD$
C_d	drag coefficient
d ( )	differential
D	diameter, in.
D_{cr}	critical particle diameter, micron
$\bar{e}$	unit vector
f	function
f_a	depth of erosion, mils
f_d	normalized severity factor
g	acceleration due to gravity, ft/sec^2
h_{is}	insentropic head, ft lb/lb
l	length, in.
L	axial distance downstream from splitter lip, in.
m	particle mass, lb
M	Mach number
N	speed - rpm
N_s	specific speed
P	pressure, lb/in^2
Q	volume flow, ft^3/sec

LIST OF SYMBOLS - Continued

R	radius, in.
R_1	outer wall radius at the separator inlet, in.
Re	Reynolds number
SF	scale factor
t	time, sec
t_m	maximum vane thickness, in.
u	gas velocity, ft/sec
U	blade section tangential velocity, ft/sec
v	particle velocity, ft/sec
v_n	particle velocity normal to impacted surface, ft/sec
v_t	particle velocity tangential to impacted surface, ft/sec
V	relative particle velocity, ft/sec
V_θ	air circumferential velocity, ft/sec
W	mass airflow, lb/sec
z	axial distance downstream from compressor station zero, in
Z	particle shape factor
β_1	particle incidence angle, deg
β_2	particle rebound angle, deg
ΔP_T	total pressure loss, lb/in^2
η	separation efficiency
η_c	separation efficiency based on sand concentration
η_w	separation efficency based on sand weight

η_v	vane passage efficiency
μ	air viscosity, lb sec/ft^2
ρ	air density, lb/ft^3
ΣA_t	sum of areas, in.^{2}
ψ	stream function
$\partial( )$	partial differential
%	weight fraction of sand with particle diameter less than D_p

SUBSCRIPTS

a	refers to air
c	refers to core
g	refers to gas
ℓ	refers to local conditions
m	indicates maximum
o	refers to average conditions
p	refers to particle
r	radial coordinate
s	refers to sand
t	indicates stagnation conditions
V	refers to relative velocity
Z	axial coordinate
Θ	circumferential coordinate

8175-75